KATHOLIEKE UNIVERSITEIT LEUVEN
FACULTEIT LANDBOUWKUNDIGE EN TOEGEPASTE BIOLOGISCHE WETENSCHAPPEN
DEPARTEMENT LANDBEHEER
LABORATORIUM VOOR BODEM- EN WATERBEHEER
KASTEELPARK ARENBERG 20
B-3001 LEUVEN

DISSERTATIONES DE AGRICULTURA

Doctoraatsproefschrift nr 581 aan de Faculteit Landbouwkundige
en Toegepaste Biologische Wetenschappen van de K.U.Leuven

LEACHING OF CADMIUM AND ZINC FROM SPODOSOLS: FROM LABORATORY TO FIELD SCALE

Promotor:

Prof. E. Smolders, K.U.Leuven

Leden van de examencommissie:

Prof. R. Schoonheydt, K.U.Leuven, Voorzitter

Dr M. Benedetti, UPMC, Paris, France

Prof. A. Cremers, K.U.Leuven

Prof. J. Feyen, K.U.Leuven

Prof. A. Maes, K.U.Leuven

Prof. R. Merckx, K.U.Leuven

Proefschrift voorgedragen tot het behalen van de graad van Doctor in de Toegepaste Biologische Wetenschappen

door

Jozefien DEGRYSE

November 2003

Het duurt altijd langer dan je denkt,
ook als je denkt
het zal wel langer duren dan ik denk
dan duurt het toch nog langer
dan je denkt.

Het duurt veel korter dan je denkt,
ook als je denkt
het zal wel korter duren dan ik denk
dan duurt het toch
nog korter dan je denkt
(Judith Herzberg)

De vier voorbije jaren zijn voorbijgevlogen. Ik kan me die eerste oktober waarop ik dacht te beginnen aan een doctoraat over cesium nog moeiteloos voor de geest halen. En meer dan eens heb ik verzucht 'Is het al zo laat?'. Maar toch, soms leek de tijd ook stil te staan; van die eindeloze dagen in het labo, of achter het scherm, waarbij het langzaam tot je doordringt dat het schrijven van een proefschrift zoiets is als de processie van Echternach – drie zinnen schrijven en er twee van schrappen. Ik ben dan ook niet rouwig dat het erop zit. Tijd voor iets nieuws... Maar niet zonder eerst deze woorden van dank.

Erik, je hielp en hield me op de weg. Je deur stond steeds open, en je drukke agenda belette je niet geregeld ons bureau binnen te springen met ideeën, raadgevingen of wetenswaardigheden. Dankjewel voor de interesse, de schouderklopjes, het grondige nalezen, voor alles wat ik van je heb geleerd.

Veerle Vlassak, tijdens mijn ingenieursthesis zag ik jou naarstig bezig: kolommetjes 'slachten', metingen met de grafietoven,... Ik had toen geen flauw benul dat je noeste arbeid zou leiden tot hoofdstuk 7 en 9 van dit proefschrift. Dankjewel dat ik je gegevens mocht gebruiken.

Piet, dankjewel voor de praktische hulp, het gebruik van de putten, en het berijden van de cadmiumweg. Het zal je wellicht plezieren te horen dat ik jouw 'boekje' – wegens veelvuldig raadplegen - hoognodig moet herinbinden.

Professor Cremers, ik mag dan al vrij snel van het cesiumpad zijn afgedwaald, u hebt toch een stempel gedrukt op dit werk. Dank ook aan de overige leden van mijn jury, voor het nalezen van de eerste versie van dit werk en de opbouwende kritiek.

Doctor Scott Young, thanks for giving me the opportunity to come to Nottingham, where I carried out the work described in chapter 4. Those three 'English months' were an enjoyable and interesting time.

Professor Maes, Agnes en Jacqueline wil ik danken voor het gebruik van hun labo-infrastructuur. Dank ook Agnes voor alle praktische raadgevingen.

Het Fonds voor Wetenschappelijk Onderzoek (FWO-Vlaanderen) ben ik erkentelijk voor de beurs die dit onderzoek mogelijk maakte.

Joke, Jurgen, Tim en Inge, ik heb het getroffen met mijn thesisstudenten. Of het nu over Cs, Cd of U ging, het was zeer fijn samenwerken met jullie. Dank jullie wel.

Alle collega's van het labo wil ik danken voor de aangename sfeer, de ontspannende koffiepauzes, de praktische hulp wanneer nodig. Kris, we zijn samen gestart, jij hebt mij blauwe plekken zien oplopen in Canada en ik jou in Zweden, en we hebben elkaar de laatste maanden zien zwoegen (en soms ook vloeken, de één hardop, de ander inwendig) achter het scherm: dat verdient een aparte vermelding.

Alle huisgenootjes en 'aanverwanten' van de Vermeylenstraat en van Safraan, door jullie was het 's avonds fijn thuiskomen. Machteld en Reza, al hebben jullie (iets te?) vaak met mijn accent gelachen, 't waren toch hezellihe avonden. Ook de anderen die mijn avonden kleuren – partners in muziek en ander vertier – wil ik hier graag bedanken.

Mama, papa, Pol en Liesbet, Kaat en Leon, Anne en Trudo, en ook de neefjes en nichtjes, het is een zegen zo een lieve en leuke familie te hebben. Dank jullie voor alle gezellige momenten samen. Ma en pa, dank jullie voor de goede zorgen, de nooit aflatende steun, de goede raad. Al was de les niet voor mij bedoeld, ik ben toch niet vergeten dat je een olifant alleen in schelletjes kan opeten, en dat besef is me de voorbije jaren goed van pas gekomen. Eén olifant heb ik alvast achter de kiezen. Ongetwijfeld zal ik er nog andere te verorberen krijgen, maar daar wil ik vandaag niet aan denken.

Fien
oktober 2003

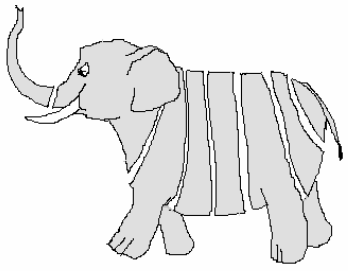

Contents

Abstract

A large area of sandy soils at the Dutch-Belgian boundary is contaminated with cadmium (Cd) and zinc (Zn) from historical pollution of non-ferrous metal smelters. Groundwater contamination with these metals is a growing concern. Earlier studies have revealed that Cd and Zn transport in soil is mainly controlled by the sorption strength of the metal in soil. This study is devoted to the role of sorption kinetics on the transport of Cd and Zn in field contaminated soils and to the effect of soil acidification on Cd transport at the field scale.

The isotopic dilution technique was used to discriminate between the labile (*E* value) and non-labile metal pool. In general, more than half of Cd in the soil was in labile form. Only in the upper horizon of contaminated soils, the %*E* value (*E* relative to total metal concentration) was less than 50%. The %*E* values of Zn were generally smaller than 50%.

Column studies showed that Cd and Zn desorption rates are large enough to maintain effluent concentrations at pore water velocities up to 30 cm d^{-1} in these soils. The Cd and Zn transport was well predicted assuming that labile metals were in equilibrium with the solution phase and that non-labile metals could not be desorbed. The transport was greatly overestimated if it was assumed that all metal was in equilibrium with the solution phase, i.e., if the (total) K_d was used for the calculations. However, a slow release of non-labile Cd and Zn was observed when the labile metal pool was nearly depleted, resulting in a longer tailing of the breakthrough curve than predicted with the equilibrium model. This tailing of the breakthrough curve could be well predicted with a two-site model, using a small rate constant for desorption of non-labile metals.

Field observations (with wick samplers) confirmed that the metal transport at field scale can be predicted with the local equilibrium assumption (LEA). The Cd and Zn transport in these soils was modelled with sorption characteristics derived from batch experiments. Present-day vertical Cd concentration profiles in a moderately polluted field with acid sandy soils were calculated based on the emission history of the nearby smelter. Predicted and observed profiles agreed reasonably well, but total Cd concentrations in the topsoil were generally underestimated, which was probably related to the presence of Cd in a partly insoluble form. It was predicted that the Cd concentration in the seepage water will remain above the groundwater threshold of 5 µg l^{-1} for the next 170 years and that the Zn concentration will remain above 0.5 mg l^{-1} for the next 40 years.

The future Cd transport was also modelled for a heavily contaminated field that was set-aside in 1992 and where slow soil acidification accelerates metal leaching. The coupled transport of Cd and protons was calculated for 48 profiles sampled in that field, and an averaged breakthrough curve was calculated. The model simulations indicated that the field-averaged concentration in the seepage water will increase from 6 to 300 µg Cd l^{-1} in the next 100 years. A later breakthrough and a larger peak Cd concentration was predicted when the Cd transport was modelled with field-averaged soil properties, illustrating the impact of spatial variability on transport of reactive solutes. Liming the topsoil was predicted to be an effective method to reduce the Cd transport to the groundwater, since most Cd is still present in the plough layer. It was calculated that the Cd concentration in the seepage water will only increase from 6 to 7 µg l^{-1} in the next 100 years when the soil pH is maintained through liming.

It is concluded that sorption kinetics have a minor effect on leaching of Cd and Zn from the labile fractions in soil. Groundwater contamination with Cd and Zn is a major risk for the contaminated area in the foreseeable future and control of soil pH by liming is therefore recommended.

Samenvatting

Een groot oppervlak in het Nederlands-Belgisch grensgebied (de Kempen) is vervuild met cadmium (Cd) en zink (Zn) door atmosferische depositie van zinksmelters. Het transport van deze metalen naar het grondwater is relatief snel in deze zandige bodems. Nu al worden verhoogde Cd en Zn concentraties in het grondwater vastgesteld, maar de verontreiniging van het grondwater door uitspoeling van deze metalen zal in de toekomst waarschijnlijk nog toenemen. Vroegere studies hebben aangetoond dat het transport van deze metalen voornamelijk afhangt van de sterkte waarmee het metaal op de vaste fase van de bodem wordt vastgelegd. In dit onderzoek werd de rol van sorptiekinetiek en het effect van bodemverzuring op het transport van Cd en Zn in deze bodems onderzocht.

Isotopische verdunning werd gebruikt om de labiele hoeveelheid (of *E* waarde) aan Cd en Zn te bepalen. Over het algemeen was ruim de helft van de totale Cd hoeveelheid in de bodem in labiele vorm. Enkel in de bovenste horizonten van de vervuilde bodems was vaak minder dan de helft in labiele vorm. Voor Zn waren de %*E* waardes (*E* waarde relatief ten opzichte van de totale concentratie in de bodem) meestal kleiner dan 50%.

Het transport van adsorberende stoffen in poreuze media wordt meestal gemodelleerd in de veronderstelling van lokaal evenwicht tussen de vaste en de vloeibare fase. Deze veronderstelling is geldig als de sorptiereactie snel is ten opzichte van de poriewatersnelheid. Experimenteel werd aangetoond dat deze veronderstelling correct is in gestoorde kolommen bij poriewatersnelheden tot 30 cm dag^{-1} (i.e., 100 maal hoger dan in veldomstandigheden). Het snelle evenwicht geldt echter enkel voor de labiele fractie. Wanneer verondersteld werd dat ook de niet-labiele fractie in evenwicht is met de oplossing, werd het transport van Cd en Zn sterk overschat. Toch werd een vrijzetting van niet-labiel Cd en Zn waargenomen wanneer de labiele hoeveelheid nagenoeg uitgeput was. Deze trage vrijzetting kon worden beschreven met een twee-site model, waarbij de desorptie van niet-labiel metaal beschreven werd met een eerste-orde-reactie.

Veldobservaties toonden aan dat de concentratie aan Cd en Zn in het percolerend bodemwater (opgevangen door een glasvezel-koord) overeenstemt met de concentratie in de bodemoplossing verkregen door centrifugatie. Deze overeenkomst duidt erop dat het Cd en Zn transport in het veld kan voorspeld worden in de veronderstelling van lokaal evenwicht. In een matig verontreinigd veld met zure zandige bodems (Spodosols) werden 10 profielen op verschillende dieptes bemonsterd. Het Cd en Zn transport in dit veld werd

berekend met sorptiekarakteristieken bepaald in batch experimenten. De verticale verdeling van Cd over het bodemprofiel werd berekend uit het verloop van de Cd emissies in de voorbije 100 jaar, en kwam vrij goed overeen met de geobserveerde verdeling. De totale Cd concentratie in de bovenste horizont werd echter onderschat. Cadmium in de depositie is wellicht deels aanwezig in slecht oplosbare vorm, wat deze onderschatting kan verklaren. Volgens de voorspelling zal de Cd concentratie in het poriewater ter hoogte van de grondwatertafel nog 170 jaar boven de grondwaternorm van 5 µg l^{1} blijven en de Zn concentratie nog 40 jaar boven de norm van 0.5 mg l^{-1}.

Het Cd transport werd ook voorspeld voor een zwaar gecontamineerd veld dat in 1992 werd braakgelegd, en waar bodemverzuring leidt tot een versnelde uitloging van de metalen. Het gekoppelde transport van Cd en protonen werd gemodelleerd voor elk van de 48 bemonsterde profielen, en een gemiddelde doorbraakcurve werd berekend. Er werd voorspeld dat de veldgemiddelde poriewaterconcentratie ter hoogte van de grondwatertafel zal stijgen van 6 tot 300 µg Cd l^{1} in de komende 100 jaar. Een latere doorbraak en een hogere piekconcentratie werd voorspeld wanneer de ruimtelijke variabiliteit buiten beschouwing werd gelaten en het veld werd beschouwd als één kolom met veldgemiddelde bodemeigenschappen. Cadmium in dit veld is hoofdzakelijk in de ploeghorizont aanwezig. Bekalken van de topbodem zal daarom een doeltreffende methode zijn om de uitloging van Cd naar het grondwater in te perken. Volgens de modellering zal de poriewater-concentratie ter hoogte van de grondwatertafel slechts stijgen van 6 tot 7 µg Cd l^{1} in de komende 100 jaar als bodemverzuring wordt vemeden door de topbodem te bekalken.

Samenvattend, sorptiekinetiek heeft weinig effect op de uitloging van labiel Cd en Zn. Op termijn kan echter ook de niet-labiele fractie langzaam vrijkomen, en dit is vooral voor Zn van belang, aangezien meestal een grote fractie van dit element in niet-labiele vorm aanwezig is. Grondwaterverontreiniging door uitspoeling van Cd en Zn zal in de toekomst nog toenemen. Controle van de bodem pH door bekalken is daarom aanbevolen.

Symbols and abbreviations

Symbol	name	unit [a]
Al_{ox}	ammonium oxalate extractable Al	mmol kg^{-1}
BS	base saturation	
c	concentration in the solution phase	mg l^{-1}
CEC	cation exchange capacity	$cmol_c$ kg^{-1}
d	layer thickness	cm
D	dispersion coefficient	cm^2 d^{-1}
D_0	diffusion coefficient in water	cm^2 d^{-1}
E	radio-labile metal concentration	mg kg^{-1}
%E	E relative to total metal concentration	
f	fraction of equilibrium sorption sites	
F	complexation coefficient	
Fe_{ox}	ammonium oxalate extractable Fe	mmol kg^{-1}
IS	ionic strength	mol l^{-1}
k	Freundlich sorption constant	mg^{1-n} l^n kg^{-1}
K_c(X/Y)	selectivity coefficient of ion X versus ion Y	
K_d	solid–liquid distribution coefficient	l kg^{-1}
K_d^*	distribution coefficient of radio-isotope	l kg^{-1}
K_d^{lab}	distribution coefficient between labile pool and solution	l kg^{-1}
K_s	saturated hydraulic conductivity	cm d^{-1}
L	length of soil column	cm
m	proton exponent of Freundlich isotherm	
M_{lab}	labile metal concentration	mg kg^{-1}
$M_{profile}$	metal amount in the soil profile	kg ha^{-1}
M_{tot}	total metal concentration	mg kg^{-1}
$[M]_{pw}$	metal concentration in the soil solution	mg l^{-1}
n	(Cd or Zn) exponent of Freundlich isotherm	
n_{Ca}	Ca exponent of Freundlich isotherm	
OC	organic C content	%

Symbol	**name**	**unit** [a]
pH BC	pH buffer capacity	$cmol_c\ kg^{-1}\ pH^{-1}$
q	water flux density	$cm\ d^{-1}$
R	retardation coefficient	
s	sorbed concentration	$mg\ kg^{-1}$
t	time	d
T_c	response time	d
v	pore water velocity	$cm\ d^{-1}$
V	volume of solution	l
W	mass of soil	kg
z	depth	cm
Z_{Ca}	equivalent fraction of Ca on the exchange complex	
α	first order rate coefficient	d^{-1}
γ	activity coefficient	
ε_n	fractional change in the n^{th} central moment	
θ	volumetric soil water content	
θ_m, θ_{im}	volumetric water content of mobile and immobile liquid phase	
λ	longitudinal dispersitivity, or dispersion length	cm
μ_n	n^{th} central moment	
ρ	soil bulk density	$kg\ l^{-1}$
τ	tortuosity factor	
ω	dimensionless mass transfer rate coefficient	

[a] most commonly used unit, other units with same dimensions may be used

CHAPTER 1

Leaching of Cd and Zn in polluted soils: an overview

1.1 Background and objectives

The behaviour of Cd and Zn in the terrestrial environment has received much attention during the last decades because of the widespread contamination of soil by these metals. Background concentrations of Cd and Zn are difficult to determine, since most soils are enriched by diffuse contamination in industrialized countries. The concentrations of Cd and Zn in unpolluted soils tend to be larger in soils with heavier texture and larger organic matter content (Tack *et al.*, 1997, see Table 1.1).

Table 1.1 Expected Cd and Zn concentration (mg kg^{-1}) in surface soils of Flanders as a function of clay and organic C (OC) content (Tack *et al.*, 1997)

	5% clay		15% clay	
	1% OC	3% OC	1% OC	3% OC
Cd	0.1	0.3	0.4	0.7
Zn	32	43	45	57

Anthropogenic activities have increased Cd and Zn concentrations in soils. Application of fertilizers, sludge, and waste to soils may contribute significant amounts of heavy metals to soils. Another important source of Cd and Zn contamination is the atmospheric deposition from the ferrous and non-ferrous industry, fuel combustion and incinerators. These point-source emissions have contaminated large areas of land. The metal deposition on the soil depends on the metal emission, the distance to the source, the wind direction, the stack height and the local topography. The soil pollution within 1–2 km of metal smelters may be quite severe, and background concentrations may be reached only at distances of more than 20 km from the source (Tiller, 1989).

Increased Cd concentrations in the soil may involve a risk for human health. The soil to plant transfer of Cd is relatively large. Consumption of plants grown on polluted soils where no phytotoxic effects were observed may have adverse affects on humans and animals. Cadmium is concentrated in the kidney after inhalation or gastrointestinal

absorption. The biological halflife time is estimated in the order of 20 years. Elevated concentrations of microproteins in the urine are a first indication of renal dysfunction caused by chronic exposure to Cd (Lauwerys *et al.*, 1990). Unlike Cd, the transfer of Zn to the food chain is limited since Zn is phytotoxic at concentrations where consumption of the plants does not pose any health risk. Therefore, soil pollution with Zn is mainly relevant from an ecotoxicologic viewpoint. Increased metal concentrations in groundwater used for drinking water supply may also increase the exposure. However, the risk of heavy metal leaching is usually small, since the metals are strongly sorbed in the soil. The solid–liquid distribution coefficient or K_d (i.e., the ratio of total metal concentration to concentration in solution) of Cd is in most soils larger than 100 l kg^{-1}, and therefore, travel velocities are usually smaller than 2 mm $year^{-1}$. However, heavy metal displacement may be relatively fast in acid sandy soils, where K_d values of Cd and Zn are usually below 100 l kg^{-1}.

An example of an extensive pollution caused by atmospheric deposition can be found in the Kempen, at the Dutch-Belgian boundary. Zinc smelters have been active in this region since the end of the 19^{th} century (Figure 1.1). Emissions have been drastically reduced since the 1970's, when a change was made from pyrometallurgical to electrolytic process technology. As a result of the historic emissions, an area of about 280 km^2 is enriched with Cd: the Cd concentration is higher than 1 mg Cd kg^{-1}, while background values for these sandy soils are around 0.3 mg Cd kg^{-1} (Ide, 1992). The soils in this area are mainly acid sandy soils, and therefore vulnerable to heavy metal leaching. At present, elevated concentrations of Cd and Zn in groundwater and surface water are already observed in this region. Mean groundwater concentrations of four fields in the Kempen region were 45 µg Cd l^{-1} and 5.2 mg Zn l^{-1} (Wilkens, 1995), while the maximum permissible concentration (MPC) for groundwater in Flanders is 5 µg Cd l^{1} and 0.5 mg Zn l^{-1}. The groundwater contamination will probably persist for a long time, since large metal amounts are still present in the soil. This thesis focuses on the transport of Cd and Zn in soils in this region.

The mobility of Cd in sandy soils has been the subject of several studies. The transport of Cd is very sensitive to the sorption parameters. The sorption of Cd depends on the soil solution composition, e.g., pH, Ca concentration and the presence of complexing ligands (Temminghoff *et al.*, 1995), and on the soil composition, e.g., organic matter content (Wilkens, 1995). Because of field heterogeneity in soil properties, Cd sorption may vary considerably within one field (Boekhold, 1992). This variation in soil chemical properties should be taken into account when modelling Cd transport at field scale (Seuntjens, 2000).

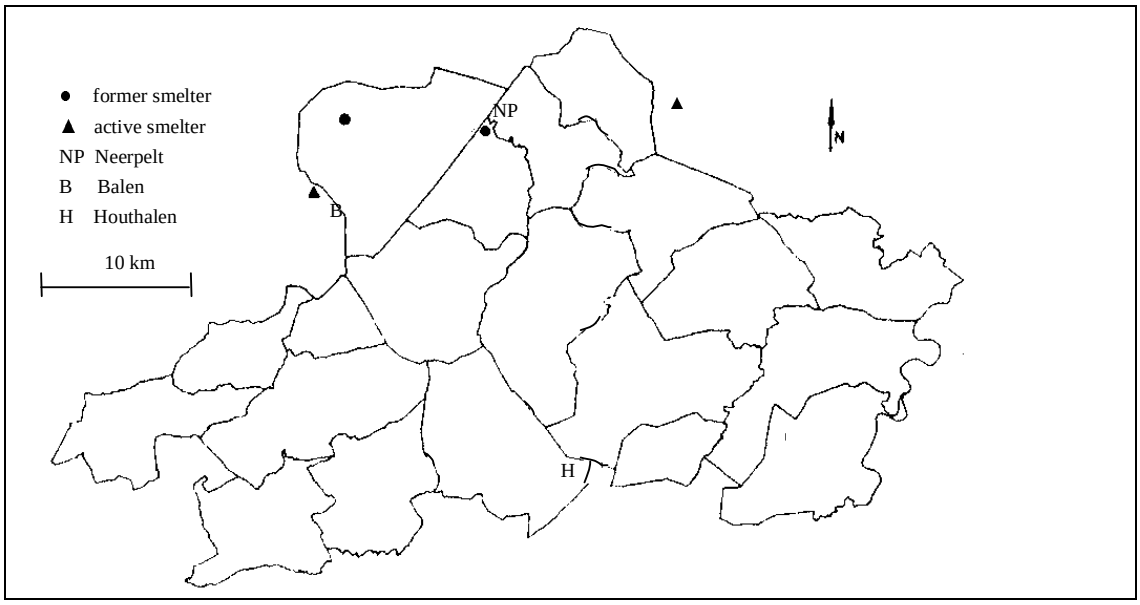

Figure 1.1 Map of the research area (northern part of Belgium), showing the location of the Zn smelters (symbols) and of the experimental fields (letters) (adapted from Ide, 1992)

In spite of the extensive research on Cd transport in soil, some questions remain unanswered. Transport of sorbing solutes in soil is often modelled with the local equilibrium assumption (LEA), but it is not clear whether this is a valid assumption to model transport of Cd and Zn in the field. Non-equilibrium transport of Cd has been observed in column experiments, but these column studies were often conducted at large pore water velocities. Moreover, most column experiments have been carried out with freshly added metal salts. Only few studies have addressed the transport of Cd and Zn in field contaminated soils, where metals have resided in the soil for a long time and have possibly been added in an insoluble form. Another unresolved issue is the effect of acidification on the transport of Cd and Zn. It has been suggested that set-aside of agricultural land contaminated with heavy metals might lead to a strong and sudden increase in leaching of these metals (Stigliani *et al.*, 1993), but until now, little effort has been made to describe quantitatively the effect of afforestation on metal transport.

The objectives of this thesis are to assess the role of reaction kinetics on transport of Cd and Zn in field contaminated soils, and to assess long term effects of soil acidification on leaching of these metals. The effectiveness of liming as a countermeasure will be investigated. Batch and column experiments, and model simulations at the field scale will be used to meet this objectives.

1.2 The solid–liquid distribution of Cd and Zn

The mobility of heavy metals in soil is strongly dependent on the solid–liquid distribution, expressed by the distribution coefficient, K_d (l kg^{-1}):

$$K_d = \frac{M_{tot}}{[M]_{pw}} \quad (1.1)$$

where M_{tot} is the total metal concentration in the solid phase (mg kg^{-1}), and $[M]_{pw}$ is the pore water concentration (mg l^{-1}). The fraction of metals in the solid phase is usually much larger than that in the solution phase and, therefore, the concentration in the solid phase may be approximated by the total metal concentration in the soil. Metals in the solid phase may be adsorbed on the soil surface, or may be precipitated. In most soils, the Cd and Zn concentrations in solution are not controlled by precipitation reactions, since sorption reactions are usually strong enough to keep the solution concentration below the value where precipitates form.

The solid–liquid distribution of Cd and Zn is mainly affected by the pH. Multivariate analyses of K_d values of Cd in topsoils have repeatedly shown that the pH is the most important factor explaining the K_d (e.g., Gerritse and van Driel, 1984; Anderson and Christensen, 1988), with K_d values increasing with a factor 3 to 5 per unit increase in the pH. This evidence suggests competitive binding of free metal ions on pH dependent sorption sites, such as surfaces of oxides or organic matter. Introducing soil organic matter as a second variable improved the regressions in some studies (e.g., Gerritse *et al.*, 1984; Christensen, 1989), but the effect was mostly small, indicating that the sorption site capacity does not vary greatly among soils. Larger concentrations of Ca and of other competing heavy metals lead to a decrease in the distribution coefficient. Christensen (1984) found that a tenfold increase in the Ca concentration reduced the Cd sorption by a factor of 3. Complexation of the metal with inorganic or organic ligands also results in larger solution concentrations, since only the free ion is buffered by the labile pool (see Figure 1.2). E.g., in the presence of 0.02 M Cl^-, about 50% of Cd in solution is present as $CdCl_n^{2-n}$ complexes that do not adsorb (Temminghoff *et al.*, 1995).

Relatively few measurements of the *in situ* K_d (i.e., based on pore water concentrations) have been reported. Römkens and Salomons (1998) measured the *in situ* K_d of Cd, Cu and Zn in 30 unpolluted soils from The Netherlands. De Groot *et al.* (1998) determined *in situ* K_d values of Cd and Zn in 46 Dutch soils, both polluted and unpolluted. Most of the reported K_d values of Cd or Zn, however, are based on adsorption studies in dilute salt

extracts of soils. These K_d values may overestimate the metal mobility *in situ*, because metals in field contaminated soils may be present in non-labile form (Figure 1.2). Metals may be in non-labile form because of ageing reactions that remove metals from the sorption surface to interior sorption sites (section 1.3), or because they entered the soil in a sparingly soluble form. Non-labile metals do not contribute to the immediate solid–solution distribution that occurs between the labile pool on the solid phase and the solution phase. The partitioning between the labile metal pool (M_{lab}, mg kg^{-1}) and solution phase may be expressed by the 'labile' distribution coefficient:

$$K_d^{lab} = \frac{M_{lab}}{[M]_{pw}} \tag{1.2}$$

where M_{lab} is the labile metal concentration on the solid phase (mg kg^{-1}). The K_d^{lab} is smaller than the K_d if the metals are partly in non-labile form:

$$K_d^{lab} = K_d \cdot \frac{M_{lab}}{M_{tot}} \tag{1.3}$$

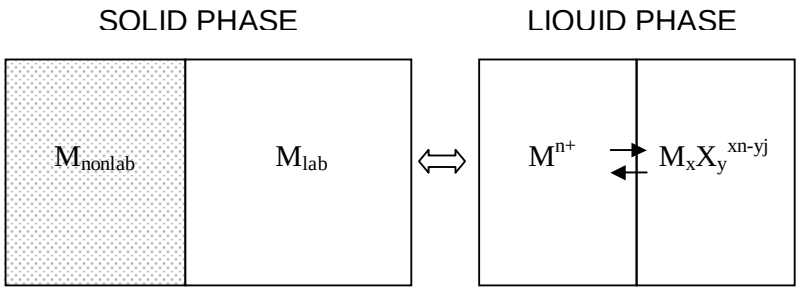

Figure 1.2 Schematic presentation of the solid–liquid distribution. The metals in the liquid phase are present as free ion (M^{n+}) or as complex with a ligand X^{-j}. The metals in the solid phase are in labile (M_{lab}) or non-labile form (M_{nonlab}).

The sorption isotherms of Cd and Zn tend to curve; the metals are held less strongly at large concentrations, because the sites with the strongest affinity are already occupied. As a result, the buffer capacity, which is essentially the slope of the sorption isotherm, is smaller than the labile distribution coefficient (Figure 1.3). At low Cd and Zn concentrations, the sorption isotherms are approximately linear, and in this case, the K_d^{lab} may serve as a reasonable estimate of the buffer capacity.

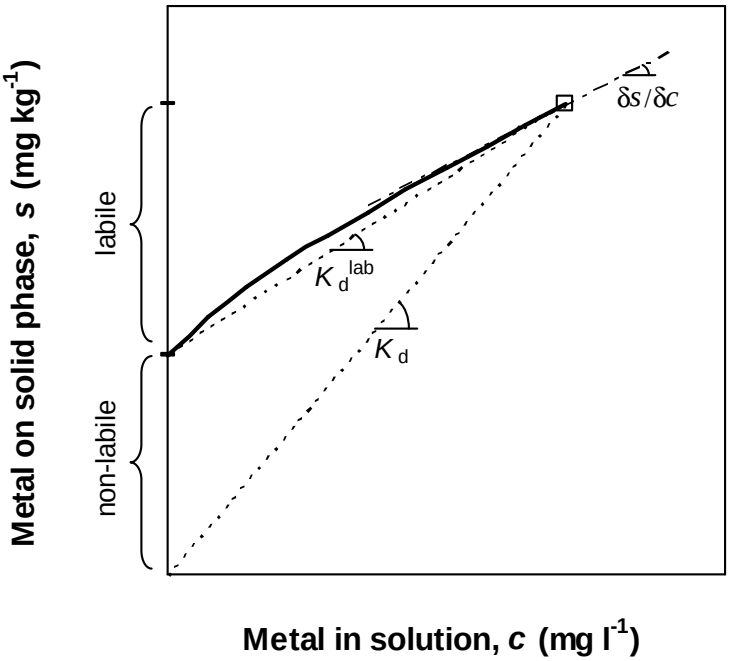

Figure 1.3 A non linear sorption isotherm (full line). The K_d represents the partitioning between the total metal pool and the solution phase, the K_d^{lab} that between the labile pool and solution phase, and $\delta s/\delta c$ gives the buffer capacity for the actual situation ( ).

In this thesis, the isotope dilution technique was used to discriminate between the labile and the non-labile metal pool. A small quantity of a suitable radio-isotope is added to a water or a dilute salt extract, and the specific activity of the metal is measured after a set equilibration time, which allows one to calculate the radio-labile metal concentration (also called *E* value). This technique has been widely used during the last decade to measure labile fractions of Cd and Zn in soils (e.g., Nakhone *et al.*, 1993; Smolders *et al.*, 1999). These studies have shown that fractions labile Cd and Zn may vary over about one order of magnitude. Labile fractions of Zn are generally smaller than those of Cd, indicating that Zn is generally added in a less soluble source and that ageing reactions are more pronounced for Zn than for Cd (Degryse *et al.*, 2003b). A multivariate analysis of *in situ* K_d values of 74 polluted soils demonstrated that the prediction of K_d values of Cd and Zn improved when metals in solution were assumed to be in equilibrium with the (radio-)labile metal pool instead of the total metal pool (Degryse *et al.*, 2003a). However, the improvement was rather small as most of the variation in K_d was explained by pH.

1.3 Reaction kinetics of metals in soil

Metals added to soil adsorb fast on the soil surface. The reaction of metals with the soil surface may be described with first-order kinetics:

$$\frac{\delta s}{\delta t} = k_f c - k_r s \tag{1.4}$$

where s is the concentration on the solid phase (mg kg^{-1}), c is the solution concentration, (mg l^{-1}), t is the time (d), k_f is the forward first order rate constant (l kg^{-1} d^{-1}) and k_r is the backward first order rate constant (d^{-1}). The response time, T_c, for this reaction is defined as:

$$T_c = \frac{1}{\frac{\rho}{\theta} \cdot k_f + k_r} \tag{1.5}$$

where ρ is the soil bulk density (kg l^{-1}) and θ is the volumetric soil water content. The response time defines the time needed for the partitioning components to reach 63% of their equilibrium value (Honeyman and Santschi, 1988). Since the response time for the sorption reaction between labile pool and solution is fast (in the order of minutes), instantaneous equilibrium between the labile pool and solution phase is often assumed (cf section 1.4.2), as is illustrated in Figure 1.4.

The initial fast reaction is followed by a slow reaction that removes the metal from the labile pool into a pool from which desorption is slow, a process often referred to as 'fixation'. Slow reactions have been demonstrated by a decrease in the solution concentration of metals with time (e.g., Barrow, 1986). Evidence for ageing reactions was also found by prolonged isotope exchange studies in soil, up to 15 days (e.g., Tiller *et al.*, 1972; Sinaj *et al.*, 1999). The slow reactions of metals in soil may be related to diffusion in sesquioxides. Bruemmer *et al.* (1988) modelled the sorption of Cd, Zn and Ni on goethite with a model that assumed adsorption on external surface sites, followed by solid-phase diffusion to internal binding sites. Trivedi and Axe (2000) studied the sorption of Cd and Zn on hydrous oxides of Al, Fe and Mn. Both studies indicated that the slow reactions are more pronounced for Zn than for Cd. Transfer from the labile to the non-labile pool may also be modelled with reversible first-order kinetics (Figure 1.4):

$$\frac{ds_2}{dt} = k_1 s_1 - k_{-1} s_2 \tag{1.6}$$

where s_1 is the metal concentration on the solid phase in equilibrium with the solution phase (equivalent to M_{lab}), s_2 is the concentration of non-labile metals, t is the time, and k_1 and k_{-1} are the forward and backward first order rate constants.

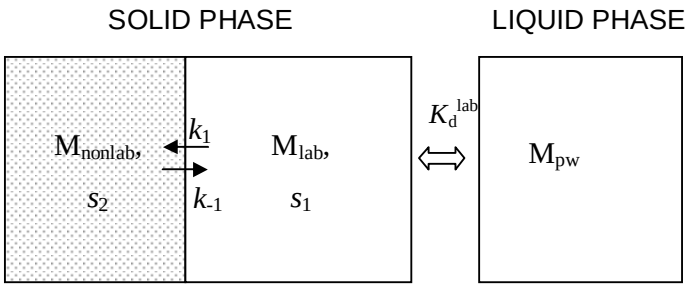

Figure 1.4 Schematic representation of the kinetic sorption model (see text).

If s_2 is initially zero (all metals labile at t=0), the solution for equation 1.6 is:

$$\frac{s_2}{s} = (1 - f) \cdot (1 - \exp(-\frac{t}{T_c})) \tag{1.7}$$

where s is the total metal concentration (s=s_1+s_2), f is the fraction of metals in labile form when equilibrium is reached, and T_c is the response time:

$$T_c = \frac{1}{k_1 + k_{-1}} \tag{1.8}$$

$$f = \frac{k_{-1}}{k_1 + k_{-1}} = k_{-1} \cdot T_c \tag{1.9}$$

Young *et al.* (2001) measured the decrease in E values of Cd and Zn with time in 24 soils amended with Cd and Zn salts in a laboratory incubation experiment. The decrease in the radio-labile fraction of Zn was reasonably well described by reversible first-order kinetics, with T_c in the order of 200 days, and the fraction f dependent on pH. The labile fraction of Zn at the end of the experiment (t=818 days) was around 0.35 at pH 6.5, and around 0.5 at pH 5. The decrease in E values of Cd was much smaller.

Theoretically, the decrease in the labile metal concentration will result in a decrease in the pore water concentration, all other parameters that affect the K_d^{lab} (e.g., pH) staying equal. In other words, the (total) K_d will increase with time (Figure 1.5).

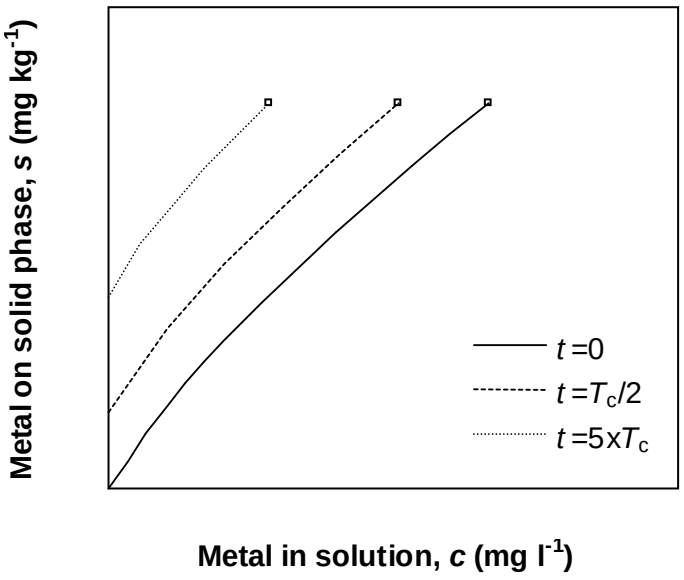

Figure 1.5 The change in solid–liquid distribution as a result of ageing reactions (f=0.5, model explained in text).

1.4 Effects of sorption kinetics on solute transport

1.4.1 Transport models

The solute transport in case of local equilibrium can be described by the convection-dispersion equation:

$$\frac{\delta c}{\delta t} + \frac{\rho}{\theta} \cdot \frac{\delta s}{\delta t} = D \frac{\delta^2 c}{\delta z^2} - v \frac{\delta c}{\delta z} \qquad (1.10)$$

where c is the solution concentration (mg l^{-1}), s is the concentration on the solid phase (mg kg^{-1}), ρ is the soil bulk density (g cm^{-3}), θ is the volumetric water content (cm^3 cm^{-3}), D is the dispersion coefficient (cm^2 d^{-1}), v is the pore water velocity (cm d^{-1}), t is the time (days), and z the distance (cm).

The local equilibrium assumption (LEA) may not hold if the rate of the concentration change due to sorption reactions is slow in comparison with the rate of the flow-induced concentration change. Non-equilibrium models have been developed that consider time-dependent sorption (e.g., van Genuchten and Wagenet, 1989). In the one-site model (Figure 1.6), the sorption between liquid and solid phase is described by first-order kinetics (eq. 1.4). Alternatively, equation 1.4 can be written as:

$$\frac{\delta s}{\delta t} = \alpha \cdot (K_d \cdot c - s) \tag{1.11}$$

where α is the first order rate coefficient (equal to k_r), and K_d the equilibrium distribution coefficient (l kg^{-1}):

$$K_d = \frac{k_f}{k_r} \tag{1.12}$$

where k_f is the forward first order rate constant (l kg^{-1} d^{-1}) and k_r is the backward first order rate constant (d^{-1}).

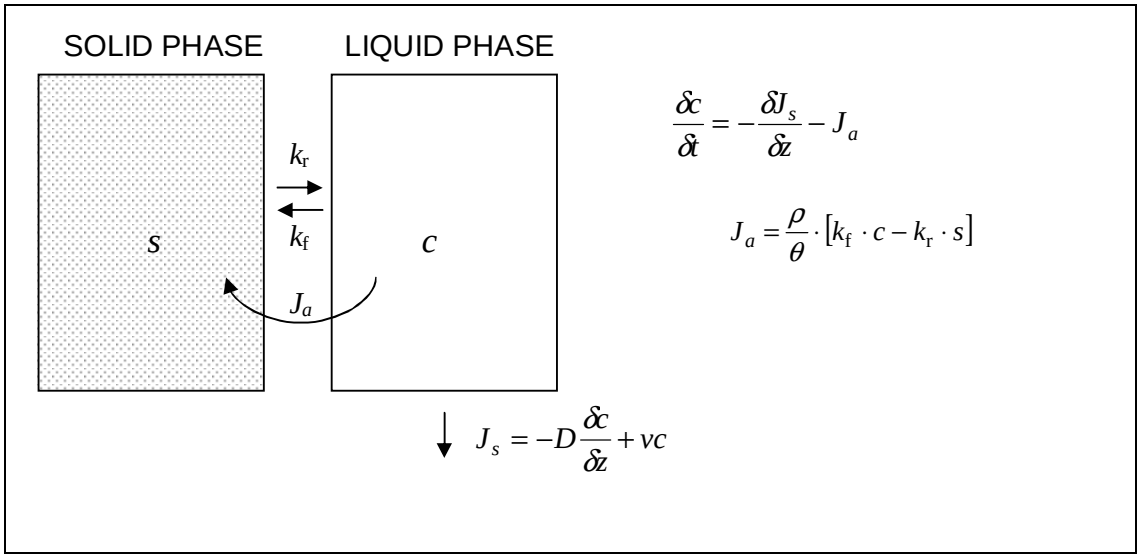

Figure 1.6 Schematic representation of the one-site model (adapted from van Genuchten and Wagenet, 1989). J_a is the sorption rate from the solution to the solid phase (mass per volume per time), and J_s is the solute flux (mass flowing per area per time)

The two site model (Figure 1.7) distinguishes type-I sites, on which the sorption is instantaneous, and type-II sites, on which sorption is time-dependent:

$$s_1 = f \cdot K_d \cdot c = K_d^{\,lab} \cdot c \tag{1.13}$$

$$\frac{\delta s_2}{\delta t} = k_f \cdot c - k_r \cdot s_2 \tag{1.14}$$

where f is the fraction of exchange sites in equilibrium with the solution phase. Alternatively, equation 1.14 can be written as

$$\frac{\delta s_2}{\delta t} = \alpha[(1 - f) \cdot K_d \cdot c - s_2] \tag{1.15}$$

This parallel model is conceptually different from the serial model presented in Figure 1.4. However, these two models are mathematically equivalent. It can be shown that the rate constants of the two models are related as follows:

$$k_{-1}=k_r \tag{1.16}$$

$$k_1 = \frac{k_f}{f \cdot K_d} \tag{1.17}$$

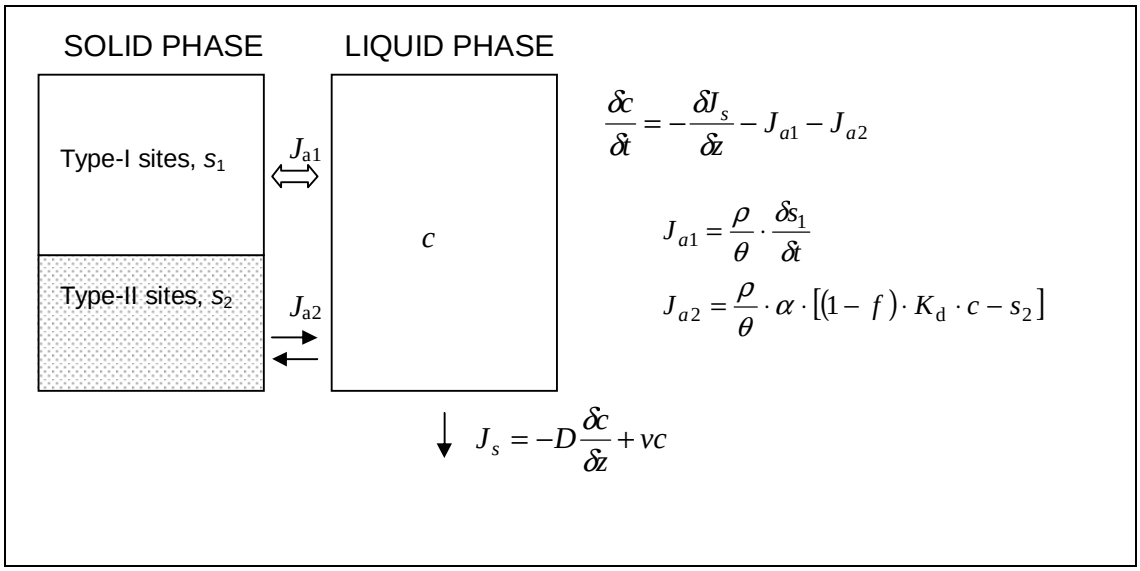

Figure 1.7 Schematic representation of the two-site model (adapted from van Genuchten and Wagenet, 1989). J_{a1} and J_{a2} are the sorption rates from the solution to the type-I sites and type-II sites, respectively, and J_s is the solute flux.

Criteria to assess the validity of the LEA have been derived by a number of researchers (e.g., Valocchi, 1985; Bahr and Rubin, 1987). Valocchi (1985) used ε_n, the fractional change in the n^{th} central time moment (μ_n), as an indicator of the error associated with the use of the LEA:

$$\varepsilon_n = \frac{\mu_n{}^K - \mu_n{}^E}{\mu_n{}^E} \tag{1.18}$$

where superscripts K and E refer to the kinetic (one-site) and equilibrium models respectively. The fractional change (due to non-equilibrium) in the 2nd central moment μ_2, which gives the spreading of the breakthrough curve, for a Dirac (impulse) imput, was shown to be:

$$\varepsilon_2 = \frac{v \cdot T_c}{\lambda} \cdot \frac{1}{1 + \dfrac{\theta}{\rho \cdot K_d}} \tag{1.19}$$

where T_c is the response time (see eq. 1.5), and λ is the dispersion length ($\lambda = D/v$). For strongly sorbing solutes ($\theta/\rho/K_d << 1$), equation 1.19 can be written as:

$$\varepsilon_2 \cong \frac{v \cdot T_c}{\lambda} \tag{1.20}$$

Equation 1.20 implies that the error associated with the use of a LEA model will become larger as the pore water velocity v increases and the response time of the sorption reaction increases (i.e., the reaction is slower). When $\varepsilon_2 < 0.1$, the breakthrough curve (for a Dirac input) is reasonably described with the LEA, as is illustrated in Figure 1.8.

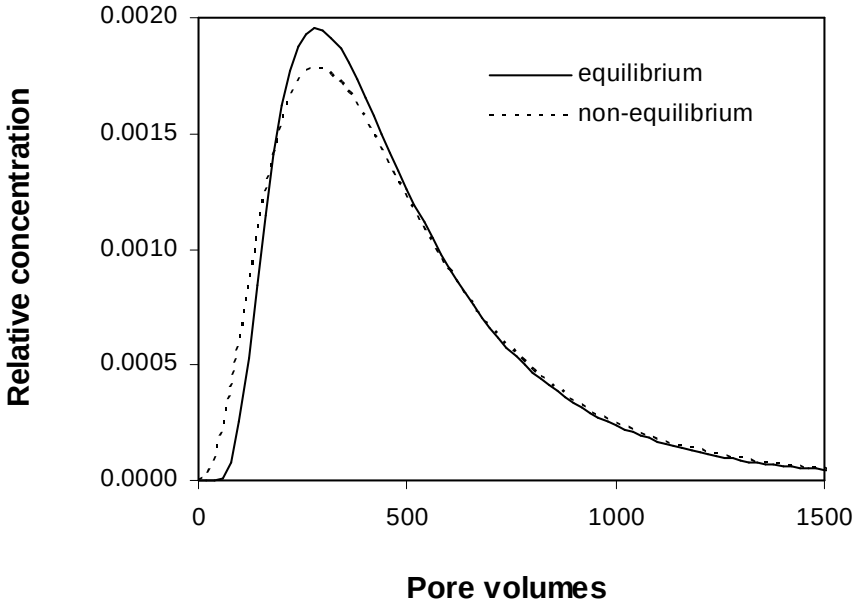

Figure 1.8 Comparison of an equilibrium and a non-equilibrium breakthrough curve (ε_2=0.1). The equilibrium breakthrough was calculated with the convection-dispersion equation (Dirac impulse, v = 10 cm d^{-1}, L = 5 cm, λ = 1 cm, K_d = 100 l kg^{-1}, ρ/θ = 5 kg l^{-1}), and the non-equilibrium breakthrough was calculated with a chemical non-equilibrium model (T_c = 0.01 d, other parameters as for the equilibrium model).

1.4.2 Transport of Cd and Zn

Instantaneous equilibrium between the labile pool and solution phase may be assumed if the sorption reaction between labile pool and solution is fast relative to the rate of convective transport. The technique of diffusive gradients in thin-films (DGT) has been used to estimate the response time for the sorption reaction between the solution and the labile pool (Ernstberger *et al.*, 2002). Values in the order of 5 minutes (0.003 d) were derived for Cd and Zn. Thus, if λ=1 cm, the breakthrough curve (for a Dirac impulse) would be reasonably (ε_2 < 0.1) described based on the LEA for pore water velocities smaller than 30 cm d^{-1}. Several transport studies where non-equilibrium in the transport of freshly added Cd was observed, were conducted at large pore water velocities, in the order of 50 cm d^{-1} and more (e.g., Kookana *et al.*, 1994; Boekhold and van der Zee, 1992). The non-equilibrium observed in these studies was probably related to the large water fluxes used. Pore water velocities in the field are usually smaller than 1 cm d^{-1}. Therefore, the transport at the field scale (Part 3) was modelled assuming that (radio-)labile Cd and Zn are in equilibrium with the solution phase.

The non-labile pool is a much more slowly reacting pool. The metals in this pool are less available because of ageing reactions, or because they were added as an insoluble source. Therefore, predicting the transport of Cd and Zn with the (total) K_d will probably result in an overestimation of the metal amount leached to the groundwater within a certain time period for field contaminated soils. However, though non-labile metals are often considered as being fixed, it cannot be excluded that these metals may be mobilized with time (e.g., by diffusion out of oxides or dissolution of mineral phases).

1.5 Thesis outline

The thesis outline is illustrated in Figure 1.9. The objectives of this thesis are to assess the role of reaction kinetics on transport of Cd and Zn in field contaminated soils, and to assess the effect of soil acidification on Cd transport at field scale. Batch experiments (Part 1), column studies (Part 2) and model simulations at the field scale (Part3) are used to meet this objectives.

The distribution of Cd and Zn between the solid phase and the soil solution (Part 1) is a key issue in the prediction of solute transport in soil. In Chapter 2, the isotope dilution

technique was used to discriminate between the labile and non-labile pool. The fraction that is isotopically exchangeable within the equilibration time (3 days) is – by definition – (radio)labile. Chapter 3 and 4 focus on the solid–liquid distribution of Cd and Zn between the labile pool and the solution phase. The effects of soil and soil solution characteristics on the distribution of Cd and Zn were quantified in Chapter 3. Chapter 4 discusses an incubation experiment where the effect of liming on pore water concentrations of Cd and Zn was studied.

In the second part, the transport of Cd and Zn was studied in column experiments with disturbed (sieved) soil. Chapter 5 describes the transport at various pore water velocities in a field contaminated soil and in a soil where Cd and Zn were freshly added to the soil (and therefore fully labile). In Chapter 6, the effect of liming on the transport of Cd and Zn was studied, while the effect of acidification was assessed in Chapter 7. Transport calculations were made with the LEA assuming that only the radio-labile Cd and Zn fractions are in equilibrium with the solution phase, or assuming that the total amount of Cd and Zn on the solid phase is in equilibrium with the solution. In Chapter 6, the transport was also modelled with a two-site model (Figure 1.7) where labile Cd and Zn were considered to be in equilibrium with the solution and non-labile metals were considered to be subject to kinetic desorption. Pore water velocities used in the column experiments (6–30 cm d^{-1}) were relatively small in comparison with most experiments reported in the literature, but still twentyfold higher than the averaged pore water velocity in the field (~ 1m y^{-1}). The larger pore water velocities in the column experiments are necessary to obtain meaningful observations within a reasonable time period (in the order of months).

The third part discusses the transport of Cd and Zn at field scale. In Chapter 8, the transport in an acid sandy soil was studied. To assess the validity of the local equilibrium assumption, wick samplers were installed in the field, and the 'flux' concentrations (measured in the solution collected by the wicks) were compared with concentrations in soil solutions obtained by centrifugation. A reconstruction of the present-day Cd profiles was made by retrospective modelling, and modelled and observed profiles were compared. Chapter 9 investigates the effect of the set-aside of polluted agricultural land on the Cd transport. Special attention was paid to the effect of field heterogeneity.

Distribution of Cd and Zn between solid phase and solution phase (Part I, Chapters 2–4)

Which parameters control the solid–liquid distribution of Cd and Zn ?

↓

Transport of Cd and Zn in sandy soils

	In laboratory columns (Part II) →	At the field scale (Part III)
No change in pH:	Chapter 5 - *Is the LEA valid for modelling transport of Cd and Zn at moderate pore water velocities?* - *Is the transport of Cd and Zn better predicted when using radio-labile concentrations?*	Chapter 8 - *Is the LEA valid for modelling transport of Cd and Zn at field scale?* - *For how long and in which concentrations will Cd and Zn leach to the groundwater in a field with acid sandy soils?*
Liming :	Chapter 6 - *Can non-labile Cd and Zn be mobilized?* - *Does liming decrease metal concentrations in the leachate?*	Chapter 8 (section 8.3.5) - *Is liming a possible method to reduce leaching of Cd and Zn to the groundwater?*
Acidification:	Chapter 7 - *Does acidification result in mobilisation of Cd?*	Chapter 9 - *Will the set-a-side of polluted agricultural land result in a large increase in Cd leaching?* - *Must field heterogeneity be taken into account when predicting solute transport at the field scale?*

Figure 1.9 Schematic representation of the thesis outline and the questions addressed (in italic)

1.6 Experimental fields

The soils used were sampled on four fields (see Figure 1.1). Three fields are situated in northern Belgium, in a region that is contaminated with heavy metals. The other field is situated in Houthalen, about 25 km southwards from this region, outside the sphere of influence of the Zn smelters.

The field in Balen (description in Chapter 2) is located at a distance of about 1 to 2 km east from a Zn smelter. Total Cd concentrations in the upper horizon are in the order of 1 mg Cd kg^{-1}. The soils are acid sandy soils (Placohumod).

The soils of the field in Houthalen (description in Chapter 2) are also classified as Placohumod. The field is further referred to as 'unpolluted'. This term should not be interpreted literally, since this field may also be slightly enriched with heavy metals (see section 1.1).

The two other fields are situated in Neerpelt, about 2 km north-east from a Zn smelter that was operative until 1995. One of these fields (description in Chapter 9) has been used as agricultural land until 1992. The other field (description in Chapter 3) has been used as arable field in the 1970s for some years. The soils in both fields are classified as typic Haplaquod.

Part I

Distribution of Cd and Zn in soils

CHAPTER 2

Vertical distribution and speciation of cadmium and zinc in polluted and unpolluted Spodosols

Abstract

The historic emission of Cd and Zn from non-ferrous metal smelters has contaminated soils in a large area of northern Belgium. A survey was conducted to assess the vertical distribution and speciation of these metals. Spodosol profiles were sampled in the contaminated area and in an uncontaminated field as a reference. Average metal concentrations in the upper horizon were 0.2 mg Cd kg^{-1} and 9 mg Zn kg^{-1} in the unpolluted field, and 0.8 mg Cd kg^{-1} and 71 mg Zn kg^{-1} in the contaminated field. In the unpolluted field, the total Cd concentrations were larger in the surface horizon than in the deeper horizon, whereas the reverse was true for Zn. This may be related to an accumulation of Cd and a loss of Zn. Mass balance analyses did not allow to give a decisive answer as to the net metal balance.

The isotope exchange technique was used to measure radio-labile Cd and Zn concentration (*E* value). The %*E* values (*E* value relative to *aqua regia* soluble metal) of Cd were generally larger than 50%, while %*E* values of Zn were mostly smaller than 50%. The smallest %*E* values of Zn were found in the deeper horizons, where Zn is probably enclosed in mineral lattices. The %*E* values of Zn were smaller in the upper horizons of the contaminated soil than in those of the unpolluted soil, indicating that Zn in the contaminated soil was added as an insoluble Zn source. The *E* values of Cd and Zn correlated well with organic matter content.

2.1 Introduction

Sandy soils at the Dutch-Belgian border (the 'Kempen') are contaminated with Cd and Zn by atmospheric deposition of Zn smelters, that have been active in this region since the second half of the 19th century. At present, primary Cd emissions are almost eliminated due to improved technology. Removal of heavy metals by leaching is usually slow, since these metals are strongly sorbed by the soil (e.g., Černík *et al.*, 1994). However, soils in the 'Kempen' area are mainly acid sandy soils, and, as a result, Cd and Zn are relatively mobile in these soils.

The transport of Cd and Zn can be assessed with solute transport models that typically rely on sorption parameters obtained from adsorption isotherms. This approach may be successful in describing the transport of freshly added Cd and Zn salts (e.g., Christensen, 1985). However, metals in polluted soils may originate from sparingly soluble components (e.g., Roberts *et al.*, 2002), that are less mobile than metal salts. In addition, slow immobilization reactions may result in increased fixation of metals with time (Bruemmer *et al.*, 1988). Extractants have been used to determine the amount of metal participating in sorption–desorption processes. Streck and Richter (1997b) used the EDTA (0.025 M)-extractable Cd and Zn to measure this available fraction of Cd and Zn in a sandy soil. The isotope dilution method is a conceptually attractive method to discriminate between labile and non-labile metals in soil. A small quantity of a suitable radio-isotope (as metal salt) is added to a soil sample suspended in water or a dilute salt extract, and the specific activity of the metal is measured after a set equilibration time. This measurement allows calculating the radio-labile metal concentration, i.e., the amount of metal that is in equilibrium with the solution within this equilibration time. Radio-labile fractions of Cd or Zn have been measured in soils polluted by sewage sludge, mine spoil and smelting, in soils amended with metal salts and in soils with background values of Cd and Zn (e.g., Nakhone and Young, 1993; Smolders *et al.*, 1999; Tye *et al.*, 2003). Labile fractions of Zn were generally smaller than those of Cd, indicating that Zn is generally added in a less soluble form or that ageing reactions are more pronounced for Zn than for Cd. Only a few studies have used the radio-labile metal concentration to predict metal solubility in soil (e.g., Tye *et al.*, 2003). The prediction of the solid–solution distribution of Cd and Zn, using linear regression equations with soil properties, improved when using radio-labile instead of total metal concentrations (Degryse *et al.*, 2003a).

In this study, we measured total and labile concentrations of Cd and Zn in Spodosol profiles of an unpolluted field and a field contaminated by atmospheric deposition of heavy metals. A desorption experiment was carried out to assess whether the radio-labile fraction corresponds to the amount of metal that can be desorbed. The polluted and unpolluted field were compared in terms of the labile fractions of Cd and Zn, and of the distribution of Cd and Zn within the soil profile.

2.2 Materials and methods

2.2.1 Soils and soil characterisation

Soils were sampled in a polluted and an unpolluted area in northern Belgium. The uncontaminated field is located in Houthalen, and is part of a nature reserve (Tenhaagdoornheide). The main vegetation is heath (*Calluna vulgaris*) and grass (*Molinea caerulea*). The contaminated area is situated in Balen, in the 'Kempen' at the Dutch-Belgian border. This area is contaminated with Cd and Zn because of atmospheric deposition by Zn factories during more than 100 years. The area is an old land dune area, mainly covered with grasses (*Molinea caerulea, Festuca ovina*).

Soils were sampled in 2000, to the depth of the groundwater table or to a depth of 4 m. Six profiles were sampled in the unpolluted field, over an area of about 4 ha, and ten profiles were sampled in Balen over an area of about 100 ha. The samples were taken with an Edelman screw auger, at 5 or 6 depths according to the pedological division.

The soils were sieved (< 2 mm) and air-dried at room temperature. The cation-exchange capacity (CEC) was measured at the soil pH with silverthiourea as index cation (Chhabra *et al.*, 1975). The organic C content was measured by dry combustion (Skalar CA 100). The pH was determined in 0.01 M $CaCl_2$ in a soil:solution ratio of 1:10 kg l^{-1} after 3 days of equilibration. The 'total' metal concentration was determined by *aqua regia* digestion. Amorphous Fe and Al oxides were measured by extraction with ammonium oxalate-oxalic acid (Schwertmann, 1964).

2.2.2 Measurement of radio-labile metal

The labile Cd and Zn in soil was measured by isotopic exchange. Duplicate samples of 2.5 g soil were weighed in polypropylene centrifugation tubes, 25 ml of a 0.01 M $CaCl_2$ solution was added, and the suspensions were spiked with between 0.25 and 0.35 ml carrier-free ^{109}Cd (~ 4000 Bq ml^{-1}) and ^{65}Zn (~ 7000 Bq ml^{-1}). The suspensions were shaken end-over-end for 3 days. The tubes were centrifuged at 3000 *g* (10 or 20 minutes) and two 5-ml samples were removed from each tube. The γ-activity of ^{109}Cd (energy window: 15-40 keV) and ^{65}Zn (1000-1200 keV) was measured (Minaxi, 5530 auto Gamma) on one sample. The other sample was acidified to pH 1 with HNO_3, prior to analysis of stable Cd and Zn with ICP-OES, or with graphite furnace atomic absorption spectrophotometry (GFAAS) if the Cd concentration was smaller than 5 µg l^{-1}. The radio-labile concentration (E, mg kg^{-1}) of Cd and Zn was calculated as

$$E = [M]\,(K_d^{*} + \frac{V}{W}), \qquad (2.1)$$

where $[M]$ is the Cd or Zn concentration (mg l^{-1}) in the supernatant, K_d^{*} is the distribution coefficient of the radioisotope (l kg^{-1}), V is the volume of solution (l), and W is the mass of soil (kg). The $\%E$ value is the E value relative to the total metal concentration (M_{tot}):

$$\%E = \frac{E}{M_{tot}} \cdot 100 \qquad (2.2)$$

The effect of electrolyte composition ($Ca(NO_3)_2$ 0.5 to 10 mM, $CaCl_2$ 0.5 to 10 mM, $NaNO_3$ 1.5 to 30 mM), of supernatant filtration (0.45 µm), and of equilibration time (1-18 days) was examined for 3 soil samples.

2.2.3 Desorption isotherms

Desorption isotherms were carried out on a topsoil from Balen in 10^{-3} M $CaCl_2$, by measuring Cd and Zn concentrations in solution at different soil:solution ratios. Filius *et al.* (1998) have shown that desorption isotherms of metals determined by this technique are in good agreement with isotherms determined by repeated extraction.

The soil:solution ratios ranged from 5 to 460 l kg^{-1}. The soil was weighed into a dialysis bag (Visking 12-14000 Daltons, Medicell, London), and 5 ml of a 10^{-3} M $CaCl_2$ solution was added. The dialysis bag was transferred in the remaining $CaCl_2$ solution. Concentrations of Cd and Zn in the equilibrium solution were measured with ICP-OES after 2 days of end-over-end shaking. The same experiment was also carried out with 7 days equilibration time.

2.3 Results and discussion

2.3.1 Effect of experimental conditions on *E* values

Supernatant filtration had no significant effect (P>0.05) on solution concentrations (Table 2.1) and *E* values of Cd and Zn, measured in 0.01 M $CaCl_2$ (data not shown). Young *et al.* (2000) found no effect of filtration over 0.2 µm on *E* values of Cd measured in 0.1 M $Ca(NO_3)_2$. Sinaj *et al.* (1999) found that filtration over 0.2 µm was necessary to remove colloidal Zn. However, they measured *E* values in a water extract, while *E* values in this study were determined in 0.01M $CaCl_2$, in which colloidal particles are (more) flocculated.

Table 2.1 Effect of filtration (<0.45 µm) on solution concentration of Cd and Zn in the 0.01 M $CaCl_2$ extract used for the determination of *E* values. Standard deviation of 2 replicates in parentheses.

	Cd_{sol} (µg l^{-1})		Zn_{sol} (mg l^{-1})	
	filtered	unfiltered	filtered	unfiltered
Neerpelt [a]	212 (0.5)	211 (2.4)	14.5 (0.14)	14.4 (0.14)
Houthalen	10.4 (0.03)	10.2 (0.4)	0.37 (0.02)	0.31 (0.02)
Balen	23.4 (0.29)	23.7 (0.01)	0.24 (0.01)	0.22 (0.03)

[a] soil from contaminated field (description in Chapter 3)

The *E* values of Cd and Zn were measured in $Ca(NO_3)_2$, $CaCl_2$ and $NaNO_3$ at ionic strengths of 1.5 mM to 30 mM. No effect of the electrolyte composition on the *E* values was observed (details not shown), although the solid–liquid distribution coefficient of the Cd and Zn isotopes differed strongly between the different solutions.

Little change (<10%) in solution concentrations and *E* values of Cd and Zn was found between 1 and 18 days of equilibration. Smolders *et al.* (1999) and Young *et al.* (2000) also found little change in *E* values of Cd beyond 1 day of equilibration. Sinaj *et al.* (1999) found an increase in the *E* value of Zn with 50% for two soils with pH 5.9 and 6.6 and an increase with 80% for a soil with pH 7.2 between 1 day and 15 days of equilibration. The more pronounced effect of equilibration time in the latter study may be related to the use of a water extract (instead of a $CaCl_2$ or $Ca(NO_3)_2$ extract).

2.3.2 Comparison between *E* value and desorbable Cd and Zn

Desorption isotherms obtained by widening the soil:solution ratio showed that a fraction of Cd and Zn could not be extracted. This fraction corresponded well with non-labile fraction determined by isotopic dilution (see Figure 2.1).

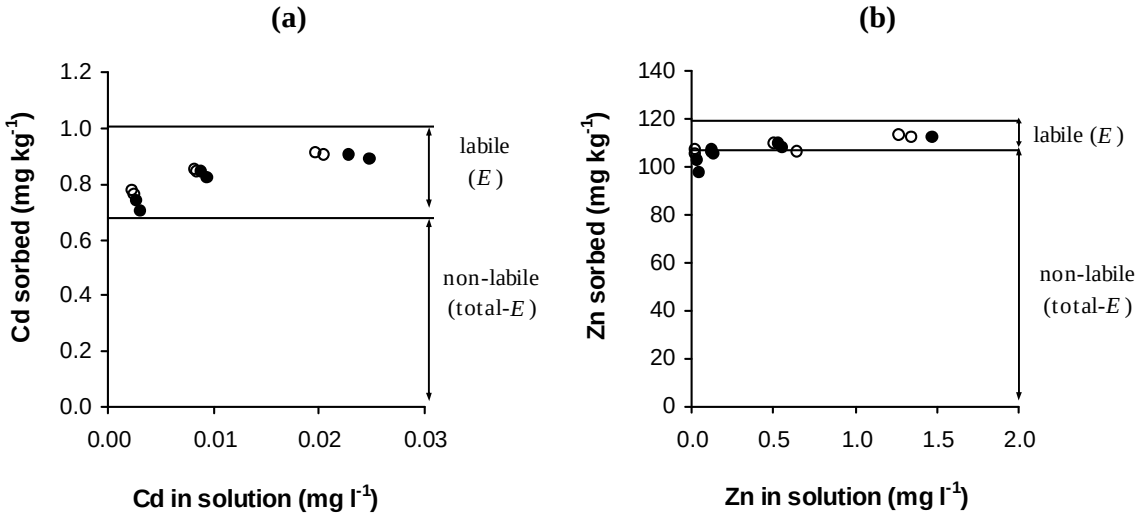

Figure 2.1 Desorption isotherms (in 10^{-3} M $CaCl_2$) of a sandy soil with pH 3.9 obtained by widening soil:solution ratio for (a) Cd and (b) Zn, after 2 days (open circles) or 7 days of equilibration (full circles). Labile and non-labile metal concentrations, as determined by isotopic dilution, are indicated by the horizontal lines.

Differences between the isotherms obtained after 2 days and after 7 days of equilibration were small, indicating fast exchange reactions in these low pH soils. Filius *et al.* (1998) found also little change in desorption isotherms of Cd between 2 and 50 days of equilibration in a low pH soil (pH 4.7), while there was a clear difference in soils with higher pH.

Desorption of metals from polluted soils is the first step in leaching of these metals. The presence of a metal fraction that cannot be extracted, and which is in agreement with the non-labile metal pool, suggests that labile metal concentrations rather than total metal concentration should be used to predict metal leaching in soil.

2.3.3 Soil characteristics

A full description of the soil characteristics can be found in Appendix A.I (Houthalen) and A.II (Balen). For both fields, the soils are classified as dry podzols (typic Humod). The main soil characteristics are summarized in Table 2.2. Total Cd and Zn concentrations in the soil from Houthalen are within the background range for sandy soils in Flanders (Tack *et al.*, 1997). The soil from Balen is enriched with heavy metals due to atmospheric deposition of heavy metals from the nearby smelter.

Table 2.2 Soil properties, total and labile concentrations (*E*) of Cd and Zn for the soils of Houthalen and Balen. Values are averages for 6 (Houthalen) or 10 (Balen) profiles (standard deviations between brackets).

Horizon [a]	pH	OC	Fe_{ox} [b]	Cd_{tot}	Zn_{tot}	E_{Cd}	E_{Zn}	$\%E_{Cd}$	$\%E_{Zn}$
		%	mmol kg^{-1}	mg kg^{-1}					
Houthalen									
A	3.27	3.35	18.5	0.18	9.4	0.11	4.46	62	46
	(0.08)	(1.31)	(7.8)	(0.07)	(4.7)	(0.05)	(3.14)	(8)	(12)
E	3.32	2.24	15.8	0.17	4.5	0.12	2.13	72	49
	(0.08)	(0.70)	(5.5)	(0.07)	(2.1)	(0.06)	(1.00)	(11)	(14)
B_h	3.70	1.38	30.8	0.15	6.3	0.13	1.88	85	32
	(0.19)	(0.80)	(10.4)	(0.07)	(2.9)	(0.07)	(1.04	(15)	(14)
BC	4.00	0.38	11.4	0.03	9.5	0.03	1.09	104 [c]	12
	(0.09)	(0.20)	(4.9)	(0.03)	(2.5)	(0.02)	(0.42)	(27)	(5)
C_1	4.00	0.15	8.9	0.02	10.6	0.02	1.21	106 [c]	11
	(0.02)	(0.06)	(6.3)	(0.01)	(4.4)	(0.01)	(0.67)	(25)	(3)
C_2	3.95	0.10	6.4	0.01	13.3	0.01	1.85	108 [c]	16
	(0.13)	(0.04)	(1.0)	(0.01)	(4.7)	(0.01)	(0.40)	(14)	(7)
Balen									
A	3.70	2.57	26.9	0.82	70.7	0.42	10.9	50	19
	(0.17)	(0.59)	(14.8)	(0.40)	(43.0)	(0.33)	(6.8)	(21)	(11)
E	3.85	1.57	24.0	0.73	27.1	0.52	7.2	80	31
	(0.24	(0.90)	(21.9)	(0.84)	(25.0)	(0.60)	(9.6)	(24)	(21)
B_h	3.96	1.58	29.8	0.94	19.9	0.81	10.1	90	39
	(0.31	(1.10)	(19.0)	(0.86)	(17.9)	(0.78)	(17.2)	(16)	(25)
BC	4.18	0.85	10.9	0.24	11.4	0.21	3.2	91	25
	(0.20	(1.22)	(7.0)	(0.24)	(4.8)	(0.21)	(4.3)	(15)	(22)
C_1	4.27	0.28	6.3	0.22	14.4	0.20	4.5	91	20
	(0.17	(0.41)	(6.0)	(0.48)	(9.9)	(0.44)	(9.3)	(19)	(21)
C_2	4.35	0.13	3.7	0.07	10.8	0.07	2.5	89	24
	(0.12)	(0.10)	(1.7)	(0.09)	(5.7)	(0.08)	(1.3)	(11)	(11)

[a] approximately (not all profiles showed clear podzolisation)
[b] ammonium oxalate extractable Fe
[c] %*E* values > 100 probably because of inaccuracy in total Cd determination at these low concentrations

The soil pH increases with depth, as was also observed by Ronse *et al.* (1988) who found that the pH decreased about 0.6 pH units in the upper layer of sandy soils in the Kempen region between 1960 and 1985. The organic matter content and Fe oxide content are largest in the upper horizons and, as a result, these variables are positively correlated with each other and negatively correlated with pH (Table 2.3).

Table 2.3 Correlation coefficients between soil characteristics

	Houthalen				Balen			
	pH	%OC	Fe_{ox}	Al_{ox}	pH	%OC	Fe_{ox}	Al_{ox}
pH	1				1			
%OC	-0.81	1			-0.81	1		
Fe_{ox}	-0.27	0.48	1		-0.55	0.68	1	
Al_{ox}	0.37	-0.08	0.63	1	-0.09	0.26	0.63	1

Total and radio-labile Cd concentrations are positively correlated with organic matter content and with Fe oxide content (Table 2.4). The correlation between Zn concentrations and organic matter content is much larger when using radio-labile instead of total concentrations (Table 2.4, Figure 2.2b). The strong correlation between organic C content and labile metal concentrations suggests that labile Cd and Zn are mainly associated with organic matter in these soils. Weng *et al.* (2001) used a multi-surface model to evaluate the contribution of various sorption surfaces to the control of heavy metal activities in sandy soils. Their results also indicated the important role of organic matter for binding of heavy metals in sandy soils with low pH. Total Zn concentrations are much less correlated with organic C content than the labile concentrations. Non-labile Zn is presumably enclosed in primary minerals of the parent material, or – in the topsoil of the polluted soil – in Zn-bearing minerals from the smelter emissions.

Table 2.4 Correlation coefficients of Zn and Cd concentrations with soil characteristics

	Houthalen				Balen			
	pH	% OC	Fe_{ox}	Al_{ox}	pH	% OC	Fe_{ox}	Al_{ox}
Cd_{tot}	-0.73	0.90	0.71	0.15	-0.75	0.79	0.71	0.39
E_{Cd}	-0.61	0.81	0.76	0.29	-0.59	0.64	0.71	0.51
Zn_{tot}	0.36	-0.02	-0.15	0.06	-0.58	0.56	0.24	-0.08
E_{Zn}	-0.48	0.83	0.32	-0.04	-0.76	0.77	0.62	0.26

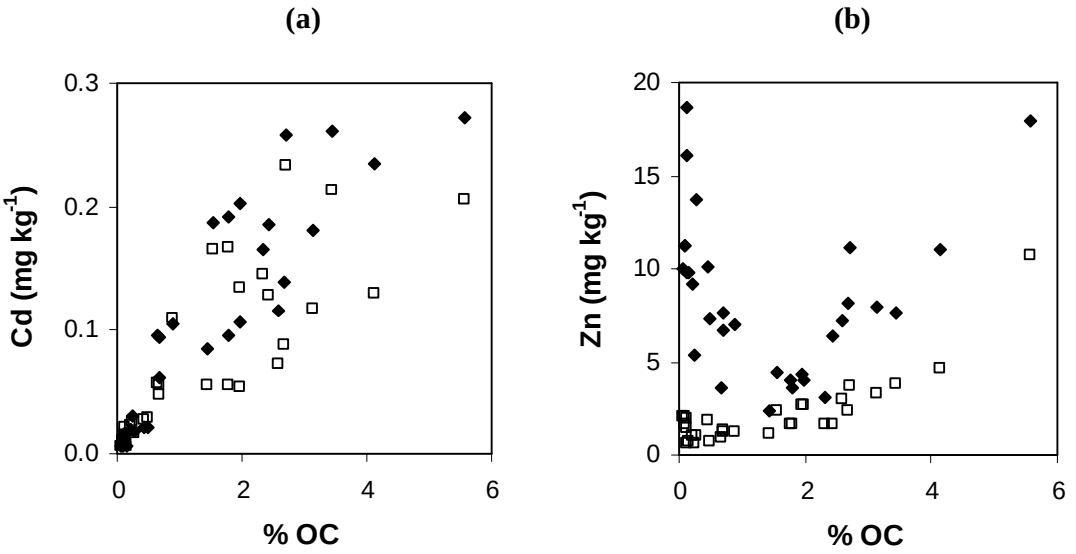

Figure 2.2 Total (♦) and radio-labile (□) concentration of (a) Cd and (b) Zn as a function of organic C content (data from Houthalen, unpolluted field).

2.3.4 Depth profiles of total and radio-labile Cd and Zn

Total Cd concentrations decrease with depth in the unpolluted soil (Houthalen), and total Zn concentrations increase with depth except for the A horizon, where Zn concentration is higher than in the underlying horizons (Table 2.2, Figure 2.3a). The higher concentrations in the upper horizon are likely related to cycling of metals in the soil-plant environment (Johnson and Petras, 1998; Nowack *et al*., 2001). Most Cd is labile throughout the profile, while labile fractions of Zn are small in the lower horizons. Zinc in the parent material is probably enclosed in mineral lattices, explaining the small labile fractions of Zn in the lower horizons (Johnson *et al.*, 1998). The increase in Zn concentration with depth indicates a loss of Zn by leaching. This loss of Zn implies that 'non-labile' Zn may be released on large time-scale, e.g., by mineral weathering. Jersak *et al.* (1997) calculated a loss of between 32 and 508 kg Zn ha^{-1} (or between 12% and 56%) of the mineral-soil profiles of three northeastern U.S. Spodosols (age ~ 12000 years). Dawson *et al.* (1991) calculated Zn losses of around 90% in the upper 38 cm of New Zealand Spodosols (age ~ 100000 years).

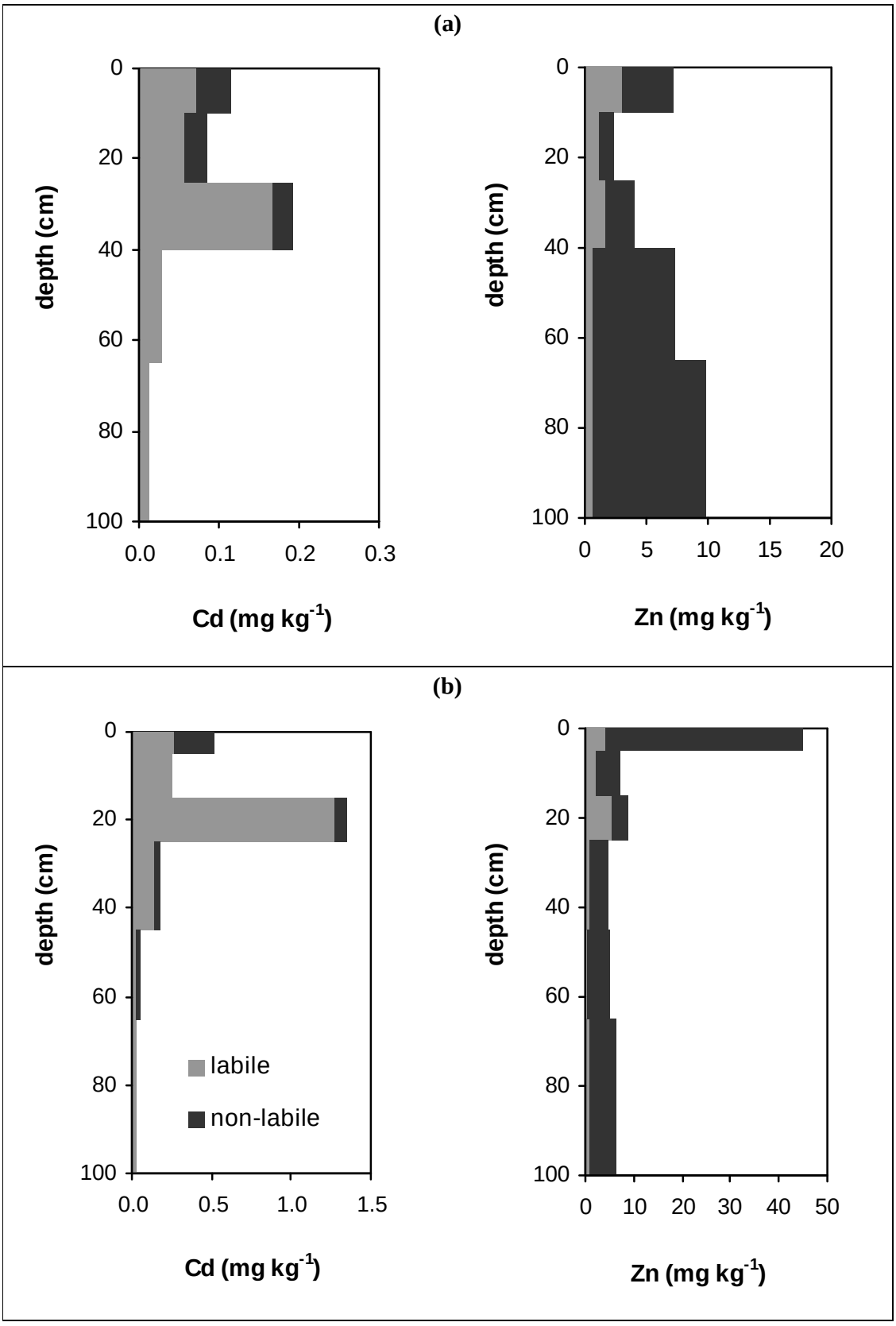

Figure 2.3 Depth profiles of radio-labile and non-labile Cd and Zn for (a) an unpolluted soil (Houthalen, profile 3) and (b) a polluted soil (Balen, profile 1)

Total Cd and Zn concentrations both decrease with depth in the polluted soil of Balen (Figure 2.3b). Despite the low pH, and consequently high mobility of Zn in the soil from Balen (see Chapter 3 and 8), a large fraction of the added Zn is present in the upper horizon. The fraction of labile Zn in the A-horizon is smaller than in the E- and the B-horizon (Table 2.2 and Figure 2.3b). The presence of Zn in insoluble form in the upper horizon, preventing Zn to be leached (cf. Figure 2.1), may therefore explain the high Zn concentration in the topsoil. The age of contamination, which is ± 50–100 years, apparently is not large enough to mobilize all non-labile Zn. Also for Cd, labile fractions are smaller in the topsoil than in the subsoil of the contaminated site. Differences in solid phase speciation of Zn between top- and subsoil of a smelter contaminated soil were also observed by Roberts *et al.* (2002). They found that Zn in the topsoil was mainly in the form of franklinite ($ZnFe_2O_4$) and sphalerite (ZnS). In contrast, aqueous (outersphere) Zn^{2+} prevailed in the subsoil (~ 60%). The difference in speciation between subsoil and topsoil was also reflected in the desorption behaviour of Zn. Only 10% of the total Zn amount in the topsoil was leached in a stirred-flow experiment, while 70% of the total Zn was leached in the subsoil.

2.3.5 Total Cd and Zn in the soil profile and the current mass balance

The total amount of Cd and Zn present in the profile (M_{profile}, kg ha^{-1}) was calculated by summing up the metal amount in all horizons:

$$M_{\text{profile}} = \sum_i 0.1 \cdot d_i \cdot \rho_i \cdot M_{\text{tot},i} \qquad (2.3)$$

where d is the horizon thickness (cm), ρ is the bulk density (g cm^{-3}) (determined by Seuntjens *et al.* (2001a) for similar soils adjacent to the site of this study), and M_{tot} is the total metal concentration (mg kg^{-1}) of the soil horizon.

The current mass balance reads:

$$\frac{\mathrm{d}M_{\text{profile}}}{\mathrm{d}t} = I - L \qquad (2.4)$$

where I is the input rate (kg ha^{-1} y^{-1}) and L is the leaching rate (kg ha^{-1} y^{-1}). In equation 2.4, it is assumed that there is no removal of crops. The input of Cd and Zn is mainly from atmospheric deposition, since no fertilizers or other soil amendments are added to these

soils. The leaching rate can be calculated from the pore water concentration ($[M]_{pw}$, mg l^{-1}) and the annual precipitation surplus (F, m y^{-1}), which is in the order of 0.2 m y^{-1}:

$$L = [M]_{pw}.10.F \quad (2.5)$$

The Cd concentration in the pore water of the unpolluted field is in the order of 1 µg l^{-1} (details not shown), and the estimated loss by leaching is, therefore, 2 g Cd ha^{-1} y^{-1}. Estimates of the input rate I of Cd for the unpolluted soil during the last century are between 1 and 7 g ha^{-1} y^{-1}, based on data of atmospheric deposition from the literature. Tjell and Christensen (1985) estimated that atmospheric deposition of Cd in Denmark was around 7 g Cd ha^{-1} y^{-1} between 1923 and 1980. Atmospheric deposition of Cd in a rural site in Belgium (Knokke) was 3.6 g ha^{-1} $year^{-1}$ (VMM, 1999, personal communication). Current atmospheric deposition of Cd in Western Europe, which is in the order of 1 g ha^{-1} y^{-1} (RIVM, 2001ab), is lower than historical input, due to increased emission control. The net effect (accumulation or loss) is uncertain. However, the deposition in rural areas has likely been higher than 2 g Cd ha^{-1} y^{-1} during the last decennia, and therefore, there has probably been a net accumulation during this period. Presently, the Cd balance is presumably close to steady state, due to the reduced deposition.

The Zn concentration in the pore water of the unpolluted field is in the order of 50–200 µg Zn l^{-1} (details not shown), and the estimated loss by leaching is therefore between 100 and 400 g Zn ha^{-1} y^{-1}. The atmospheric deposition of Zn is estimated to be in the order of 100-150 g Zn ha^{-1} y^{-1} (RIVM, 2001ab). Since input rate and leaching rate are of the same order of magnitude, no conclusion can be made whether accumulation or loss of Zn has occurred in this soil. However, as mentioned above, the increase in Zn concentration with depth indicates that a net loss of Zn has occurred (Figure 2.3a).

Assuming that the metal concentrations in the C-horizon of the unpolluted soil (~ 0.02 mg Cd kg^{-1} and 10 mg Zn kg^{-1}) are equal to the concentrations in the parent material, the amount in the upper 2 m of the parent material is estimated to be about 0.5 kg Cd ha^{-1} and 300 kg Zn ha^{-1}. Since the present-day amounts of Cd are larger (Table 2.5), this would indicate that also the unpolluted soil of Houthalen is considerably enriched in Cd. However, the estimated concentration in the parent material is uncertain, since also in the deeper horizons, enrichments or losses of metals may have occurred.

Table 2.5 Amount of Cd and Zn (in kg ha^{-1}) present in the profiles of the unpolluted field (Houthalen). Calculations were made for the upper 2 meters.

Profile	1	2	3	4	5	6	mean
Cd	1.27	1.2	1.04	1.84	0.75	2.01	1.35
Zn	340	287	271	388	331	290	318

The metal amount in the polluted soil, averaged for the 10 sampled profiles, is 7.2 kg Cd ha^{-1} and 461 kg Zn ha^{-1} (Table 2.6). The (relative) difference in metal amount between the polluted and unpolluted soil is much larger for Cd than for Zn, which is indicative of the higher mobility of Zn in low pH soils. The variation in metal amount between the profiles is large. The largest amounts are found in profiles 8 and 10, which were located close to a smelter waste dump. The Cd amount is between 4 and 6 kg ha^{-1} in most other profiles. Lower amounts were observed in profiles 2 and 6. These profiles had low organic matter content (<0.7%) below the A-horizon, and showed no podzolisation. The low Cd accumulation in these profiles may therefore be due to higher leaching of Cd. A more detailed discussion of Cd and Zn transport in this polluted soil will be given in Chapter 8.

Table 2.6 Amount of Cd and Zn (in kg ha^{-1}) present in the profiles of a polluted field (Balen). (Calculations made for the upper 2 meters)

Profile	1	2	3	4	5	6	7	8	9	10	mean
Cd	3.7	1.2	3.7	5.1	5	1.3	5.8	13.8	6.2	25.6	7.2
Zn	213	291	361	463	406	365	513	633	480	889	461

CHAPTER 3

The solid–liquid distribution of Cd and Zn in Spodosols as affected by soil properties

Abstract

Risk assessment of heavy metals in soils requires knowledge about the solid–liquid distribution of these metals. The distribution of Cd and Zn was studied in a series of batch experiments where solution composition was varied and by a multivariate approach with 141 different soil samples. Spodosols were sampled at different depths of two contaminated fields and one unpolluted field. Batch experiments showed that the solid–liquid distribution coefficient (K_d) of Cd and Zn increased with a factor 5 to 6 per unit increase in pH. The K_d of these metals increased 2- to 3-fold when the Ca concentration decreased tenfold. The K_d values were nearly unaffected by the pH at low ionic strength between pH 6.5 and 7, because of competition for heavy metal binding between soil and dissolved organic matter solubilized under these conditions.

The *in situ* K_d values of Cd and Zn (i.e., the ratio of total metal concentration to the concentration in the soil solution) of 141 soil samples were correlated with soil properties. Between 59 and 85% of the variation of logK_d was explained by organic matter content, pH and pore water concentration of Ca. The prediction of K_d of Zn strongly improved for two of the three fields, when metals in solution were assumed to be in equilibrium with the radio-labile metal pool instead of the total metal pool. No such improvement was found for Cd, since non-labile fractions were generally small (< 50% of total metal concentration).

3.1 Introduction

An accurate estimate of the solid–liquid distribution coefficient, K_d, is necessary when modelling heavy metal transport in soil, because the K_d largely influences the outcome of the transport predictions. The K_d is mainly affected by solution parameters such as pH, Ca concentration, the presence of other competing heavy metal, and the presence of complexing ligands (cf section 1.2).

Relatively few measurements of the *in situ* K_d (i.e., based on pore water concentrations) have been reported. *In situ* K_d values have been measured on 30 unpolluted soils by Römkens and Salomons (1998) and on 46 (polluted and unpolluted) soils by de Groot *et al.* (1998). The K_d values varied over almost 4 orders of magnitude. In both studies, the pH explained most of the variation in logK_d of Cd and Zn.

In this chapter, the distribution coefficients of Cd and Zn were determined for a number of Spodosols (described in Chapter 2). Two methods were used to determine the factors that influence the K_d of Cd and Zn.

(i) The effect of changing electrolyte composition (pH, Ca concentration) on the solution concentration of Cd and Zn was measured in batch experiments.

(ii) *In situ* K_ds of Cd and Zn were measured and correlated with soil properties. A comparison was made between predictions that were either based on total metal concentrations or on radio-labile metal concentration.

3.2 Materials and methods

3.2.1 Effect of electrolyte composition on sorption of Cd and Zn

3.2.1.1 Theory

The solid–liquid distribution of cadmium is often described with a Freundlich isotherm (e.g., Christensen, 1984). From theoretical considerations of sorption on heterogeneous soil surfaces, Temminghoff *et al.* (1995) derived a three-species Freundlich model (3SF) in which pH, complexation, Ca competition and ionic strength effects were taken into account:

$$s_{Cd} = K \cdot (Cd^{2+})^{n_{Cd}} \cdot (Ca^{2+})^{n_{Ca}} \cdot (H^{+})^{m} \qquad (3.1)$$

where s_{Cd} is the amount of adsorbed metal (in mol kg^{-1} or mg kg^{-1}), (Cd^{2+}) and (Ca^{2+}) are the free ion activities of Cd^{2+} and Ca^{2+} (in mol l^{-1} or mg l^{-1}), (H^{+}) is the free proton activity (in mol l^{-1}), and K, n_{Cd}, n_{Ca} and m are the empirically derived parameters.

The Cd concentration is related to the free ion activity of Cd:

$$(Cd^{2+}) = [Cd] \cdot \gamma_{Cd} \cdot F \qquad (3.2)$$

where γ_{Cd} is the activity coefficient of Cd, and F is the complexation coefficient which is the ratio of free Cd concentration to total Cd concentration in solution. Cadmium may form complexes with inorganic (e.g., Cl^{-}) or organic ligands.

In case of linear sorption (i.e., at low metal load), eq. 3.1 can be written as:

$$K_d = \frac{s_{Cd}}{[Cd]} = K \cdot \gamma_{Cd} \cdot F \cdot (Ca^{2+})^{n_{Ca}} \cdot (H^{+})^{m} \qquad (3.3)$$

3.2.1.2 Experiments

Topsoils were sampled from two sites situated in Balen (soil A) and Neerpelt (soil B), that are polluted by atmospheric deposition of Zn smelters.

The distribution of Cd and Zn was measured at constant ionic strength (0.03 M), and at varying Ca concentrations or varying pH. Duplicate samples of 2 g soil (Soil A, Table 3.1) were weighed in polypropylene centrifugation tubes, and 20 ml of a solution spiked with ^{109}Cd and ^{65}Zn was added. The background electrolytes were $Ca(NO_3)_2$ (0.01 M) : $NaNO_3$ (0.03 M), mixed in volume ratios of 100:0, 50:50, 10:90, 5:95 or 1:99 for the experiment with varying Ca concentration, and 0.01 M $Ca(NO_3)_2$ with different concentrations of NaOH or HCl (0.01 and 0.02 meq OH^{-} or H^{+} g^{-1}) for the experiment with varying pH. The suspensions were shaken end over end for three days.

The influence of pH on the K_d of Cd and Zn was studied in two background electrolytes (0.5 mM $Ca(NO_3)_2$ and 10 mM $Ca(NO_3)_2$). Duplicate samples of 2.5 g soil (Soil B, Table 3.1) were weighed in polypropylene centrifugation tubes, and 25 ml of the electrolyte solution spiked with ^{109}Cd and ^{65}Zn and with varying $Ca(OH)_2$ concentrations (0, 0.02, 0.04, and 0.06 meq OH^{-} g^{-1}) was added. The suspensions were shaken end over end for four days.

In all cases, phase separation was achieved by centrifugation (3000*g*, 30 min). The pH of the supernatant was measured, the ^{109}Cd and ^{65}Zn activities were determined (gamma scintillation) and concentrations of Cd, Zn and major cations (Ca, Mg, Na, and K) were measured with ICP-OES.

Table 3.1 Selected characteristics of the soils used in the batch experiments

	pH ($CaCl_2$)	OC %	Cd_{tot}	E_{Cd}	Zn_{tot}	E_{Zn}
			mg kg^{-1}			
Soil A	3.5	2.3	0.8	0.6	18	9
Soil B	4.2	2.3	3.1	2.3	239	130

3.2.2 Relationship between sorption of Cd and Zn and soil properties

Sandy soils were collected from an unpolluted field in Houthalen, a contaminated field in Balen, and a contaminated field in Neerpelt. The main soil characteristics of these fields are summarized in Table 3.2. The field in Neerpelt is part of a nature reserve (Hageven), and has been used as arable field in the 1970s for some years. The soil is classified as a typic haplaquod, a wet sandy soil with a plough layer. The groundwater table is between 60 and 120 cm of depth.

Six (Houthalen) or ten (Balen) profiles were sampled at 5 or 6 depths (see section 2.2.1). For the field in Neerpelt, 10 soil profiles were sampled in 2000 over an area of about 4 ha. The samples were taken with an Edelman screw auger, at 5 or 6 depths up to the groundwater table, which was located around 1 meter of depth.

The soils were sieved (< 2 mm) and air dried. The organic C content, pH, oxide content (Fe_{ox} and Al_{ox}), and total metal concentration (M_{tot}) were measured (section 2.2.1). The radio-labile Cd and Zn concentration (E, mg kg^{-1}) was measured by isotopic exchange, as described in section 2.2.2. Soil solution was isolated by centrifuging the field moist soils for 1 hour at 3000*g* (within 2 days after the soil sampling). The soil solution was filtered through a 0.45-µm membrane filter and acidified to pH=1 with HNO_3. Pore water concentrations of Cd and Zn ($[M]_{pw}$) and concentrations of macrocations (Ca, Mg, Na and K) in the soil solution were measured with ICP-OES.

The partitioning of Cd and Zn between solid and solution phase was expressed in terms of K_d ($M_{tot}/[M]_{pw}$) or K_d^{lab} ($E/[M]_{pw}$). These K_d values were correlated to soil properties by stepwise regression analysis, using SAS (Release 6.12). All variables were transformed to their logarithms, except for pH which is already a logarithm. The logarithmic transformation was used to normalize the data and to linearize relationships.

Table 3.2 Mean and range of selected soil characteristics for the three fields

	Balen (*n*=61)			Houthalen (*n*=31)			Neerpelt (*n*=56)		
	mean	min	max	mean	min	max	mean	min	max
pH	4.1	3.4	4.5	3.7	3.1	4.1	5.2	3.9	6.1
% OC	1.1	0.4	4.0	1.4	0.1	5.6	1.3	0.2	2.8
CEC ($cmol_c\ kg^{-1}$)	1.1	0.05	3.6	1.0	0.09	2.6	2.5	0.06	5.1
Fe_{ox} ($mmol\ kg^{-1}$)	17	1.2	76	17	3.6	50	9.6	0.5	38
Al_{ox} ($mmol\ kg^{-1}$)	33	6.7	87	27	7.2	69	35	33	59
Cd_{tot} ($mg\ kg^{-1}$)	0.5	0.01	2.9	0.10	0.01	0.27	2.3	0.05	7.6
Zn_{tot} ($mg\ kg^{-1}$)	23	1.2	140	8.4	2.3	18.7	208	12.6	758

Metal concentrations and soil properties were also determined on a collection of polluted topsoils collected in Belgium, France, Hungary and the UK, covering a wide range of soil properties, metal concentration and contamination source (sewage sludge, smelter, metal salts, mining, alluvial deposition) (Table 3.3).

Table 3.3 Mean and range of selected soil characteristics for an independent dataset of polluted soils (*n*=57 for Cd and *n*=61 for Zn).

	pH	Organic C	Ca_{pw}	Cd_{tot}	Zn_{tot}
		%	mM	$mg\ kg^{-1}$	
Mean	5.7	3.5	5.1	18.4	1080
Minimum	3.5	0.9	0.3	0.2	23
Maximum	7.2	23.1	18.6	3.5	34100

3.3 Results and discussion

3.3.1 Effect of electrolyte composition on the sorption of Cd and Zn

The distribution of Cd and Zn was measured at an ionic strength of 0.03 M, at varying pH or at varying Ca concentrations. Solution concentrations of Cd and Zn decreased and K_d values increased as the pH increased (Figure 3.1). Lower Ca concentrations increased sorption of Cd and Zn. This effect could partly be explained by the higher pH at lower Ca concentration. However, also a pure Ca competition effect was observed (Figure 3.1).

The distribution coefficient of the free ion was calculated as:

$$K_{d\,free}^{lab} = \frac{K_d^{lab}}{\gamma \cdot F} \tag{3.4}$$

where γ is the activity coefficient of Cd or Zn predicted by the Debye-Hückel equation (equal to 0.52 for IS=0.03 M), and F is the ratio of free concentration to total concentration in solution. The complexation coefficient F was assumed to be 1 since complexation with NO_3^- is negligible at the concentration used, and complexation of Cd and Zn with dissolved organic matter is also not of much importance at pH values below 4.5. Equation 3.3 may then be written as:

$$\log K_{d\,free}^{lab} = k + n_{Ca} \cdot \log(Ca^{2+}) - m \cdot pH \tag{3.5}$$

Parameters of this regression equation are given in Table 3.4. For Cd, a value of -0.70 was found for m, which implies that an increase of the pH with one unit increases the K_d with a factor of 5. A value of -0.23 was found for n_{Ca}, i.e., a tenfold increase of the Ca concentration decreases the K_d with a factor 1.7. The pH factor and Ca factor of Zn were both slightly larger (in absolute values) than those of Cd (Table 3.4).

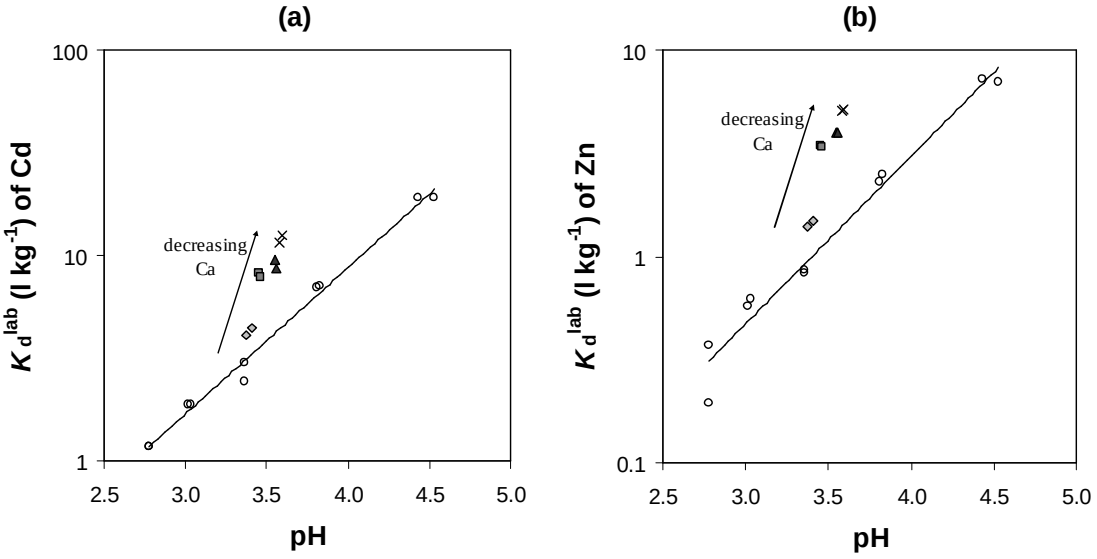

Figure 3.1 Effect of pH on the labile distribution coefficient (ratio of *E* value to concentration in solution) of (a) Cd and (b) Zn, measured in 0.01 M $Ca(NO_3)_2$ (open circles). Also shown are labile K_d values measured at the same ionic strength (0.03M), but lower Ca concentrations (x, 0.0001 M; ▲, 0.0005 M; ■ , 0.001 M ; ◇, 0.005 M Ca). (Data for soil A, Table 3.1)

Figure 3.2 shows the effect of pH on the distribution of Cd and Zn measured in two background electrolytes (0.5mM $Ca(NO_3)_2$ and 10 mM $Ca(NO_3)_2$). At low pH values, sorption was weaker in the background electrolyte with the higher ionic strength, which may be explained by the competition of Ca for sorption sites and the reduced activities. At high pH values, the increase of K_d with pH levelled off at low ionic strength. Concentrations of dissolved organic matter (DOM) are larger and the complexation of DOM with Cd and Zn is stronger at higher pH and lower ionic strength (Kinniburgh *et al*., 1996). Therefore, a reduction in free ion activity caused by a stronger complexation of Cd and Zn with DOM might explain this observation. To test this hypothesis, Cd and Zn in solution were speciated using the Windermere Humic Aqueous Model (WHAM), a chemical speciation model that incorporates model VI to describe complexation of metals with humic substances (Tipping, 1998). The soil solution pH and the concentrations of Ca, Mg, Na, K, Zn, Cd and dissolved organic matter were used as input data. The DOM concentrations in the extracts were not measured, but were estimated based on data from Oste *et al.* (2002). They measured DOM concentrations in soil suspensions at different pH and Ca concentrations, for a sandy soil from the same area as the soil used in this study, and with similar organic matter content (%OC 2.2). Predicted fractions of solution Cd and

Zn complexed with DOM were lower than 0.20 in 10 mM $Ca(NO_3)_2$, but ranged up to 0.85 in 0.5 mM $Ca(NO_3)_2$. Estimates of the parameters of the regression equation 3.5, obtained by linear regression analysis, are given in Table 3.4. The pH factors were very close to those obtained for soil A, whereas the effect of Ca competition was significantly larger for Cd, for unknown reasons. The labile K_d predicted from the regression equation and the free ion fractions calculated with WHAM agreed well with the observed values (Figure 3.2).

Table 3.4 Results of multiple regression results for $\log K_{d\,free}^{lab}$ (l kg^{-1}) with respect to $\log(Ca^{2+})$ (in mmol l^{-1}) and pH. (Values ± standard error)

	Cd				Zn			
	k	m	n_{Ca}	R^2	k	m	n_{Ca}	R^2
Soil A	-1.40	-0.70	-0.23	0.98	-2.15	-0.79	-0.31	0.98
	± 0.09	± 0.03	± 0.02		± 0.16	± 0.05	± 0.03	
Soil B	-1.56	-0.70	-0.44	0.99	-2.18	-0.76	-0.25	0.98
	± 0.09	± 0.02	± 0.04		± 0.10	± 0.02	± 0.04	

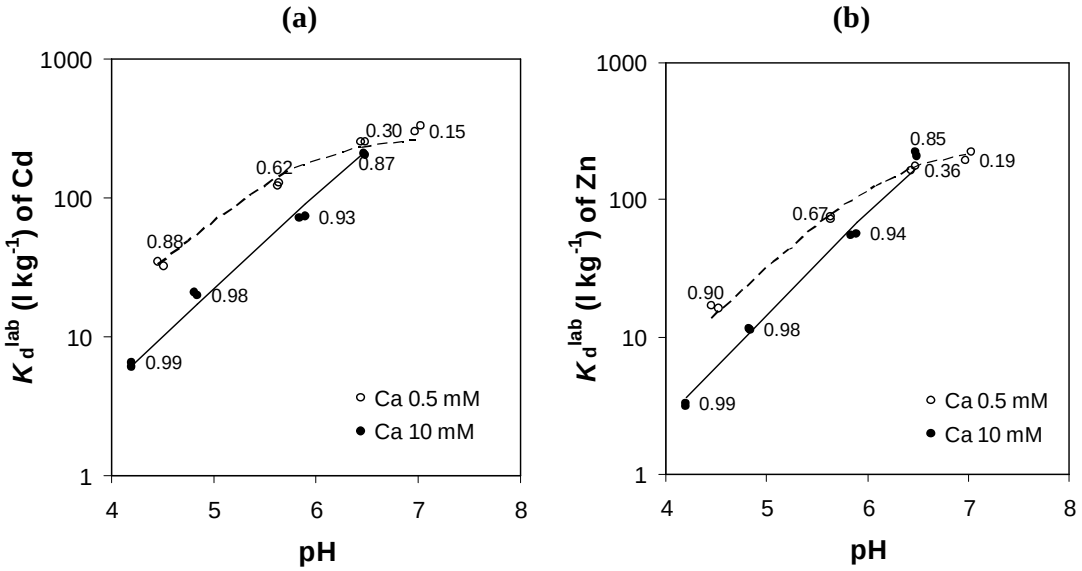

Figure 3.2 Effect of pH on K_d^{lab} of (a) Cd and (b) Zn, measured in 0.5 mM $Ca(NO_3)_2$ or 10 mM $Ca(NO_3)_2$. The lines represent the modelled values and data labels indicate the free ion fraction, as calculated with WHAM. (Data for soil B, Table 3.1)

These results indicate that liming may be an option to reduce the mobility of Cd and Zn in these acid sandy soils, since the K_d increases with about a factor 5 (Cd) to 6 (Zn) per unit increase in pH (Table 3.4). However, these soils have low ionic strength (Ca_{pw} ~ 0.1 mM), and liming will cause an increase in ionic strength, which may partly counteract the effect of increase in pH. Complexation of Cd and Zn with dissolved organic matter (DOM) may also result in a smaller increase in the K_d than is expected based on the increase in pH. Heavy metal binding by DOM may become of importance when the pH of these acid soils (pH ~ 4) is increased with more than 2 units.

3.3.2 Relationship between K_d of Cd and Zn and soil properties

The *in situ* K_d was calculated as the ratio of total metal concentration and the concentration measured in the soil solution, for all soil samples of the three fields (Table 3.5). The K_d values varied strongly among soil horizons and soil cores within one field (details not shown).

Table 3.5 Mean and range of the K_d values of Cd and Zn for the three fields.

	Houthalen		Balen		Neerpelt	
	Cd	Zn	Cd	Zn	Cd	Zn
Mean	46	26	57	40	169	80
Minimum	3	8	2	2	9	10
Maximum	108	77	446	237	590	306

The soil organic matter content explained most of the variation in logK_d: 70% for Cd and 33% for Zn. The Fe oxide content, that is positively correlated with the organic C content (r=0.57, P<0.001), explained much less of the variation in logK_d: only 14% for Cd and 9% for Zn. Introducing the soil pH as a second component improved the R^2 to 0.85 for Cd and 0.59 for Zn (Table 3.6). The pH is usually the most important factor explaining the K_d of Cd and Zn (e.g., Anderson *et al.*, 1988; Sauvé *et al.*, 2000). For this dataset, the organic matter content explained most of the variation in K_d, which may be explained by the strong variation in organic C content (from 0.05 to 5.6%), because soils were sampled at different depths. This becomes even clearer when only the fields of Houthalen and Balen, that have comparable pH (Table 3.2), are considered in the regression analysis. The organic C content explained 85% of the variation in logK_d for Cd (Table 3.7). Introducing the pH

into the regression model had no significant effect in this case. The coefficient for logOC was near 1 for Cd, effectively predicting that the K_d is proportional to the organic matter content in these soils. In various studies (e.g., Gerritse *et al.*, 1984; van der Zee and van Riemsdijk, 1987; Tye *et al.*, 2003), the Cd concentration has been normalised with respect to organic C content, the underlying assumption being that Cd only adsorbs on soil organic matter.

Table 3.6 Summary of linear regression for $\log K_d$ and $\log K_d^{lab}$ (in l kg^{-1}) of Cd and Zn with respect to soil properties for all soils (n=141). Organic C content (OC) is expressed in %. The pH was measured in 0.01 M $CaCl_2$ (S:L 1:10 kg l^{-1})

	$\log K_d$				$\log K_d^{lab}$			
		regression coefficients				regression coefficients		
	R^2	intercept	logOC	pH	R^2	intercept	logOC	pH
cadmium								
Value	0.85	-0.05	1.19	0.42	0.84	-0.29	1.09	0.45
SE		0.15	0.04	0.04		0.03	0.04	0.04
P-level			<0.0001	<0.0001			<0.0001	<0.0001
zinc								
Value	0.59	-0.08	0.62	0.38	0.84	-1.21	0.88	0.56
SE		0.18	0.05	0.04		0.13	0.04	0.03
P-level			<0.0001	<0.0001			<0.0001	<0.0001

Table 3.7 Summary of linear regression for $\log K_d$ and $\log K_d^{lab}$ (in l kg^{-1}) of Cd and Zn with respect to soil properties for the soils of Houthalen and Balen (n=85). Organic C content (OC) is expressed in %.

	$\log K_d$			$\log K_d^{lab}$		
		regression coefficients			regression coefficients	
	R^2	intercept	logOC	R^2	intercept	logOC
cadmium						
Value	0.85	1.52	0.99	0.84	1.40	0.87
SE		0.03	0.05		0.03	0.04
P-level		<0.0001	<0.0001		<0.0001	<0.0001
zinc						
Value	0.24	1.46	0.31	0.72	0.86	0.55
SE		0.04	0.06		0.02	0.04
P-level		<0.0001	<0.0001		<0.0001	<0.0001

No improvement in R^2 was found for Cd when the solid–liquid distribution was expressed with respect to the E value instead of total Cd concentration. Non-labile fractions of Cd were generally small, which explains this lack of improvement. In contrast, the R^2 improved strongly when the K_d of Zn was expressed with respect to radio-labile instead of total Zn concentration (Table 3.6 and Table 3.7). Non-labile fractions were larger and more variable for Zn than for Cd (section 2.3.3). The %E values of Zn varied between 5 and 88% in the field of Balen, and between 6 and 68% in the field of Houthalen. The variation in labile fractions of Zn was smaller in the field of Neerpelt, where the %E values ranged from 27 to 87%.

Tye *et al.* (2003) found no or only small improvements when using radio-labile instead of total metal concentration to predict pore water concentrations of Cd and Zn with an extended Freundlich model. However, the major portion of the dataset of this study consisted of metal salt spiked soils. The fraction radio-labile metal was highly pH dependent in these soils. Therefore, the variation in metal 'lability' was already partly described by the pH coefficient.

Concentrations of Cd and Zn (total, radio-labile and pore water concentrations) were also determined in contaminated soils collected in Belgium, France, Hungary and the UK, covering a wider range of soil properties (Table 3.3) than the Spodosols. The K_d ranged from 5 to 5830 l kg^{-1} for Cd and from 3 to 9660 l kg^{-1} for Zn. Stepwise linear regression analysis was performed for logK_d^{lab} with pH, organic C content (%) and pore water concentration of Ca (mM) as independent variables. The pH explained most of the variation in logK_d: 65% for Cd and 62% for Zn. Introducing organic C content and pore water concentration of Ca further improved the R^2. The following equations were obtained with all regression coefficients significant at the 0.05 level:

$$\text{for Cd: } \log K_d^{lab} = -1.80 + 0.66\ \text{pH} + 0.79\ \log\%\text{OC} - 0.26\ \log Ca_{pw} \quad (R^2 = 0.77) \qquad (3.6)$$

$$\text{for Zn: } \log K_d^{lab} = -2.54 + 0.73\ \text{pH} + 0.82\ \log\%\text{OC} - 0.46\ \log Ca_{pw} \quad (R^2 = 0.74) \qquad (3.7)$$

These equations were used to predict pore water concentrations of Cd and Zn for the sandy soils of this study. Predicted concentrations, calculated as the ratio of radio-labile metal (E) to the predicted K_d^{lab}, agreed well with observed values (Figure 3.3).

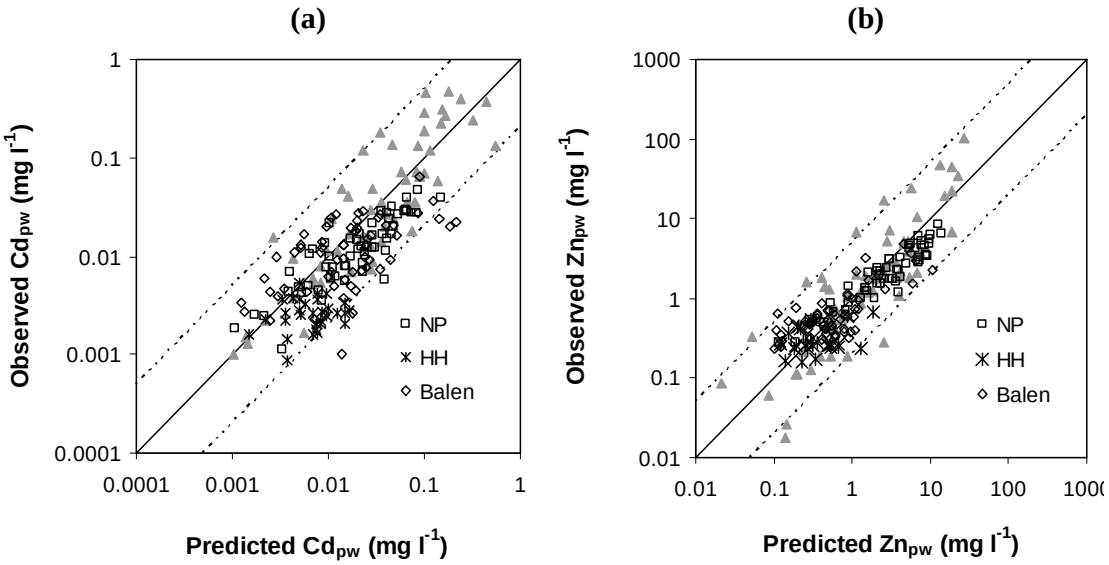

Figure 3.3 Observed versus predicted pore water concentrations of (a) Cd and (b) Zn, for the soils from Neerpelt (NP), Houthalen (HH) and Balen. Predictions were made based on radio-labile metal concentration and a regression equation derived from an independent dataset (data indicated by ▲). The dotted lines indicate 5 times under- or overprediction.

In conclusion, the batch experiments and the multivariate analysis showed that the solid–liquid distribution of *labile* Cd and Zn is mainly controlled by pH, organic matter content and ionic strength of the soil solution. For Zn, predictions of the K_d were much improved when the K_d was expressed with respect to the radio-labile metal pool (E value) instead of total metal concentration. The regression equations for K_d and K_d^{lab} were nearly equal for Cd, since Cd was – in general – mainly in labile form.

CHAPTER 4

Liming decreases pore water concentrations of Cd and Zn and stimulates soil microbial activity

Abstract

The effect of liming on pore water concentrations of Cd and Zn was tested on two acid sandy soils in a laboratory incubation experiment. One soil was contaminated with heavy metals due to smelter emission, the other soil was amended with metal salts to a same (radio-)labile metal concentration as the field contaminated soil. The soils were limed at two rates, and the soil solution was sampled and analysed at 1, 4 and 9 weeks after liming. An increase in the pH with two units resulted in a tenfold decrease of pore water concentrations of Cd and Zn in the field contaminated soil. Pore water concentrations of Cd and Zn increased up to five-fold between one and nine weeks of incubation (20°C). These increases were attributed to the increase in ionic strength and acidification of the soil solution, caused by mineralization of organic N. This laboratory experiment reveals that liming may be successful in remediation of metal contaminated soils, but also highlights that accelerated soil microbial activity may partly offset the reduction of metal concentrations in the soil solution.

4.1 Introduction

Most technologies to remediate metal contaminated soils are expensive and not applicable on a large scale. Increasing the soil pH through liming could possibly be used as a cost-effective method to reduce the metal mobility in acid soils contaminated with Cd and Zn (cf. Chapter 3).

Decreases in soil solution concentrations of heavy metals upon liming have been observed in several studies. Liming of two strongly contaminated soils decreased the pore water concentrations of Cd and Zn with about a factor of 5 per unit increase in pH (Lombi *et al.*, 2002). Two soil amendments, red mud (a waste product of the bauxite industry) and beringite (a cyclonic ash), that increased the pH to approximately the same value as the lime treatment, had a similar effect on the pore water concentrations of Cd and Zn. Filius *et al.* (1998) measured Cd concentrations in a 0.01 M $Ca(NO_3)_2$ extract in a metal contaminated soil from a liming experiment, and found that concentrations decreased with about a factor of three per unit pH increase. Knight *et al.* (1998) amended soils from a long-term liming experiment with $CdSO_4$ (3 mg Cd kg^{-1}) or $ZnSO_4$ (300 mg Zn kg^{-1}). Pore water concentrations decreased about 6 times per unit increase in pH.

Reductions in metal concentrations in solution may be achieved by an increased adsorption (i.e., an increase in the solid–liquid distribution between labile pool and solution phase), or by a decrease in the labile pool (Hamon *et al.*, 2002). The reduction in pore water concentrations of Cd and Zn upon liming is mainly caused by stronger adsorption, because of the increase in pH. However, this effect of increase in pH on metal mobility may be partly counteracted by the increase in Ca concentration upon liming. Especially in soils with low ionic strength, liming may result in a large increase in the Ca concentration. Increased complexation of Cd and Zn with dissolved organic matter may also result in a lower reduction in the pore water concentrations than is expected based on the increase in pH.

Liming may also result in a decrease in the labile pool, especially at high pH values where precipitates may form. Hamon *et al.* (2002) found a strong decrease in the radio-labile Zn concentration (*E* value) between pH 6 and 7, which was attributed to the formation of $ZnCO_3$. However, acidification returned the labile pool to values comparable with that of an unamended soil, since carbonates are readily solubilized. Other soil amendments (e.g., red mud) may promote fixation of metals in non-labile pools that are

partly resistant to acid dissolution (Hamon *et al.*, 2002). Therefore, liming is sometimes not recommended since it does not lead to irreversible fixation

The effect of liming may be assessed in laboratory incubation experiments. Changes in the soil solution composition may occur during incubation. Curtin and Smillie (1995) found a strong increase in concentration of the major cations and of nitrate and a decrease in pH for soils that were incubated for periods up to one year. These changes in soil solution composition were attributed to the mineralization and nitrification of organic N. The decrease in pH and the increase in Ca concentration during incubation increase the pore water concentrations of Cd and Zn. Curtin and Smillie (1983) found that pore water concentrations of Zn increased up to tenfold between 1 and 52 weeks of incubation in control and limed soils.

In this study, we tested the effect of liming and incubation on pore water concentrations of Cd and Zn in two acid soils. One soil was contaminated with heavy metals due to smelter emissions. The other soil was amended with Cd and Zn salts in the laboratory to a (radio-)labile metal concentration similar as the field contaminated soil.

4.2 Materials and methods

Soils were sampled from the surface horizon (0-10 cm) of a non-contaminated soil (Houthalen, H) and a soil slightly contaminated with heavy metals (Neerpelt, NP) (Table 4.1). Both soils were acid sandy soils (Spodosols). Pore water was isolated from the field moist soils by centrifugation immediately after sampling the soils, and the concentrations of Cd, Zn and Ca in the pore water (filtered over 0.45µm) were measured with ICP-OES.

Table 4.1 Selected characteristics of the soils

	pH [a]	OC [b]	CEC [c]	Cd_{tot}	Zn_{tot}	E_{Cd}	E_{Zn}
		%	$cmol_c\ kg^{-1}$	$mg\ kg^{-1}$		$mg\ kg^{-1}$	
Neerpelt	3.2	2.4	3.1	1.3	110	0.55	30
Houthalen	3.4	2.9	2.2	0.32	16	0.20	7.2

[a] $CaCl_2$ 0.01M, S:L 1/10; [b] organic C content, dry combustion (Skalar CA 100);
[c] silverthiourea method (Chhabra *et al.*, 1975)

The soils were air-dried and passed through a 2 mm sieve. Three weeks after drying, a $CdSO_4$ + $Zn(NO_3)_2$ solution was added to soil H to a final moisture content of 20% (w:w)

and a dose of 0.3 mg Cd kg^{-1} and 25 mg Zn kg^{-1}. Soil NP was only wetted, to the same water content. The moist soils were incubated in polyethylene bags at 4°C. After 3 days of incubation, lime (analytical grade $CaCO_3$) was added to the soils (0, 1.1, and 2.2 g $CaCO_3$ kg^{-1} for soil H and 0, 1.25, and 2.5 g $CaCO_3$ kg^{-1} for soil NP) and thoroughly mixed (2 replicates per treatment). Soil solution was extracted by centrifugation and filtered over 0.2 µm after one week of incubation at 4 °C. The soils were subsequently incubated at 20°C and soil solution was extracted and filtered (0.2 µm), four and nine weeks after liming. The subsamples that were used for extraction of the soil solution were wetted to 25% (w:w) moisture content three days before the pore water isolation. The solutions were analysed for pH, Ca, K, Na, Mg, Cd, Zn, dissolved organic carbon (DOC), SO_4^{2-}, NO_3^- and Cl^-. Calcium, K, Na, Mg, Al and Zn were determined by AAS and Cd by GFAAS on acidified (pH=1) samples. Total carbon in solution was measured with a Total Carbon Analyzer (Shimadzu TOC-V_{CPH}) and was assumed to be equal to the dissolved organic carbon (DOC), as it was found at the first sampling occasion that the concentration of inorganic C in solution was negligible. Sulphate, nitrate and chloride were measured with ion chromatography (Dionex).

Radio-labile Cd and Zn in soil (*E* values) were measured three and nine weeks after the metals were added to the soil, as described in section 2.2.2. The soil pH of all treatments was measured in 0.01 M $CaCl_2$ (solid:liquid ratio 1:10) at the beginning and the end of the experiment.

Total dissolved Cd and Zn in soil solutions were speciated using the Windermere Humic Aqueous Model (WHAM), a chemical speciation model that incorporates model VI to describe complexation of metals with humic substances (Tipping, 1998). The soil solution pH and the total measured concentrations of Cd, Zn, Ca, Mg, Na, K, Al, SO_4^{2-}, NO_3^-, Cl^-, and dissolved organic matter were used as input data. The temperature was set at 20°C and the partial CO_2 pressure at 3.5 10^{-3} atm. It was assumed that the dissolved organic matter contained 50%C, was fulvic in origin, and that 50% was inert (Lofts and Tipping, 2000).

Statistical analyses were based on two-way ANOVA (SAS 6.12).

In an additional incubation experiment, four topsoils of the field of Neerpelt were amended with lime at three rates (0.43, 0.86, and 1.28 g CaO kg^{-1}). After 2 weeks of incubation, the pH was determined (in 0.001 M $CaCl_2$, S/L=1/10 kg l^{-1}), and the CEC and concentrations of exchangeable bases were measured at the soil pH with silverthiourea as index cation (Chhabra *et al.*, 1975).

4.3 Results

The radio-labile metal concentration of Cd and Zn of both soils was not affected by liming. Soil H amended with metal salts had *E* values of 0.56 (± 0.02) mg Cd kg^{-1} and 29 (± 0.7) mg Zn kg^{-1}, similar to the *E* values of the field contaminated soil (Table 4.1). The difference between *E* value before and after metal salt amendment is 0.36 mg Cd kg^{-1} and 22 mg Zn kg^{-1}, or nearly equal to the amount of added metal, which means that all added labile metal remained labile. The *E* values measured after nine weeks of incubation were not lower than those measured after 3 weeks of incubation, i.e., no ageing reactions had occurred during this period. The soil pH of the highest lime treatment was 4.8 for soil NP and 5.4 for soil H. In soils with pH<5.5, no considerable decrease in labile Cd or Zn concentrations is to be expected in a two-months period (Tye *et al.*, 2003).

Liming increased the soil solution pH, and, as a consequence, decreased pore water concentrations of Cd and Zn (Table 4.2). The Ca concentration increased upon liming (Table 4.2), the concentrations of Na, Mg and K were only slightly affected, and the Al concentration decreased (details not shown). Concentrations of DOC increased (soil NP) or were unaffected (soil H). The changes in soil solution composition upon liming were similar to those observed by Curtin *et al.* (1983).

The pH of the soil solution decreased as incubation progressed (Table 4.2), except for the control treatment of soil H. The soil pH, measured in 0.01 M $CaCl_2$, of the limed soil was also lower after 9 weeks of incubation, but the decrease was less pronounced than that of the soil solution pH. The pore water concentrations of Ca increased and this was most pronounced in the lime treatments. Concentrations of DOC decreased with time. Decomposition of DOC, released after rewetting of the soil, may explain this decrease (Merckx *et al.*, 2001). The decrease in DOC with time may be also related to the increase in ionic strength and decrease in pH of the soil solution (Oste *et al.*, 2002). Concentrations of Cd and Zn increased upon incubation. The decrease in pH upon incubation partly explains this increase in pore water concentrations. However, concentrations were generally larger at a given pH value for longer incubation times (Figure 4.1), which may be explained by the increase in Ca concentration during incubation. An increase in ionic strength causes a decrease in sorption of Cd and Zn because of Ca competition and because of a decrease in free ion activity (Temminghoff *et al.*, 1995; Chapter 3).

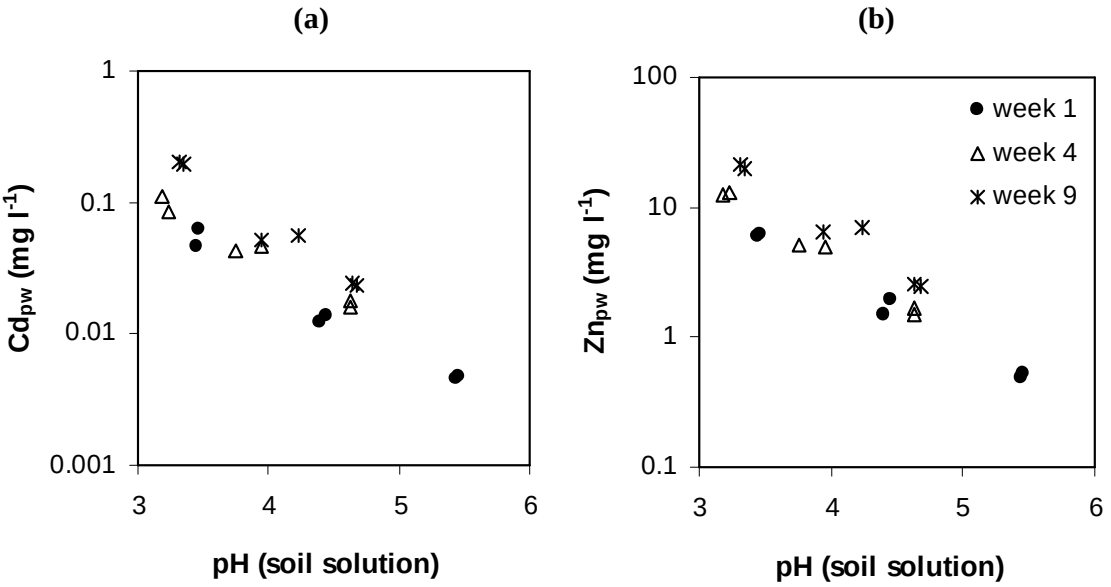

Figure 4.1 The pore water concentrations of (a) Cd and (b) Zn as a function of soil solution pH at different incubation times (for soil NP)

According to the speciation calculations with WHAM, Cd and Zn in solution were mainly present as free ion. Predicted fractions of dissolved Cd and Zn complexed with SO_4^{2-} were lower than 0.2. The fractions of solution Cd and Zn complexed with dissolved organic matter (DOM) were predicted to be below 0.2, except for the highest lime treatments after 1 week of incubation. For these treatments, it was predicted that the fraction of Cd and Zn complexed with DOM was around 0.25 for soil H and around 0.5 for soil NP.

Concentrations of NO_3^- increased during incubation, and this increase (in meq l^{-1}) agreed well with the increase in salt concentration (sum of concentrations of Ca, Mg, K, and Na; in meq l^{-1}). This relationship suggests that the increase in ionic strength and the acidification of the soil solution is caused by mineralization of organic N. The amount of N mineralized was estimated from the increase in NO_3^- concentration. More N was mineralized in the limed soils (Table 4.3). Stimulation of N and C mineralization by liming was also observed by Curtin *et al.* (1998). Dancer *et al.* (1973) found that nitrification rates in soils amended with $NH_4(SO_4)_2$ were higher in limed soils than in control soils of a field lime experiment.

Since moist storage may result in changes of the soil solution composition, it is advisable to sample soil solution immediately after soil samples are collected in the field.

Table 4.2 Effect of liming and incubation on soil solution composition. (L0 = control, L1 = low lime, L2 = high lime treatment)

Incubation time (weeks)	pH soil solution			Cd (µg l^{-1})			Zn (mg l^{-1})			Ca (mM)			NO_3^- (mM)			DOC (mg l^{-1})		
	L0	L1	L2	L0	L1	L2	L0	L1	L2	L0	L1	L2	L0	L1	L2	L0	L1	L2
Soil H																		
1	3.7	4.4	5.6	47	25	7	3.2	2.0	1.1	0.8	1.9	3.6	2.8	2.7	3.2	101	107	95
4	3.8	4.2	5.1	35	23	7	3.2	2.3	1.1	0.9	2.7	4.3	4.3	6.7	7.2	55	49	55
9	3.8	3.9	4.6	48	67	23	6.2	8.9	3.6	1.5	8.6	12.1	7.9	23.4	26.7	54	47	50
Analysis of variance																		
Lime		***			***			***			***			***			ns	
Time		***			***			***			***			***			***	
Lime x time		***			***			***			***			***			ns	
Soil NP																		
1	3.5	4.4	5.5	54	13	5	6.1	1.7	0.5	0.3	1.1	1.6	2.8	3.1	3.3	53	68	114
4	3.2	3.9	4.6	96	44	17	12.7	5.0	1.6	0.6	3.5	4.1	4.9	8.0	8.1	38	34	45
9	3.2	4.1	4.5	200	53	24	20.4	6.7	2.5	0.6	5.3	6.7	8.1	12.5	14.8	35	32	38
Analysis of variance																		
Lime		***			***			***			***			***			***	
Time		***			***			***			***			***			***	
Lime x time		***			***			***			***			***			***	

*** Significant at the 0.001 probability level; ns, not significant at the 0.05 probability level

Table 4.3 Effect of liming on the amount of mineralized N, calculated from the increase in NO_3^- concentration during incubation.

	Soil H			Soil NP		
	pH [a]	N min. (mmol kg^{-1})		pH [a]	N min. (mmol kg^{-1})	
		0-21 d	0-56 d		0-21 d	0-56 d
L0	3.3	0.2	1.1	3.2	0.5	1.3
L1	4.2	1.0	5.2	4.0	1.2	2.4
L2	5.4	1.0	5.9	4.8	1.2	2.9

[a] pH measured in 0.01M $CaCl_2$ at the start of the experiment

4.4 Discussion

4.4.1 Capacity and intensity effects of liming

The concepts of capacity and intensity are useful in interpreting the effects of liming on soil solution composition. The capacity factor stands for the total amount in the soil system, while the intensity factor corresponds to the solution concentration (Reuss and Walthall, 1990).

The reaction of $CaCO_3$ in an acid soil can be written as:

$$CaCO_3 + 2\ S\text{-}H \rightarrow S_2\text{-}Ca + CO_2 + H_2O \qquad (4.1)$$

where S represents an exchange site. Liming results in an increase of the base saturation, i.e., the fraction of the cation exchange complex that is occupied by the cations Ca^{2+}, Mg^{2+}, K^+ and Na^+. These cations are not bases in a chemical sense, but an exchange complex dominated by these 'basic' cations behaves as a dissociated acid, and will have a soil solution with a relatively high pH. On the other hand, an exchange complex dominated by the 'acidic' cations H^+ and Al^{3+} behaves as an undissociated acid and maintains the soil solution at lower pH.

The increase in Ca saturation is accompanied by an increase in the pH (intensity factor), which can be explained with the ion exchange theory (Reuss *et al.*, 1990). Exchange between Ca^{2+} and H^+ on the soil surface, can be quantified using a selectivity coefficient:

$$K_c(\mathrm{Ca/H}) = \frac{Z_{\mathrm{Ca}}}{(1-Z_{\mathrm{Ca}})^2} \cdot \frac{(\mathrm{H}^+)^2}{(\mathrm{Ca}^{2+})} \qquad (4.2)$$

where Z_{Ca} is the equivalent fraction of Ca on the ion exchange complex, (Ca^{2+}) is the free ion activity of Ca^{2+} (in mol l^{-1}), and (H^{+}) is the free proton activity (in mol l^{-1}). Equation 4.2 can be rewritten as

$$pH - \tfrac{1}{2}pCa = k + 0.5 \cdot \log \frac{Z_{Ca}}{(1 - Z_{Ca})^2} \qquad (4.3)$$

The left hand part of this equation is termed the lime potential. Thus, the lime potential does not change if the base saturation of the soil remains constant, according to the lime potential concept. At constant Ca^{2+} activity and when Ca is the main base cation on the exchange complex, equation 4.3 may be rewritten as:

$$pH = k' + 0.5 \log \frac{BS}{(1 - BS)^2} \qquad (4.4)$$

where BS is the base saturation of the ion exchange complex.

In a preliminary experiment, the pH (measured in 0.001 M $CaCl_2$), the CEC and the amount of exchangeable bases were measured for four soils (of Neerpelt) amended with lime at three rates. The theoretical curve (equation 4.4) fitted the experimental data well, when *k'* was set to 4.2 (Figure 4.2).

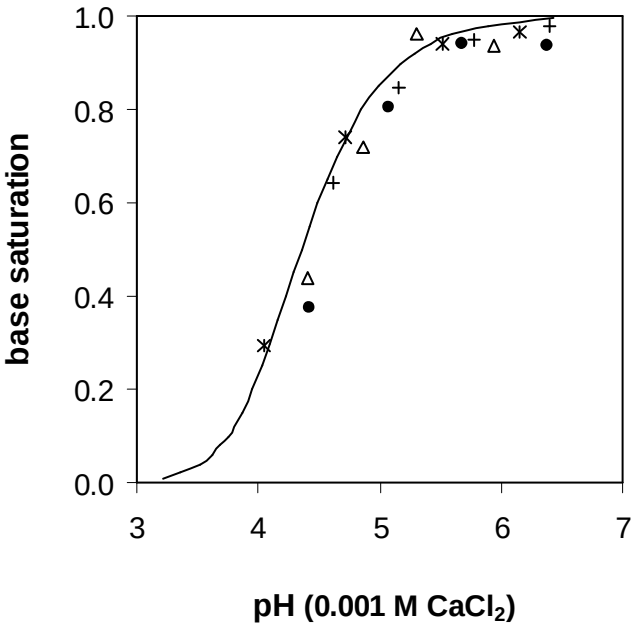

Figure 4.2 The relation between base saturation and pH. The symbols are observed values for four soils that were amended with lime at three rates. The line gives the theoretical relation derived from Ca^{2+}/H^{+} exchange.

Figure 4.3a shows the same theoretical curve of base saturation versus the lime potential (equation 4.3). Also the base saturation (estimated based on the results of the preliminary experiment) for the different treatments of soil NP are plotted against the lime potential of the soil solution.

Figure 4.3 also illustrates the effect of incubation. Mineralization and nitrification of organic N during incubation results in the production of protons:

$$R\text{-}NH_2 + 2\ O_2 \rightarrow R\text{-}OH + NO_3^- + H^+ \qquad (4.5)$$

These protons will displace cations from surface-exchange sites. Mineralization (followed by nitrification) in a closed system, where the excess ions cannot drain, therefore results in an increase in the ionic strength and a decrease in pH of the soil solution. The amount of protons produced between 1 and 9 weeks of incubation in the highest lime treatment was estimated, based on the increase in NO_3^- concentration (Table 4.3), at 3 meq kg^{-1} for soil NP and 6 meq kg^{-1} for soil H. This amount is a substantial fraction of the CEC that ranges from 20 to 50 meq kg^{-1}, depending on pH, in these sandy soils. The decrease in the base saturation, estimated from the increase in NO_3^- concentration (Table 4.3), was in good agreement with the observed decrease in lime potential (Figure 4.3a) and in soil pH (measured in 0.01M $CaCl_2$) upon incubation. The decrease in the pH of the soil solution upon incubation was much more pronounced than the decrease in the soil pH, because of the increase in the ionic strength. This effect is illustrated in Figure 4.3b where Figure 4.3a is replotted with the pH of soil solution in the x-axis. At the same Ca saturation, the soil solution pH is lower when the Ca concentration is larger. The increase in Ca concentration upon incubation was most pronounced in the limed soils, which explains why the increase in pH of the soil solution upon liming becomes smaller with time (Table 4.2).

Mineralization and nitrification in a closed system clearly results in an increase in the ionic strength and a decrease in the soil solution pH. In the field, no such increase in ionic strength is to be expected since the excess cations can freely drain. However, nitrification will also result in acidification if the rate of nitrification exceeds the nitrate uptake, which will probably be the case immediately after the lime addition. The nitrogen transformations will have little effect on the pH (if there is no net N input), once steady state is reached and mineralization equals assimilation.

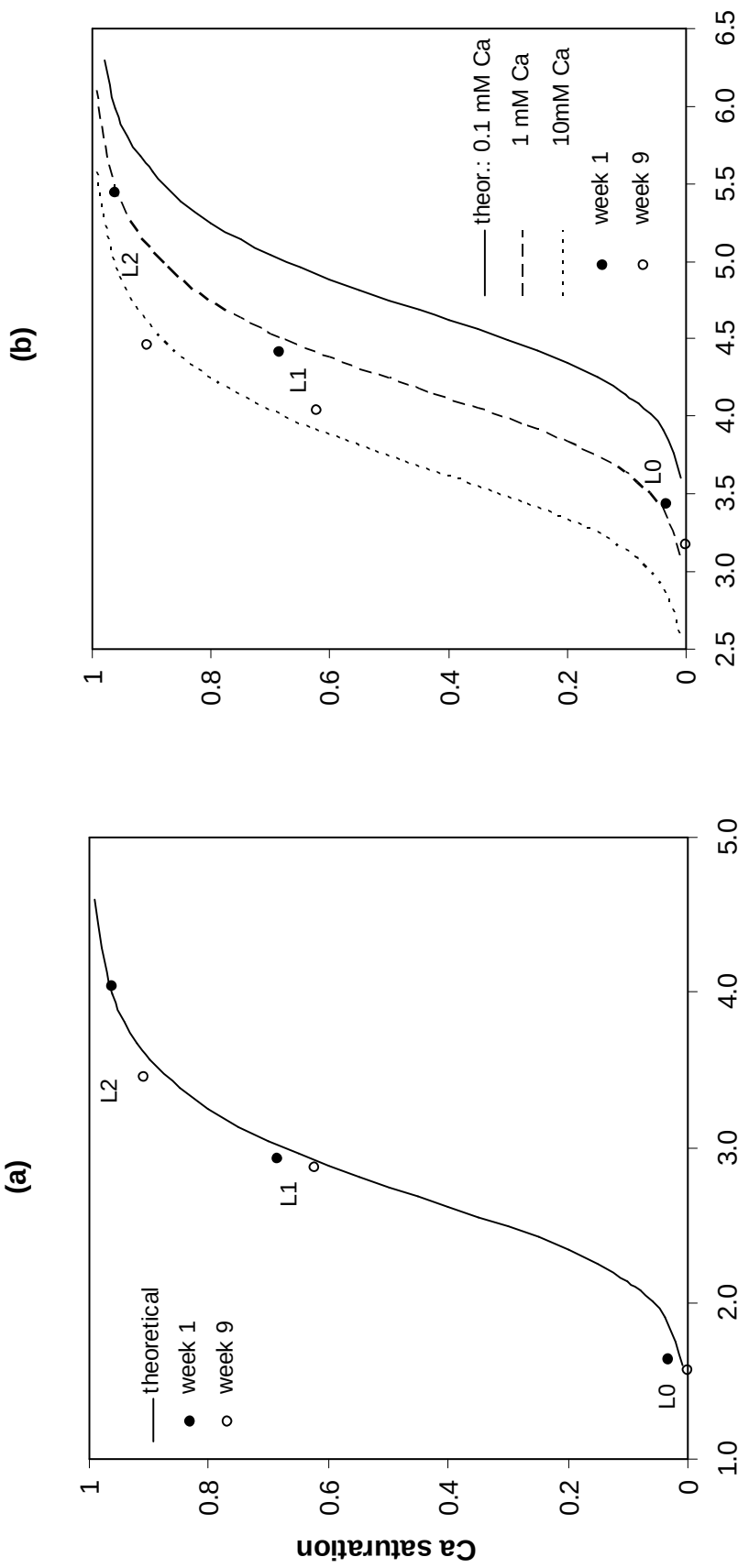

Figure 4.3 The relation between Ca saturation and (a) lime potential or (b) pH of the soil solution for control (L0) and limed (L1, low dose; L2, high dose) after one and nine weeks if incubation (soil NP). The lines give the theoretical relationships (equation 4.3).

4.4.2 Effect of liming and incubation on Cd and Zn distribution

The changes in pore water concentrations of Cd and Zn upon liming and incubation can be explained by the changes in pH and in Ca concentration. An increase in the soil pH with two units resulted in a ten-fold decrease of the pore water concentrations of Cd and Zn in the field contaminated soil from Neerpelt (Table 4.2). The effect of increase in pH upon liming, resulting in a decrease of pore water concentrations of Cd and Zn, was partly counteracted by the increase in Ca concentration and the stronger complexation with DOC at higher pH, but these effects were small in comparison with the pH effect.

The concentrations of Cd and Zn increased upon incubation because the soil solution pH decreased and the Ca concentration increased. This effect was most pronounced in the limed soils, and therefore the effect of liming on pore water concentrations of Cd and Zn diminished as incubation progressed. After 9 weeks of incubation, pore water concentrations of Cd and Zn for the low lime treatment (L1) of soil H were even larger than those in the unlimed soil (Table 4.2). The soil solution pH was similar for these two treatments, and the pore water concentration of Ca was larger in the limed soil, which explains the larger Cd and Zn concentrations in the limed soil.

Pore water concentrations of Cd and Zn in both soils were similar for treatments with nearly identical soil solution composition (pH, Ca concentration). Both soils had almost identical *E* values. Thus, the 'labile' K_d , which is the ratio of *E* value to the pore water concentration, was similar in both soils if soil solution composition was comparable. Regression equations 3.6 and 3.7 (derived from an independent dataset) were used to predict the pore water concentrations based on the *E* value and the K_d^{lab} predicted from the pH, the organic C content, and the pore water concentration of Ca. The predicted concentrations were within a factor 3 (Cd) or 2 (Zn) from the observed concentrations (Figure 4.4).

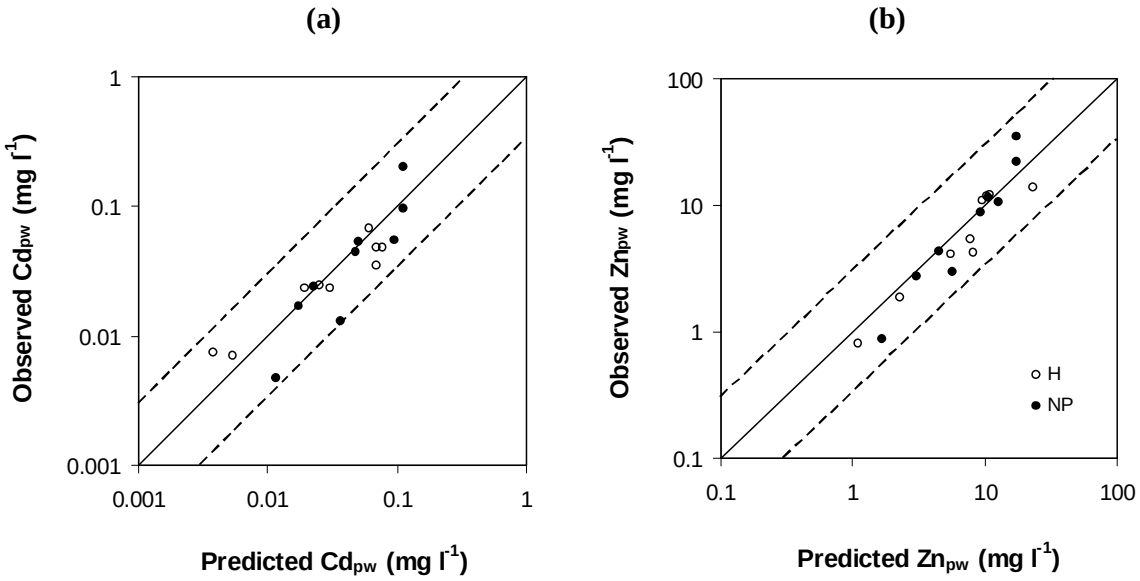

Figure 4.4 Observed versus predicted pore water concentrations of (a) Cd, and (b) Zn for soil H and soil NP. Predictions were made based on radio-labile metal concentrations and a regression equation derived from an independent dataset (equations 3.6 and 3.7). The dotted lines indicate 3 times over- or underprediction.

In conclusion, the pore water concentrations of Cd and Zn in a contaminated soil decreased tenfold when the pH was increased with two units. Incubation increases the ionic strength of the soil solution and the pore water concentrations of Cd and Zn. The pore water concentrations of Cd and Zn increased up to five-fold between one and nine weeks of incubation (20°C). These increases were attributed to mineralization of N, and were most pronounced in the limed treatments.

part II

Transport of Cd and Zn in columns

CHAPTER 5

Transport of Cd and Zn in acid sandy soils: effect of pore water velocity

Abstract

The transport of Cd and Zn at varying pore water velocities was measured to assess whether the breakthrough curves could be described based on the local equilibrium assumption (LEA). Column experiments were performed using a contaminated podzol with aged Cd and Zn and an uncontaminated podzol with freshly applied Cd and Zn. The columns were leached with 0.5 mM $Ca(NO_3)_2$, at pore water velocities of around 6, 12 and 30 cm day^{-1}.

Breakthrough curves of a non-sorbing tracer, $^{36}Cl^-$, were well described with the convection-dispersion equation (CDE) at the lowest pore water velocity. Breakthrough curves at the higher pore water velocities demonstrated increased tailing and a left-handed displacement, and could be well described with a two-region model (TRM).

The transport of Cd and Zn was modelled with the CDE model using sorption parameters obtained from batch experiments, and assuming that only radio-labile metals can be desorbed. The transport of freshly applied Cd and Zn was well described at all pore water velocities. The breakthrough curves of indigenous Cd and Zn showed an initially faster decrease of the concentration than was predicted based on the LEA. However, observed and predicted breakthrough curves of Cd and Zn were in reasonable agreement, even at the highest pore water velocity. Predicted concentrations in the column effluent differed at most 37% from the observed concentrations. It was concluded that the LEA may be used to predict the transport of Cd and Zn in field contaminated soils, if it is assumed that only labile metals are in equilibrium with the solution phase.

5.1 Introduction

Sandy soils in the northern part of Belgium are contaminated by atmospheric deposition of heavy metals. These soils show relatively low retention of Cd and Zn, and therefore, leaching of these metals is fast, thus imposing a risk of groundwater contamination. Transport models, used to predict leaching of Cd and Zn to the groundwater, should represent the chemical and physical mechanisms affecting the transport of these metals. The simplest transport models are based on the local equilibrium assumption (LEA). The validity of the LEA for Cd transport has been questioned in several studies, where evidence was found that non-equilibrium conditions existed during the transport (e.g., Kookana *et al.*, 1994). Non-equilibrium may result from physical or chemical (sorption-related) non-equilibrium. Sorbing and non-sorbing solutes are both subject to physical non-equilibrium. Sorption-related non-equilibrium may result from true chemical non-equilibrium, or from rate-limited diffusion. Bi-continuum (two-region or two-site) models describing physical or chemical equilibrium can be reduced to the same mathematical form (Nkedi-Kizza *et al.*, 1984).

Several transport studies where non-equilibrium in Cd transport was observed, were conducted at high pore water velocities, in the order of 50 cm d^{-1} and more (e.g., Kookana *et al.*, 1994; Boekhold *et al.*, 1992). Pore water velocities in the field are, on average, around 0.3 cm d^{-1} for the regions studied, and the maximum velocity is probably around 5 cm d^{-1}. Large pore water velocities may result in non-equilibrium conditions (Gaber *et al.*, 1995), and therefore, it cannot be concluded that non-equilibrium conditions will also prevail in the field.

Chemical non-equilibrium may occur when the reaction rate is small relative to the rate of the convective transport (Valocchi, 1985). Slow reactions in soil may remove metals from the sorption surface into interior sorption sites, from which desorption is very slow. In addition, metals may have entered the soil in an insoluble form (e.g., mine spoils, massive metallic forms, etc.), and may therefore not be available for leaching (Roberts *et al.*, 2002). Isotopic dilution methods have been used to discriminate between chemically reactive (labile) and non-labile metal pools (e.g., Nakhone *et al.*, 1993; Smolders *et al.*, 1999). The lability of Cd and Zn is usually high in low pH soils, though labile fractions may be small in topsoils where the metals were added in insoluble form (Degryse *et al.*, 2003b). It is usually assumed that non-labile metals do not participate in the solid–liquid distribution within a realistic time frame. Based on this assumption, the metal transport

can be calculated using sorption parameters that describe the distribution between the labile metal pool (not the total metal pool) and the solution phase. Streck and Richter (1997a) used EDTA (0.025 M)-extractable Cd and Zn to model the transport of Cd and Zn in a sandy soil, based on similar reasoning.

In this study, we measured the transport of Cd and Zn in sandy soils at varying pore water velocities. A column experiment was conducted for an unpolluted soil with freshly applied (and hence fully labile) Cd and Zn, and for a contaminated soil in which Cd and Zn were partly in non-labile form. Experimental results were compared with model predictions of the Cd and Zn transport. Model calculations were performed with independently derived sorption parameters, and assuming that only radio-labile metal could be leached from the soil.

5.2 Materials and methods

5.2.1 Soils

The uncontaminated soil was sampled from the B_h horizon of a Spodosol profile in a nature conservation area (Houthalen, Belgium). The contaminated soil was taken from the A horizon of a Spodosol profile in the northern part of Belgium (Neerpelt). This area has been contaminated with Cd and Zn during more than 100 years by atmospheric deposition of Zn smelters. The soils were sieved (< 2 mm) and air dried. The organic C content was measured by dry combustion (Skalar CA 100). The pH was determined in 0.001 M $CaCl_2$ in a soil:solution ratio of 1:10 after 3 days of equilibration. The 'total' metal concentration was determined by *aqua regia* digestion. The radio-labile concentration (*E* value) was determined as described in section 2.2.2. The main soil characteristics are summarized in Table 5.1.

Table 5.1 Characteristics of the soils used in the column experiment

	OC	pH	Cd_{tot}	E_{Cd}	Zn_{tot}	E_{Zn}
	(%)		(mg kg^{-1})			
Houthalen (H)	0.7	4.2	0.1	0.1	7.6	1.3
Neerpelt (NP)	1.9	4.6	5.6	3.6	407	259

5.2.2 Adsorption and desorption isotherms

Adsorption isotherms were measured on both soils. Two g of air-dry soil was equilibrated with 20 ml of 0.001 M $CaCl_2$ at various Cd:Zn concentrations (0:0, 0.1:10, 0.2:20 and 0.5:50 mg Cd l^{-1}: mg Zn l^{-1}) labelled with ^{109}Cd and ^{65}Zn. The suspensions were shaken end-over-end for six days, and centrifuged at 3000*g* (30min). The pH of the supernatant was measured, Cd and Zn concentrations were measured with ICP-OES, and the activity of ^{109}Cd and ^{65}Zn was determined.

A desorption isotherm was measured on the contaminated soil (Neerpelt), by measuring Cd and Zn concentrations in solution at different soil:solution ratios (ranging from 1:460 to 1:5 kg l^{-1}). The soil was weighed into a dialysis bag (Visking 12-14000 Daltons, Medicell, London), and 5 ml of a 10^{-3} M $CaCl_2$ solution was added. The dialysis bag was transferred to the remaining $CaCl_2$ solution. Concentrations of Cd and Zn in the equilibrium solution were measured with ICP-OES after 7 days of end-over-end shaking.

5.2.3 Column experiment

The transport of Cd and Zn in two soils at different pore water velocities was measured. Treatments are summarized in Table 5.2. Twelve polyvinylchloride columns (3.6 cm i.d.) were used, with a fiberglass wick or Passive Capillary Sampler (PCAPS) (AM 3/8 HI) rolled up on the bottom of the column (Figure 5.1). The free end of the wick, surrounded by a PVC tube, protruded through a hole in the centre of the bottom of the column. The wicks were used to obtain unsaturated streaming. The wicks were pre-treated by heating them during 4 hours at 400°C, washing them in 0.001 M $CaCl_2$ acidified to pH 2.6, and rinsing them in 0.001 M $CaCl_2$. A preliminary experiment showed that Cd and Zn did not adsorb on the treated wicks. The optimal length of free end of the wick was calculated according to the procedure of Knutson and Selker (1994) and was between 40 and 60 cm. A glass fibre filter was placed on top of the column to ensure homogeneous distribution of the feeding over the column. The columns were filled with moist soil (6 cm high). Sorting of the particles during packing was avoided by placing a piston of slightly smaller diameter than the column on the surface of the soil after each increment and by tapping the column. The packed columns were saturated from top to bottom with a 0.001 M $CaCl_2$ solution by slowly raising the open end of the wicks while adding water to it. The free end of the wicks was lowered again, and, after one week of equilibration, the feeding solution was

applied by a peristaltic pump at a constant flux (flow rates in Table 5.2). The feeding solution for the columns 1 to 6 (filled with contaminated soil) was 0.001 M $CaCl_2$, adjusted to pH 4.5 with H_2SO_4. Columns 7 to 12 (filled with uncontaminated soil) were initially fed with a solution of 0.001 M $CaCl_2$, 1 mg l^{-1} Zn and 0.02 mg l^{-1} Cd, adjusted to pH 4.2. When complete breakthrough was reached, a 0.001 M $CaCl_2$ solution (pH 4.2) without Cd or Zn was added to the columns. The columns were kept at a constant temperature of 4°C. The effluent samples were collected daily, the volume was recorded by weight, and the pH was measured. The samples were acidified to pH=1 with HNO_3 and analyzed for Cd, Zn and major cations with ICP-OES. Columns 5 and 6 were dismantled 41 days after the start of the experiment, columns 3, 4, 9, 10, 11 and 12 after 60 days and columns 1, 2, 7 and 8 after 128 days.

Prior to dismantlement, transport parameters (D, v) were estimated from $^{36}Cl^-$ breakthrough curves. A ^{36}Cl pulse (0.4 pore volumes) was applied to each column. Samples were regularly collected, until complete breakthrough. Activity of ^{36}Cl in the samples was determined with a liquid scintillation counter (Packard Tricarb 1600 CA). Breakthrough curves of ^{36}Cl were also determined for the wicks, after the soil was removed, to evaluate the effect of the wick on the total dispersivity.

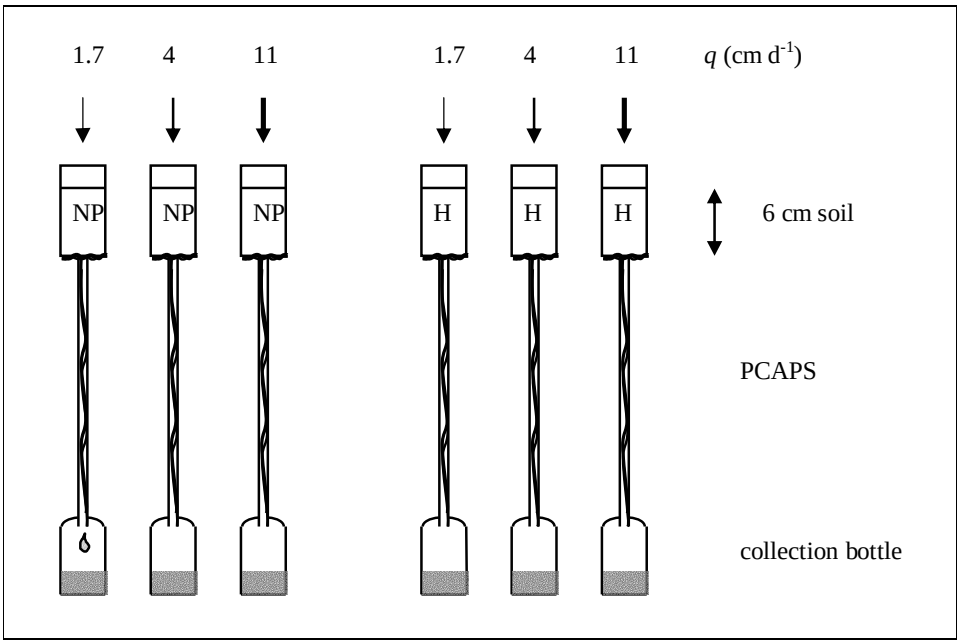

Figure 5.1 Schematic presentation of the soil column setup
(NP: Neerpelt, polluted soil; H: Houthalen, unpolluted soil)

Table 5.2 Summary of the transport experiments

	Neerpelt			Houthalen		
Column	1/2	3/4	5/6	7/8	9/10	11/12
q (cm day^{-1}) †	1.7	4.4	11.3	1.7	4.3	11.1
θ (-)	0.33	0.42	0.46	0.24	0.29	0.31
ρ (g cm^{-3})	1.42	1.42	1.42	1.60	1.60	1.60
Feeding solution	$CaCl_2$ 0.001M			1) $CaCl_2$ 0.001M + Cd 0.02 mg l^{-1} Zn 1 mg l^{-1}		
				2) $CaCl_2$ 0.001M		

† q: water flux density

5.2.4 Transport models

One-dimensional transport of a sorbing solute through soil may be described with the convection-dispersion equation (eq. 1.10), that can also be written as:

$$R \cdot \frac{\delta c}{\delta t} = D \frac{\delta^2 c}{\delta z^2} - v \frac{\delta c}{\delta z} \tag{5.1}$$

where R is the retardation coefficient, defined as:

$$R = 1 + \frac{\rho}{\theta} \cdot \frac{\delta s}{\delta c} \tag{5.2}$$

In case of linear sorption, $\delta s/\delta c$ is given by the K_d. Non-linear sorption is often described with a Freundlich isotherm:

$$s = k.c^n \tag{5.3}$$

In this case, $\delta s/\delta c$ is concentration dependent:

$$\frac{\delta s}{\delta c} = n \cdot k \cdot c^{n-1} \tag{5.4}$$

The CDE may fail to predict the transport of a solute in soil because of non-equilibrium processes. Physical non-equilibrium may be conceptualized by a two-region model (TRM) that divides the soil water into mobile and immobile (stagnant) regions. Solute exchange between the two liquid phases is often described by a first order kinetic diffusion process (van Genuchten and Wierenga, 1976):

$$\theta_m \cdot \frac{\delta c_m}{\delta t} + \rho \cdot f \cdot \frac{\delta s_m}{\delta t} = \theta_m \cdot D \cdot \frac{\delta^2 c_m}{\delta z^2} - \theta_m \cdot v_m \cdot \frac{\delta c_m}{\delta z} - \alpha \cdot (c_m - c_{im}) \tag{5.5a}$$

$$\theta_{im} \cdot \frac{\delta c_{im}}{\delta t} + \rho \cdot (1 - f) \cdot \frac{\delta s_{im}}{\delta t} = \alpha \cdot (c_m - c_{im}) \tag{5.5b}$$

where subscripts 'm' and 'im' refer to mobile and immobile regions respectively, α is the first-order mass transfer coefficient describing the transfer between the mobile and immobile liquid phases, and *f* is the fraction of sorption sites that equilibrate with the mobile water.

Sorbing solutes may also be subject to chemical non-equilibrium. The two-site model (TSM) divides the exchange sites into type-1 sites (s_1), that are in equilibrium with the solution phase, and type-2 sites (s_2), on which sorption is time-dependent (cf. section 1.4.1). Though the physical and chemical non-equilibrium models differ conceptually, they are mathematically indistinguishable (Nkedi-Kizza *et al.*, 1984).

5.3 Results and discussion

5.3.1 Sorption isotherms

The sorption isotherms could be well described with a Freundlich isotherm (Figure 5.2 and Figure 5.3). The Freundlich parameters *k* and *n* were obtained by linear regression for log*s* versus log*c*:

$\log s = \log k + n.\ \log c$

where *c* is the concentration in solution (mg l^{-1}), and *s* is the labile concentration on the solid phase (mg kg^{-1}), calculated as the product of the solution concentration and the isotopic distribution coefficient. The results are given in Table 5.3.

Table 5.3 Freundlich parameters *k* and *n*, obtained from batch experiments (adsorption isotherm for Houthalen and desorption isotherm for Neerpelt)

	Cd		Zn	
	k	*n*	*k*	*n*
Soil	$mg^{1-n}\ l^n\ kg^{-1}$		$mg^{1-n}\ l^n\ kg^{-1}$	
Houthalen	3	0.80	4	0.70
Neerpelt	14.5	0.57	65	0.60

Both adsorption and desorption isotherms were measured on the soil from Neerpelt. The low values for *n* are probably due to the high metal load of this soil. The zinc concentration of this soil is 407 mg kg^{-1}, which corresponds to 1.3 $cmol_c\ kg^{-1}$ or 45% of the CEC (3 $cmol_c\ kg^{-1}$). No discontinuity between the adsorption and the desorption isotherm

was observed (Figure 5.3). Filius *et al.* (1998) found no hysteresis in a soil with pH 4.7, while a clear discontinuity was observed for soils with higher pH, especially at short equilibration times.

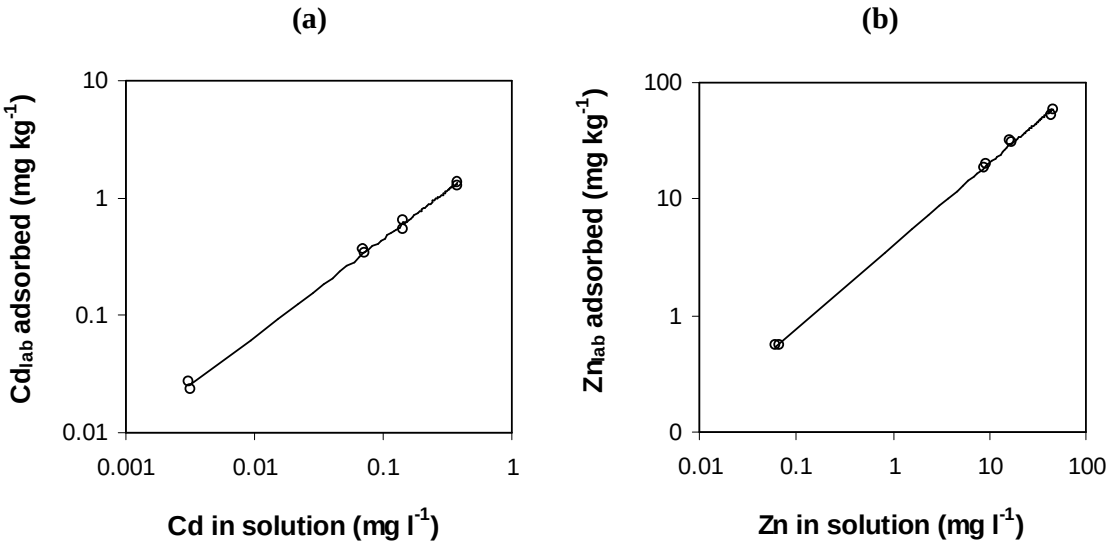

Figure 5.2 Adsorption isotherm of (a) Cd, and (b) Zn for the uncontaminated soil (Houthalen).

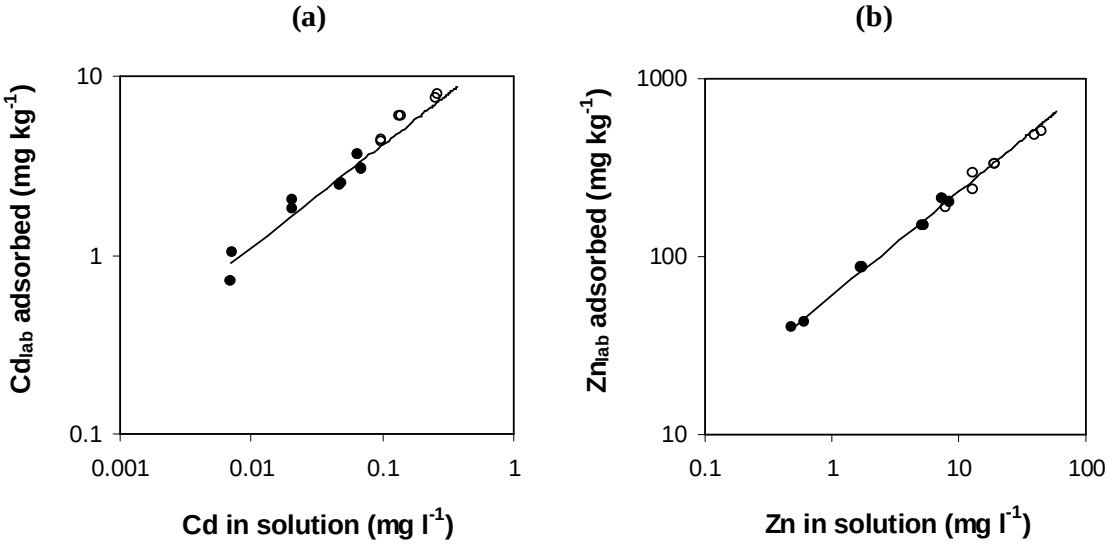

Figure 5.3 Desorption (closed symbols) and adsorption (open symbols) isotherms of (a) Cd, and (b) Zn for the contaminated soil (Neerpelt). The Freundlich isotherm is fitted on the desorption data.

5.3.2 Breakthrough of ^{36}Cl

The parameters *v* and *D* of the convection-dispersion (CDE) model were optimised with CXTFIT (Toride *et al.*, 1995).

Wicks

All curves could be well described by the CDE model. The dispersion coefficient increased with increasing pore water velocity (Figure 5.4). The dispersion length λ (=*D*/*v*) only varied slightly with pore water velocity and was, on average, 1.1 cm. This is in good agreement with the value of 1.0 cm found by Boll *et al.* (1992) for wicks with wick filaments spread on a flat plate.

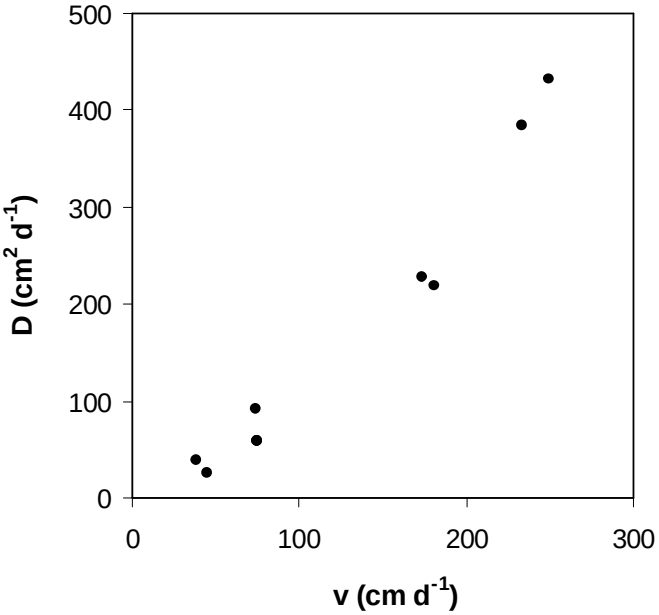

Figure 5.4 Dispersion coefficient as a function of pore water velocity in fibreglass wicks.

Columns

The breakthrough curves of ^{36}Cl at the lower pore water velocity could be well described with the CDE (Table 5.4 and Figure 5.5a). The tailing at the end of the breakthrough curves, observed at the higher pore water velocities, could not be described with the CDE model, but was well described with the TRM model (Figure 5.5). Relative mobile water contents for the treatments with pore water velocities above 10 cm d^{-1} ranged from 0.72 to 0.87 (Table 5.4). The calculated mass transfer coefficient α increased with increasing pore

water velocity, as was also observed by Seuntjens *et al.* (2001b) and Reedy *et al.* (1996). Convective mixing of the immobile liquid at higher pore water velocities may explain this increase in α (van Genuchten and Wierenga, 1977).

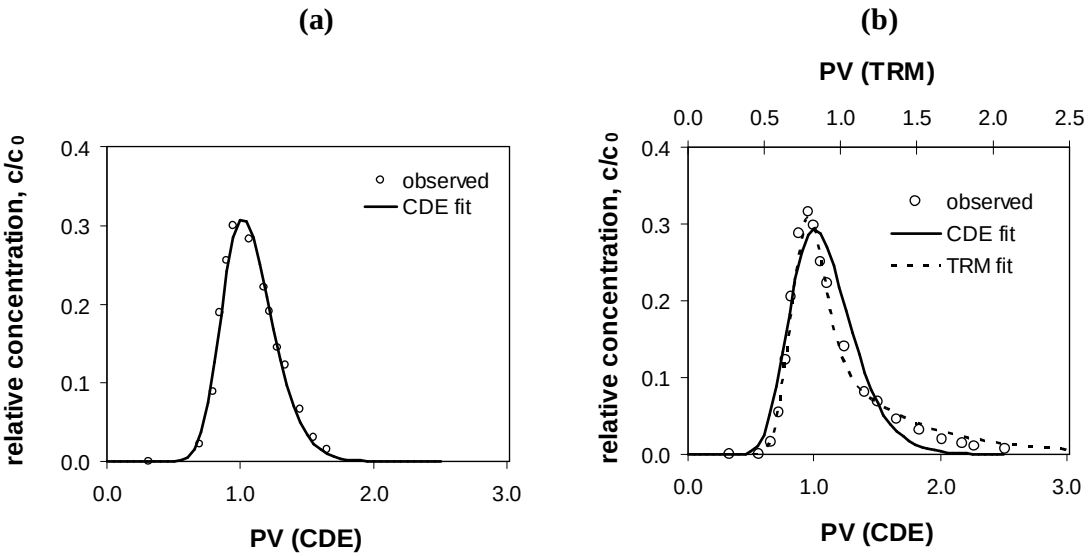

Figure 5.5 Observed and fitted breakthrough curves of ^{36}Cl in the soil from Neerpelt, using the convection-dispersion equation (CDE) or the two- region model (TRM) at a pore water velocity of (a) 6 cm d^{-1}, and (b) 12 cm d^{-1}.

5.3.3 Breakthrough of Cd and Zn

The transport of Cd and Zn was modelled with the CDE model, using the sorption parameters from the batch experiments and the transport parameters (v, D) from the ^{36}Cl breakthrough. The transport parameters obtained with the CDE model (Table 5.4) were used. At the higher pore water velocities, where non-equilibrium was observed, D optimized with the CDE model may be considered as an effective model parameter that combines two processes: actual dispersion and additional dispersion caused by physical non-equilibrium. The effect of the wick on the transport of Cd and Zn was tested with model calculations. It was found that the contribution of the wick to the dispersion of these sorbing solutes was negligible. Therefore, breakthrough curves of Cd and Zn were only corrected for the travel time in the wick. The calculations were performed with the HYDRUS-1D code (Šimůnek *et al.*, 1998).

Table 5.4 Results of the nonlinear least-square fit (with CXTFIT) of the parameters *v* (pore water velocity) and *D* (dispersion coefficient) for the convection-dispersion model (CDE), and the parameters *D*, β (= θ_m/θ) and ω of the Two-Region Model (TRM).

	CDE				TRM				
	v (cm d^{-1})	*D* (cm^2 d^{-1})	λ [a] (cm)	R^2	*D* (cm^2 d^{-1})	θ_m/θ	ω [b]	α [c] (d^{-1})	R^2
soil NP	6.3 (0.015)	0.9 (0.02)	0.15	1.00					
	6.2 (0.017)	0.8 (0.02)	0.14	1.00					
	11.9 (0.15)	3.4 (0.34)	0.29	0.95	0.96 (0.11)	0.79 (0.008)	1.04 (0.11)	0.42	1.00
	10.9 (0.08)	3.3 (0.21)	0.30	0.97	1.79 (0.11)	0.86 (0.008)	0.45 (0.07)	0.17	1.00
	28.4 (0.44)	10.1 (0.98)	0.36	0.93	2.75 (0.26)	0.72 (0.006)	0.75 (0.06)	0.72	0.99
	26.0 (0.28)	8.3 (0.57)	0.32	0.97	3.75 (0.38)	0.84 (0.015)	0.84 (0.17)	0.90	1.00
soil H	4.9 (0.04)	0.7 (0.05)	0.15	0.98					
	4.8 (0.03)	1.1 (0.08)	0.23	0.98					
	13.8 (0.12)	5.6 (0.41)	0.41	0.98	3.07 (1.9)	0.86 (0.023)	1.39 (0.46)	0.40	0.99
	14.1 (0.13)	2.8 (0.24)	0.20	0.96	1.01 (0.31)	0.87 (0.030)	1.26 (0.56)	0.37	0.99
	31.5 (0.60)	19.1 (1.15)	0.61	0.98	5.90 (1.37)	0.73 (0.035)	1.75 (0.39)	1.28	0.99
	37.8 (0.60)	13.4 (1.50)	0.36	0.93	4.22 (0.58)	0.79 (0.011)	0.89 (0.13)	0.71	0.99

[a] λ = *D*/*v*; [b] ω: dimensionless mass transfer coefficient; [c] α: mass transfer coefficient, α = $\omega\theta v/L$ (*L*: length of column)

Only the right part of the breakthrough curve (i.e., when the columns were fed with the metal free solution) was modelled for the unpolluted soil where Cd and Zn were freshly added to the column. The left part was not considered, since the wicks influenced leachate composition in the beginning of the experiment, which was reflected in the high pH (~6) during the 10 first pore volumes. This problem was also encountered by Brahy and Delvaux (2001). The breakthrough curves were reasonably well described with the independent predictions of the CDE model, even at the largest pore water velocity (Figure 5.6). The good agreement between predicted and observed breakthrough curves indicates that chemical non-equilibrium is limited and that the physical non-equilibrium observed at the higher pore water velocities has little influence on the breakthrough of sorbing solutes.

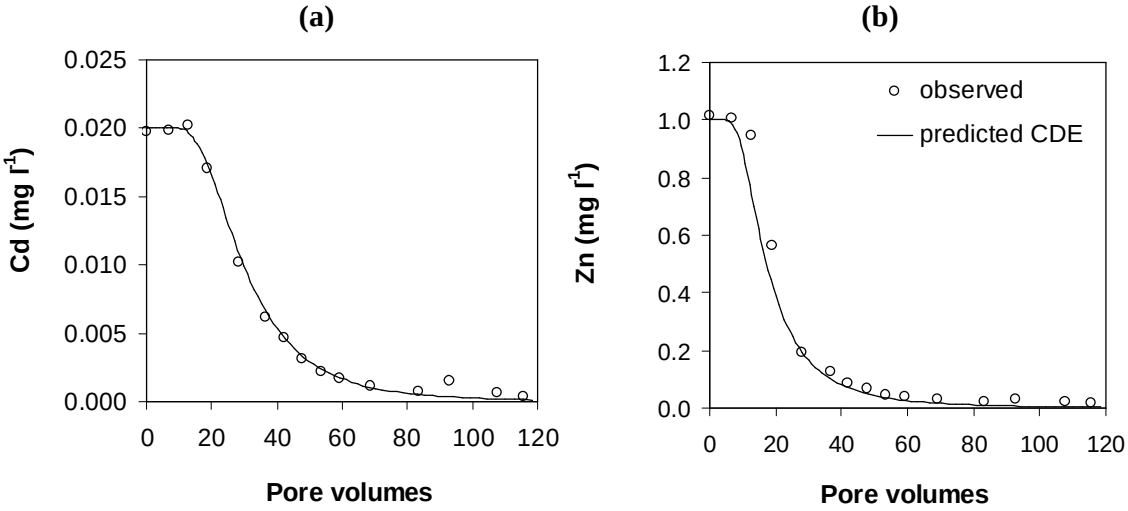

Figure 5.6 Observed and predicted breakthrough curves of (a) Cd and (b) Zn freshly applied to an unpolluted soil, at a pore water velocity of 38 cm d^{-1}. Predictions were made with the CDE model, using sorption parameters derived from batch experiments.

The small effect of the physical non-equilibrium on the breakthrough curve is also illustrated in Figure 5.7. The breakthrough curve was predicted with CXTFIT using a constant K_d value (since CXTFIT does not allow the use of a Freundlich isotherm) with the LEA, or with the non-equilibrium parameters obtained from the ^{36}Cl breakthrough (Table 5.4). The agreement between observed and predicted breakthrough curves was not as good as when using the Freundlich isotherm (Figure 5.6), but the difference was small since the Freundlich exponent was close to 1 in the unpolluted soil (0.8 for Cd). Predictions with the TRM model were very similar to these of the CDE model (Figure 5.7).

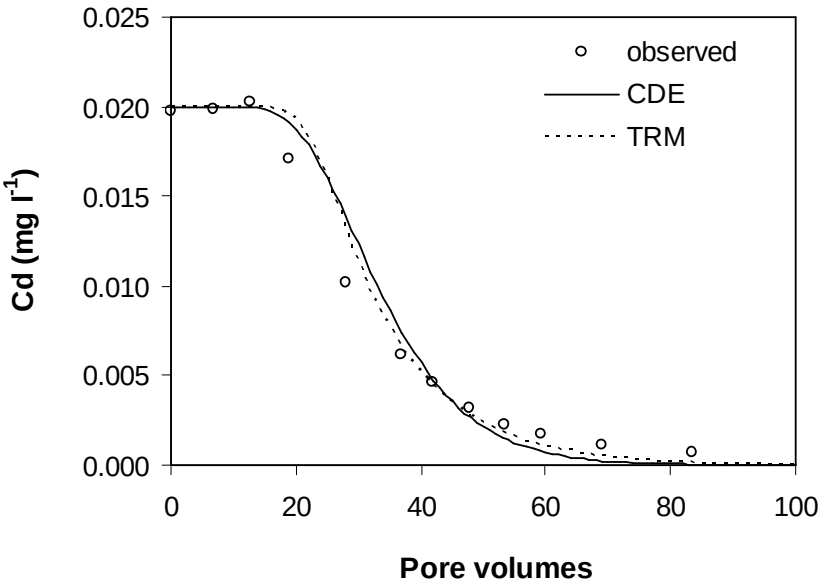

Figure 5.7 Observed and predicted breakthrough curve of Cd freshly applied to an unpolluted soil, at a pore water velocity of 38 cm d^{-1}. Predictions were made (with constant K_d value) assuming local equilibrium (CDE model, full line), or with a physical non-equilibrium model using parameters derived from the ^{36}Cl breakthrough (TRM model, dotted line).

Figure 5.8 shows the predicted breakthrough curves of indigenous Cd and Zn in a soil polluted with heavy metals due to Zn smelter activities. Predictions were made with the CDE model using sorption parameters derived from batch experiments, assuming that only the radio-labile Cd and Zn concentration can be leached from the soil (Figure 5.8, dotted lines). The predicted breakthrough curves were in reasonable agreement with the observed ones. It should be noted that the sorption parameters (Table 5.3) were measured at 20°C, while the column experiment was carried out at 4°C. A slightly smaller value for the Freundlich parameter *k* would probably have been obtained, if the sorption parameters had been obtained at 4°C (e.g. Barrow, 1986). Predicted and observed breakthrough curves would have agreed better if predictions were made with a smaller *k*. The deviation between observed and predicted breakthrough was more pronounced at higher pore water velocities, indicating that large pore water velocities enhance non-equilibrium conditions. This non-equilibrium may have been caused solely by physical constraints, but may also have been sorption-related. However, even at the largest pore water velocity, observed and predicted breakthrough curves were in reasonable agreement, considering that independently determined sorption parameters were used for the prediction.

Breakthrough curves were also modelled with the total K_d value, i.e., the ratio of total metal concentration to solution concentration at the start of the experiment. The mass of Cd and Zn leached is clearly overestimated if it is assumed that all Cd and Zn can be desorbed (Figure 5.8, full line).

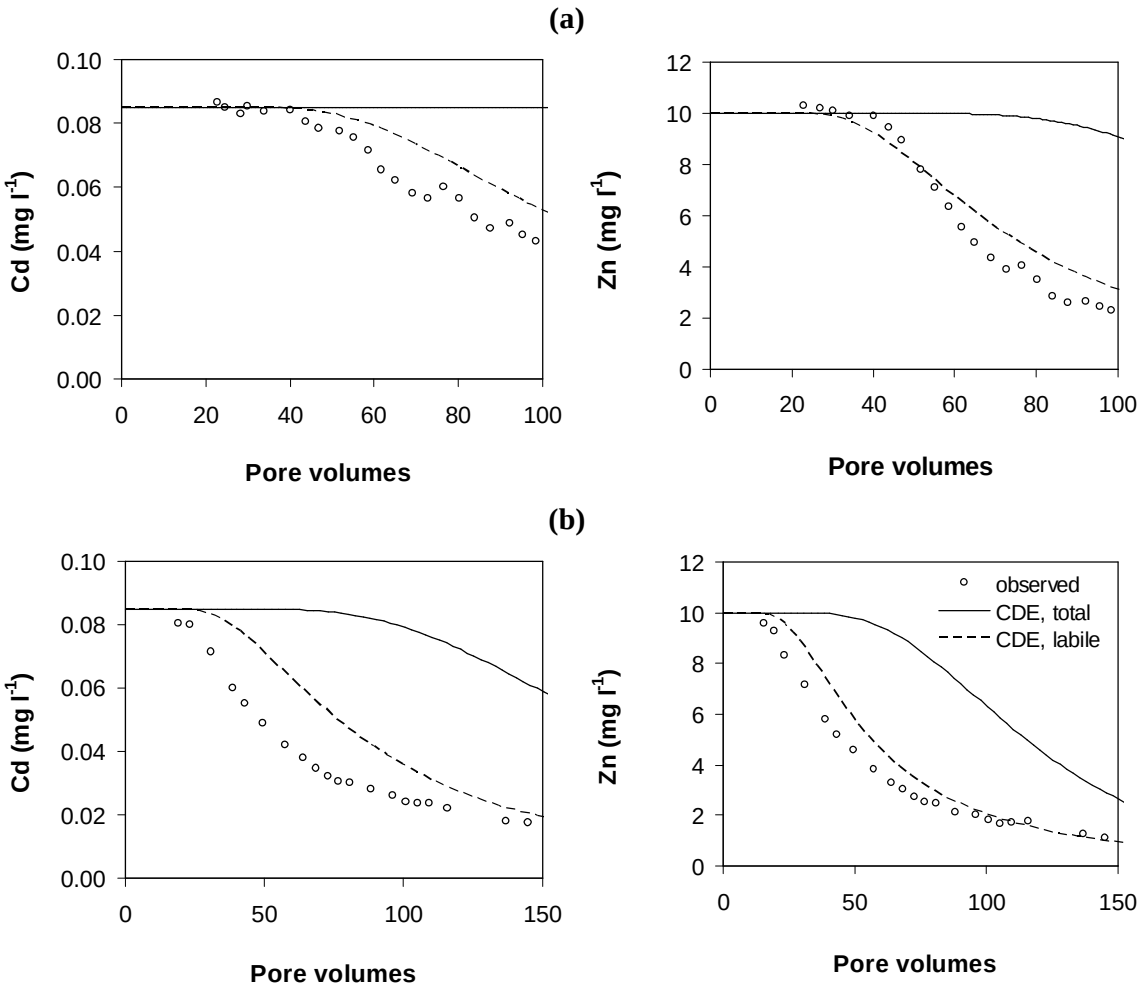

Figure 5.8 Breakthrough curves of indigenous Cd and Zn in a contaminated soil (Neerpelt) at a pore water velocity of (a) 6 cm d^{-1}, and (b) 26 cm d^{-1}. Predictions were made with the CDE model using a Freundlich equation and assuming that only radio-labile metal can be leached (dotted lines) or using the total K_d (full lines).

The results of this column experiment indicate that the local equilibrium assumption may be used to predict the transport of Cd and Zn, if it is assumed that only the labile pool is in equilibrium with the solution. The transport of Cd and Zn in field contaminated soils was greatly overestimated if it was assumed that all metal was in equilibrium with the solution phase, i.e., if the (total) K_d was used for the calculations.

CHAPTER 6
Transport of Cd and Zn in limed soils: a column study

Abstract

The effect of soil liming on transport of Cd and Zn was assessed in a column experiment. Artificial soil columns were made with 2 cm topsoil and 3 cm subsoil from a site with acid sandy soils contaminated with heavy metals due to smelter activities. The topsoil (pH 4.3) was either limed with CaO to pH 5.2, or left unlimed. Columns were leached with 0.5 mM $Ca(NO_3)_2$, at a pore water velocity of around 6 cm d^{-1}. After 4 months, the amount of Cd leached from the columns in which the topsoil was limed was about half of the amount leached from the control columns.

Concentration profiles of total and radio-labile Cd and Zn were determined after 1, 2, 3 and 4 months of leaching. Cadmium and Zn that was initially not radio-labile (i.e., not isotopically exchangeable within 3 days) was slowly released from the columns, when the radio-labile Cd and Zn was depleted. Model calculations were performed with sorption parameters derived from batch experiments. The concentrations in the leachate and the concentration profiles could be well described with a 2-site model, where it was assumed that the labile metal was in equilibrium with the solution phase and that non-labile metal was subject to kinetic desorption.

6.1 Introduction

Soils in the northern part of Belgium (Kempen) have been contaminated with Cd and Zn due to the activity of Zn smelters in the 20th century. Most soils in this area are acid sandy soils (Spodosols). Model predictions have shown that large amounts of Cd will be transported to the groundwater in the next 100 years, if no remedial actions are taken (e.g., Seuntjens, 2002).

Liming might be an option to reduce leaching of Cd and Zn to the groundwater, since the solid–liquid distribution coefficient of these metals increases about 5-fold for a pH increase with one unit (cf. Chapter 3). Total concentrations of Cd and Zn in soils from lime amendment experiments were found to be smaller in the topsoil and higher in the subsoil from control plots in comparison with limed plots (Weng *et al.*, 2001; Filius *et al.*, 1998), indicating that transport of Cd and Zn is reduced by liming.

Isotopic exchange studies have shown that not all Cd and Zn in the soil is radio-labile (e.g., Young *et al.*, 2000). In low pH soils, the lability of these metals is generally high, though labile fractions may be small in topsoils where the metals were added in insoluble form (Degryse *et al.*, 2003b; Chapter 2). Non-labile metals are often considered to be fixed; it is assumed that they do not contribute to sorption–desorption processes. In the previous chapter, it was shown that breakthrough curves of Cd and Zn in a field contaminated soil could be well predicted assuming that the radio-labile metals are in equilibrium with the solution phase, and that non-labile metals are fixed. However, it may not be excluded that slow desorption of non-labile metals may occur in the long term, when the labile pool is nearly depleted.

In this study, the changes in Cd mobility upon liming of an acid soil were assessed in a column experiment. Concentrations in the effluent solution were measured, and total and radio-labile concentration profiles of Cd and Zn were determined at various times. Model calculations were performed with independently measured transport and sorption parameters. The aim of the experiment was twofold:

(i) to quantify the effect of liming on the transport of Cd and Zn.

(ii) to assess whether metal was released that was initially not isotopically exchangeable.

6.2 Materials and methods

6.2.1 Column experiment

The soils used were sampled from a soil profile in Balen, near a Zn smelter. Topsoil was sampled from the upper 10 cm of the profile, and the subsoil was sampled between 35 and 45 cm depth, by use of an Edelman auger. Soil properties are summarized in Table 6.1.

Table 6.1 Properties of the soils used in the column experiment.

	pH †	CEC $cmol_c\ kg^{-1}$	Organic C %	Cd_{tot} $mg\ kg^{-1}$	Zn_{tot} $mg\ kg^{-1}$
topsoil	4.3	2.0	2.62	4.0	173
subsoil	4.3	1.4	0.85	1.7	44

† pH measured in 0.5 mM $Ca(NO_3)_2$ (S/L=1/10 $kg\ l^{-1}$)

Sixteen polypropylene columns (3 cm i.d.) equipped with a porous glass plate were filled with moist soils (Figure 6.1). The columns consisted of 2 layers: the lower 3 cm was filled with the subsoil and the upper 2 cm was filled with the topsoil. In eight of the columns the topsoil was limed (0.56 g CaO kg^{-1} soil, equivalent to a dose of 1.5 ton $CaCO_3$ ha^{-1} for a 10 cm layer), in the other columns the soil was applied without liming. Sorting of the particles during packing was avoided by tapping the column after each increment using a piston of slightly smaller diameter than the column. The soil was packed at a bulk density of 1.35 g cm^{-3}. On top of the soil, a glass fibre filter was placed to ensure a homogeneous inflow of the feeding solution over the column. The experiment was started after 3 weeks of incubation at 20°C. The feeding solution ($Ca(NO_3)_2$ 0.5 mM adjusted to pH=4.3 with H_2SO_4) was applied by a peristaltic pump at a flow rate of 14 ml day^{-1}. A suction of 25 kPa was applied at the bottom to ensure unsaturated streaming through the columns. The effluent was collected through a Teflon funnel into polypropylene bottles. The effluent was sampled weekly and volume was recorded by weight. The samples were acidified to pH=1 with HNO_3 and analyzed for Cd, Zn and Ca with ICP-OES.

Each month, two columns for each treatment were dismantled. The soil core was removed and sliced into 1 cm layers. Two subsamples (1g) of every layer were weighed and oven dried (3d, 105°C), to determine the water content. The pH and the *E* values of Cd and Zn were measured for all layers (in 0.5 mM $Ca(NO_3)_2$ at S/L=1/10, 3 days of equilibration). The total Cd and Zn concentration was determined by *aqua regia* digestion.

The CEC and the concentration of exchangeable bases were determined at the pH of the soil using silverthiourea as index cation (Chhabra *et al.*, 1975).

Transport parameters (D, v_{pw}) were derived from $^{36}Cl^-$ breakthrough curves measured prior column dismantling (cf. section 5.2.3).

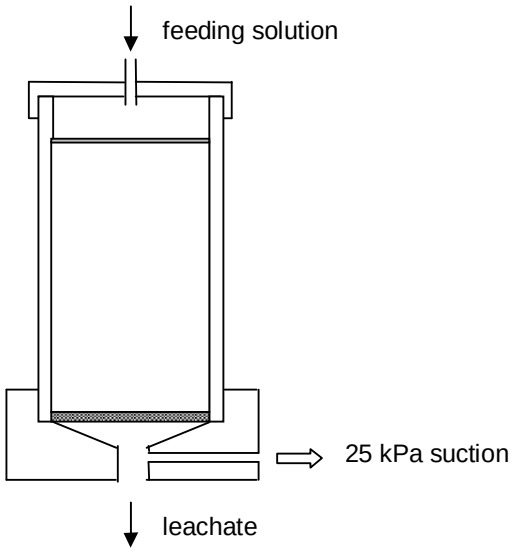

Figure 6.1 Schematic presentation of the soil columns

6.2.2 Transport models

One-dimensional transport of a sorbing solute through soil is often described with the convection-dispersion equation (CDE), assuming local equilibrium (eq. 1.10). However, physical and chemical non-equilibrium processes may cause earlier breakthrough than is predicted with the CDE. Physical non-equilibrium may be conceptualized by a two-region model (TRM) that divides the soil water into mobile and immobile (stagnant) regions (see section 5.2.4). Sorbing solutes may be subject to chemical non-equilibrium. The two-site model (TSM) divides the exchange sites into type-1 sites (s_1), that are in equilibrium with the solution phase, and type-2 sites (s_2), on which sorption is time-dependent (Figure 1.7). In case sorption is described with the Freundlich isotherm (eq. 5.3), the transport equations for the two-site model are (Šimůnek *et al.*, 1998):

$$\frac{\delta c}{\delta t}\cdot(1+\frac{\rho}{\theta}\cdot f\cdot n\cdot k_{tot}\cdot c^{n-1}) = D\frac{\delta^2 c}{\delta z^2} - v\frac{\delta c}{\delta z} - \frac{\rho}{\theta}\cdot\alpha\cdot\left[(1-f)\cdot k_{tot}\cdot c^n - s_2\right] \quad (6.1a)$$

$$\frac{\delta s_2}{\delta t} = \alpha\cdot\left[(1-f)\cdot k_{tot}\cdot c^n - s_2\right] \quad (6.1b)$$

where f is the fraction of equilibrium sites, α is the first-order rate coefficient (d^{-1}), k_{tot} and n are the Freundlich parameters (that describe the distribution between solid phase and solution at equilibrium) and the other symbols are equal to those in equation 1.10.

6.3 Results and discussion

6.3.1 Changes in pH, CEC and Ca saturation

Depth profiles of pH, CEC and exchangeable bases were determined 1, 2, 3 and 4 months after the start of the experiment. The pH of the control columns showed little variation with time (Figure 6.2). A significant increase in pH was observed in the subsoil of the limed columns.

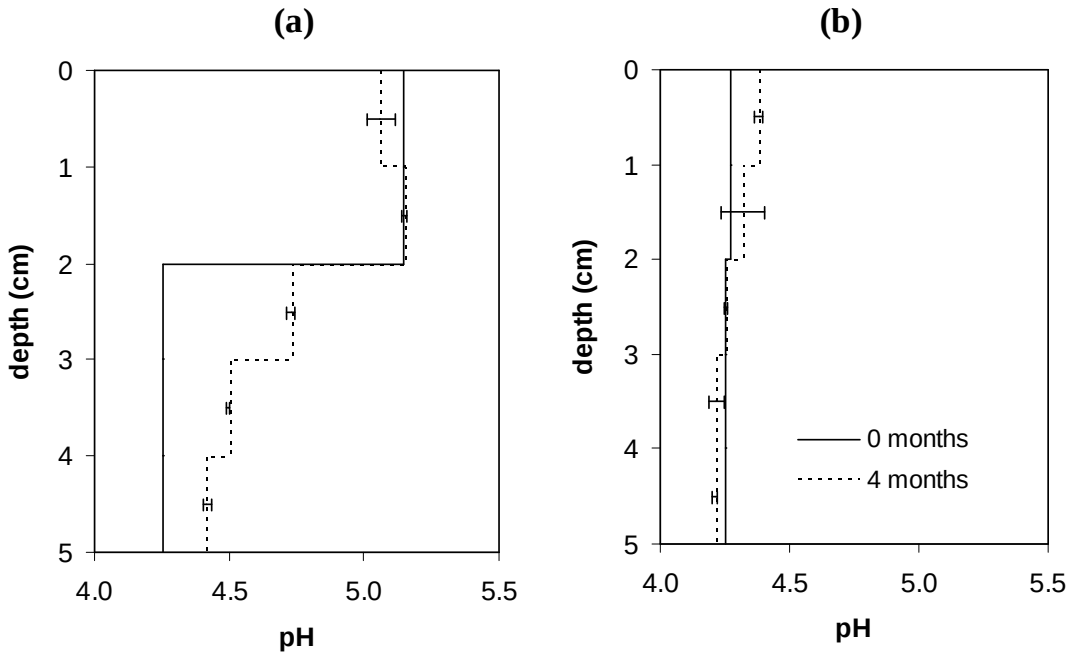

Figure 6.2 Depth profiles of pH at the start and the end of the experiment (4 months of leaching, in (a) columns where the toplayer was limed, and (b) control columns without lime addition. Mean ± standard deviation (error bars) of 2 replicates.

This increase in pH coincided with an increase in base saturation, and in exchangeable Ca content (Figure 6.3). The Ca saturation in the layer immediately beneath the limed topsoil increased from 32% initially to 63% at the experiment. The CEC was only slightly affected by the increase in pH (Figure 6.3).

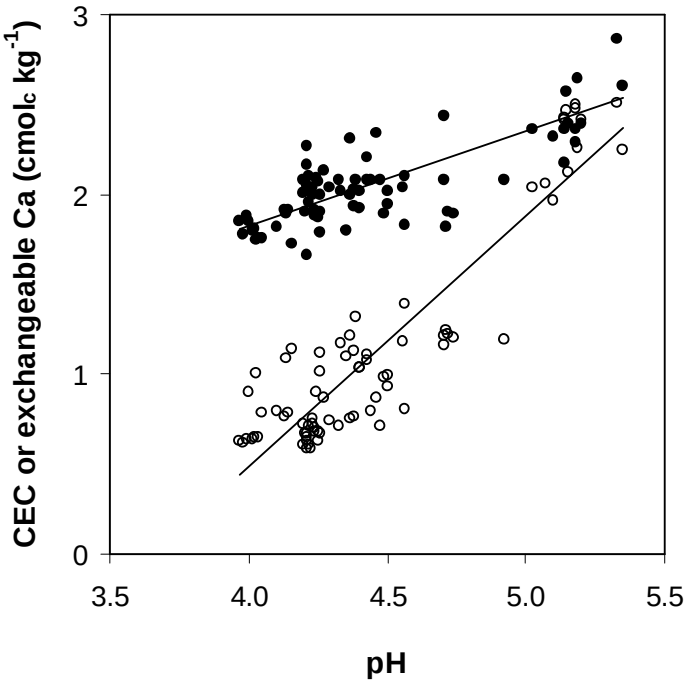

Figure 6.3 Exchangeable Ca (open symbols) and CEC (closed symbols) as a function of pH (measured in 0.5 mM $Ca(NO_3)_2$). Measurements were carried out on column layers (5 per column) at 1, 2, 3 and 4 months after the start of the experiment.

6.3.2 Distribution of Cd and Zn

The *E* values and distribution coefficients of Cd and Zn were determined in 0.5 mM $Ca(NO_3)_2$ at 1 cm-depth intervals, after 1, 2, 3 and 4 months of leaching. Liming decreased the *E* values of the topsoil (Table 6.2).

The Freundlich parameters *k* and *n* were determined for the limed and unlimed topsoil and the subsoil (of both limed and unlimed columns) (Table 6.2). These values were derived by linear regression analysis for $\log s_1$ versus $\log c$:

$\log s_1 = \log k + n.\log c$

where c is the concentration in solution (mg l^{-1}), and s_1 is the labile concentration on the solid phase (mg kg^{-1}) calculated as the product of the solution concentration and the isotopic distribution coefficient. The layer immediately beneath the limed topsoil (2-3 cm layer in the limed columns) was not considered, since sorption was time dependent in this layer because of the increase in pH.

Table 6.2 The radio-labile concentration (E) at the start of the experiment and Freundlich parameters (k and n) for the partitioning of Cd and Zn between the radio-labile pool and the solution phase. These parameters were obtained from batch experiments.

	Cd			Zn		
	E	k	n	E	k	n
	mg kg^{-1}	mg^{1-n} l^n kg^{-1}		mg kg^{-1}	mg^{1-n} l^n kg^{-1}	
topsoil - limed	2.0	100	0.85	52	80	0.85
topsoil - unlimed	2.5	18	0.78	65	15	0.80
subsoil	1.4	16	0.80	39	13	0.80

6.3.3 Transport of Cd and Zn

Table 6.3 gives the amounts of Cd and Zn lost by leaching. These amounts may be calculated from the product of leachate volume and metal concentration in the leachate, or from the decrease in total metal concentration in the soil (determined when the columns were dismantled). Both methods gave similar results (Table 6.3). The metal losses were larger in the control columns than in the limed columns.

Table 6.3 The amount of Cd and Zn lost by leaching in limed columns and in control columns, calculated from the metal amount recovered in the leachate or from the decrease in total metal concentration in the soil.

	Cd lost (µg) (initial Cd content: 118 µg)				Zn lost (µg) (initial Zn content: 4260 µg)			
time [a]	limed		control		limed		control	
(months)	leached	ΔCd_{tot}	leached	ΔCd_{tot}	leached	ΔZn_{tot}	leached	ΔZn_{tot}
1	20	20	26	25	984	838	1691	1752
2	32	28	41	40	1337	1096	2166	1971
3	40	41	63	61	1510	1428	2375	2339
4	46	50	81	80	1886	1987	2491	2572

[a] 1 month ~ 50 pore volumes

Predictions of the Cd and Zn transport were made (with the HYDRUS-1D code), using the hydraulic parameters (v, D) obtained from the ^{36}Cl breakthrough. The pore water velocity v was between 4.5 and 7.7 cm d^{-1}. The dispersivity λ (= v/D) ranged from 0.13 to 0.36 cm, and was on average 0.24 cm. The breakthrough curves of ^{36}Cl could be well described with the CDE model, indicating that there was no physical non-equilibrium.

6.3.3.1 Equilibrium transport

The transport of Cd and Zn was predicted with the CDE model assuming that all Cd and Zn was in equilibrium with the solution phase or that only the radio-labile concentration (E value) was in equilibrium. Figure 6.4 illustrates these two approaches for the limed topsoil.

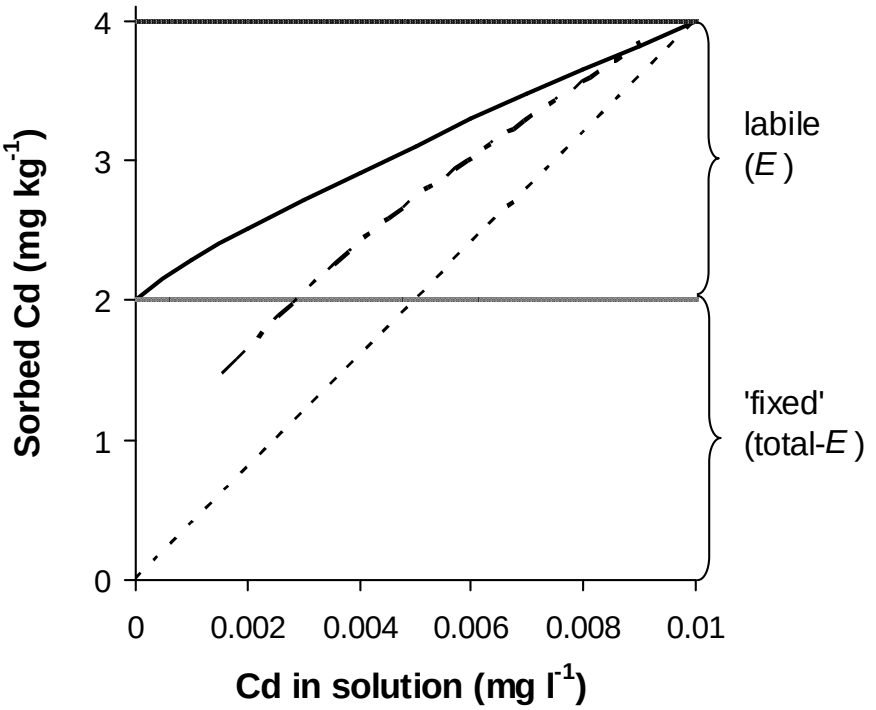

Figure 6.4 Sorption isotherms of Cd in the limed topsoil, used for the prediction of the Cd transport in the column experiment. The full line is a Freundlich isotherm where only radio-labile Cd is in equilibrium with Cd in solution (parameters in Table 6.1). The dotted line gives the sorption isotherm with constant K_d and where all Cd is assumed in equilibrium with Cd in solution. The point-dashed line gives the solid–liquid distribution predicted with the two-site model after 4 months of leaching (details in section 6.3.3.2).

The measured and predicted concentration profiles are shown in Figure 6.5 for Cd and in Figure 6.6 for Zn. Total concentrations of Cd and Zn decreased more slowly in the limed columns than in the control columns, because of the stronger retention of Cd and Zn in the limed columns. Radio-labile Zn in the topsoil was already removed after one month of leaching in the control columns. Further leaching removed Zn from the 'fixed' pool (Figure 6.6b). Zinc that was initially not radio-labile, i.e., not isotopically exchangeable within 3 days, was slowly released. Not all radio-labile Cd was removed after 1 month of leaching (Figure 6.5b), illustrating the higher retention for Cd than for Zn. However, a release of non-labile Cd was also observed after 4 months of leaching (Figure 6.5b).

Predicted concentrations were much smaller than the observed concentration in the upper layer of the control columns when all metal was assumed to be in equilibrium with the solution phase (Figure 6.5b and 6.6b, dotted lines), indicating that leaching of Cd and Zn is strongly overestimated when based on total rather than on labile metal concentrations, as was also concluded in the previous chapter. Concentrations predicted with the CDE model based on labile metal concentrations (Figure 6.5 and 6.6, full lines) were larger than observed concentrations after 4 months of leaching, especially in the control columns, where non-radio-labile metal was released from the column. In the limed columns, the metal concentration in the third layer (2-3 cm of depth) was underpredicted, since the increase in pH of this layer was not taken into account in the model.

Concentrations of Cd and Zn in the leachate were measured weekly. Leaching was overestimated when all Cd and Zn was assumed to be in equilibrium with the solution phase (Figure 6.7 and Figure 6.8), as was already concluded from the soil concentration profiles. The breakthrough curves were better described when it was assumed that only radio-labile metal was available, but the tailing of the breakthrough curves was generally underestimated, which is indicative of non-equilibrium.

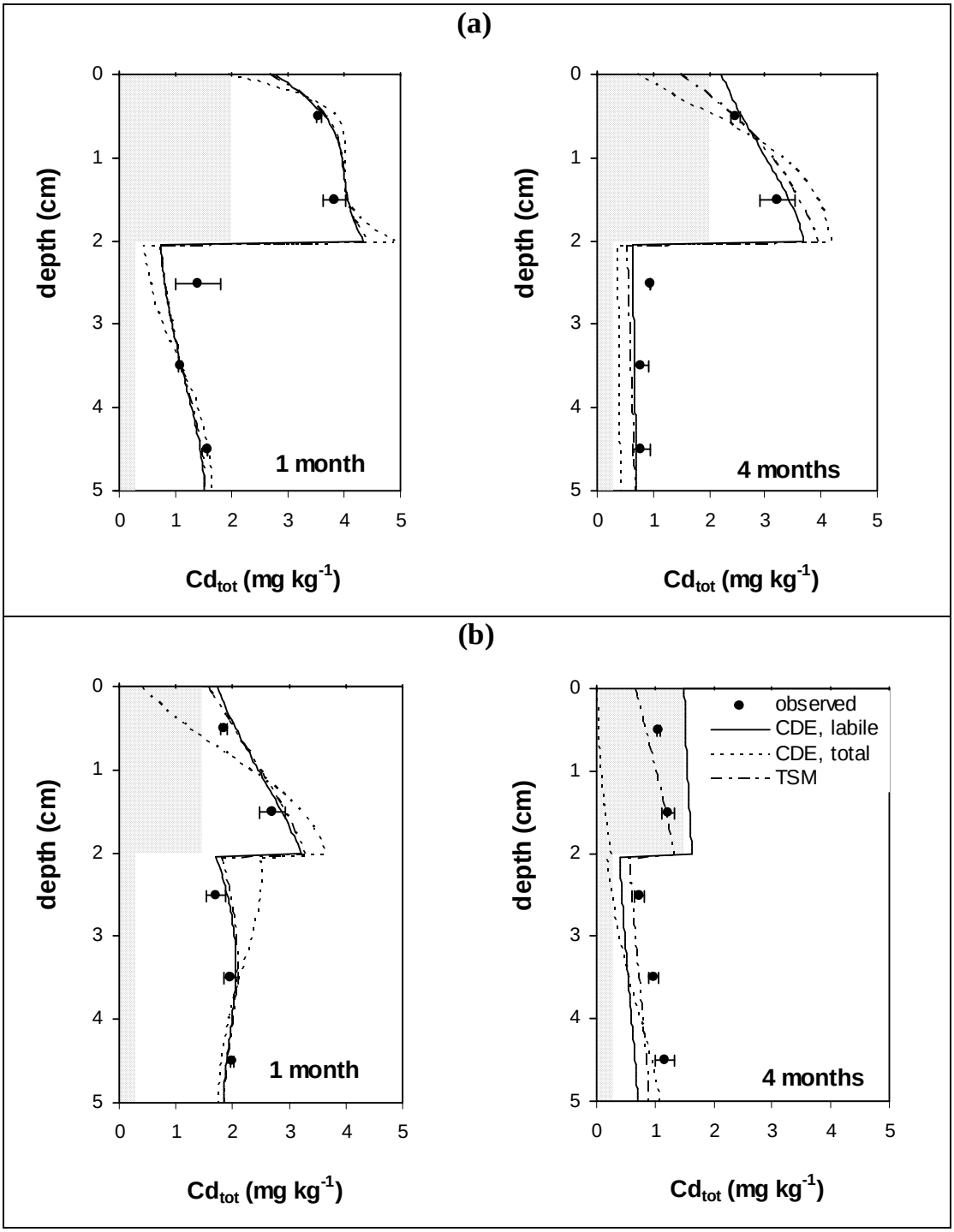

Figure 6.5 Measured (points ± SD) and predicted total Cd concentration profiles after 1 month and after 4 months of leaching, in (a) limed and (b) control columns. Predictions were made with the CDE model based on *E* values or based on total metal concentration, or with the two-site model (TSM). The shaded area represents non-labile Cd at the start of the experiment, as determined by isotopic dilution.

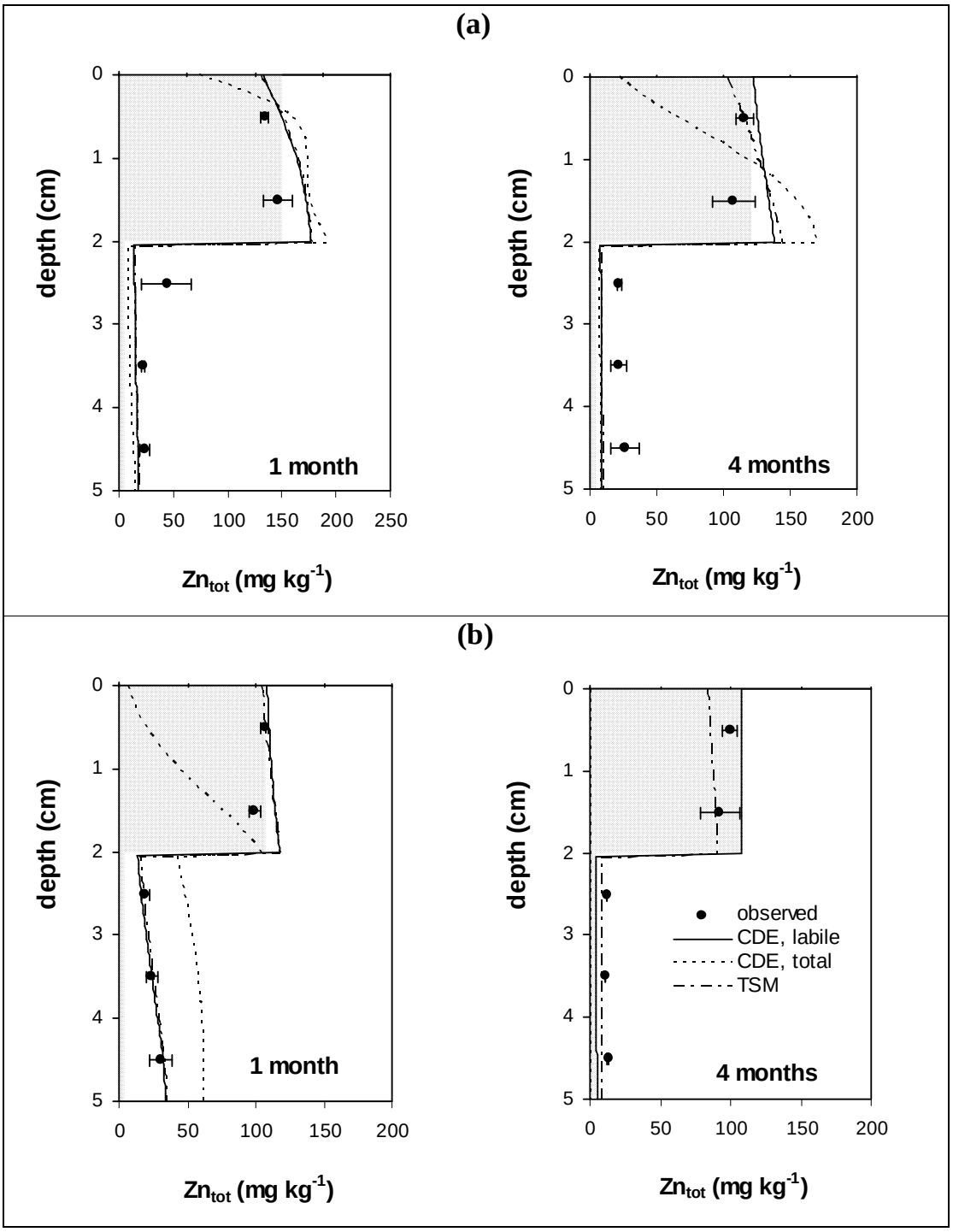

Figure 6.6 Measured and predicted total Zn concentration profiles after 1 month and after 4 months of leaching, in (a) limed and (b) control columns. Predictions were made with the CDE model based on *E* values or based on total metal concentration, or with the two-site model (TSM). The shaded area represents non-labile Zn at the start of the experiment, as determined by isotopic dilution.

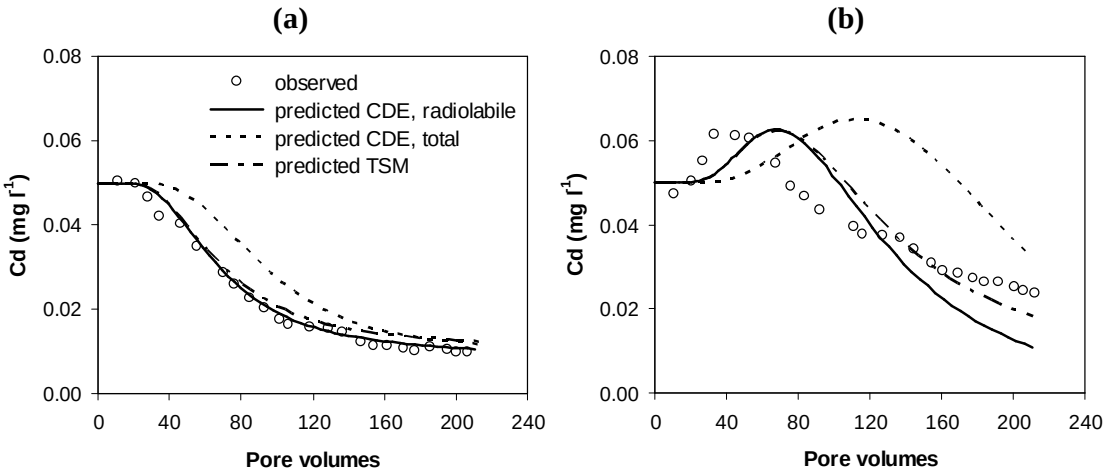

Figure 6.7 Predicted and observed breakthrough of Cd in (a) limed and (b) control columns. Predictions were made with the convection-dispersion equation (CDE), or with a non-equilibrium transport model (two-site model, TSM), using independently determined sorption parameters. The radio-labile concentration (*E* value) or the total Cd concentration was assumed to be in equilibrium with the solution phase for the predictions with the CDE model. For the two-site model, it was assumed that the radio-labile Cd was in equilibrium and that non-labile Cd was subject to kinetic desorption.

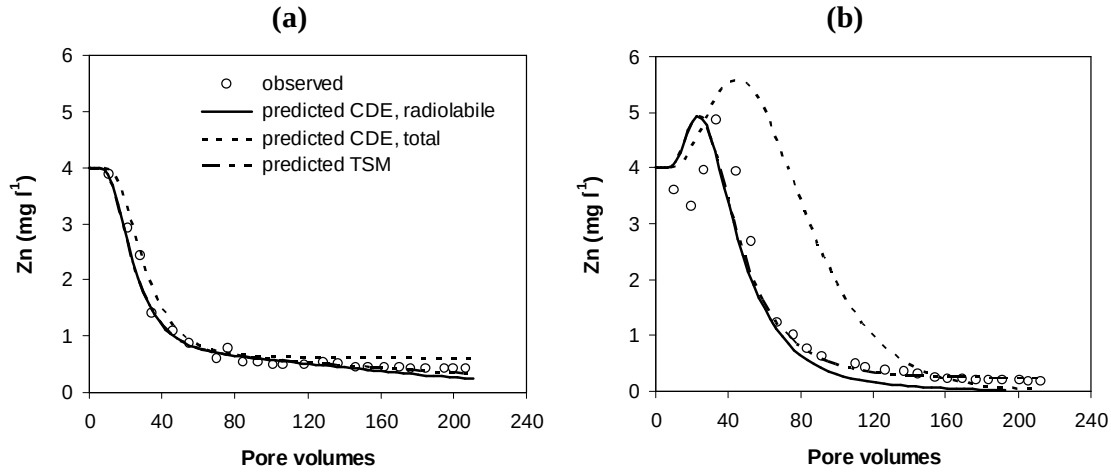

Figure 6.8 Predicted and observed breakthrough of Zn in (a) limed and (b) control columns. Predictions were made as explained in Figure 6.7.

The cumulative amount of Cd and Zn leached was compared with the radio-labile and total metal concentration at the beginning of the experiment (Figure 6.9). In the control columns, radio-labile Zn was almost completely depleted after 50 pore volumes, because of the low retention of Zn in this soil. Non-(radio)labile Zn was also released, but at a much slower rate. These finding indicate that the transport should be modelled by a two-site

model, where the radio-labile metal is in equilibrium with the metal in solution and the non-radio-labile metal is subject to kinetic desorption.

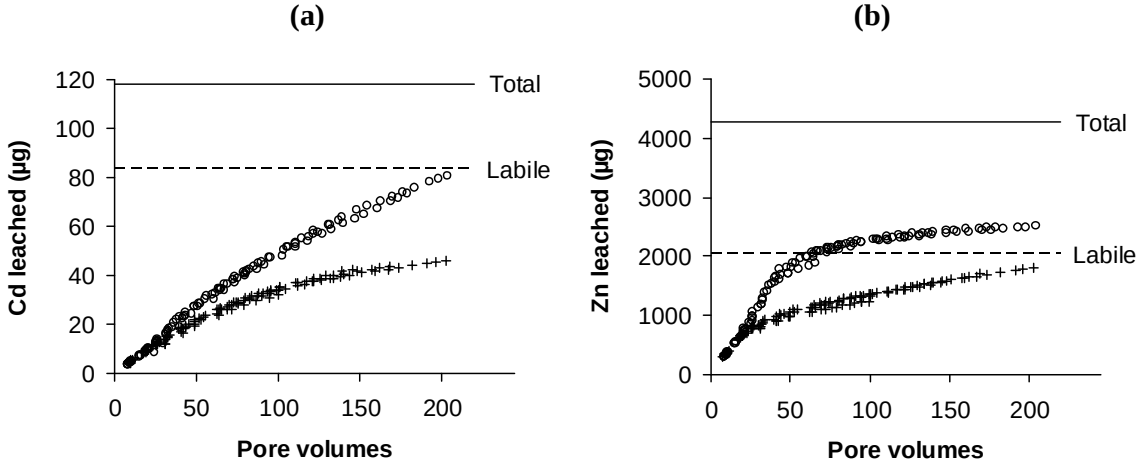

Figure 6.9 Total amount of (a) Cd and (b) Zn leached in limed columns (crosses) and control columns (open circles). The lines represent the total (aqua regia soluble) metal amount and the amount of radio-labile metal present in the column at the start of the experiment.

6.3.3.2 Non-equilibrium transport

The transport was modelled with a two-site model (eq. 6.1) assuming that the radio-labile metal was in equilibrium with the solution phase (type-1 sites), and that (initially) non-labile metal was subject to kinetic desorption (type-2 sites).

Every month, total and radio-labile concentrations were measured at 1-cm depth intervals. The non-labile metal concentration (s_2, mg kg^{-1}), calculated as the difference between total and labile concentration, decreased with time. After 2 months of leaching, labile Cd and Zn was almost completely removed from the upper part (0-1 cm) of the control columns, and solution concentrations were near zero. In this case, Eq. 6.1b can be written as

$$s_2 = s_2^0 \cdot \exp(-\alpha t) \qquad (6.2)$$

where s_2^0 is the concentration of non-equilibrium sites at t=0, which was taken two months after the start of the experiment. The observed decrease in non-labile Cd and Zn could be well described with this equation (Figure 6.10), with α set equal to 0.008 d^{-1} for Cd and 0.002 d^{-1} for Zn.

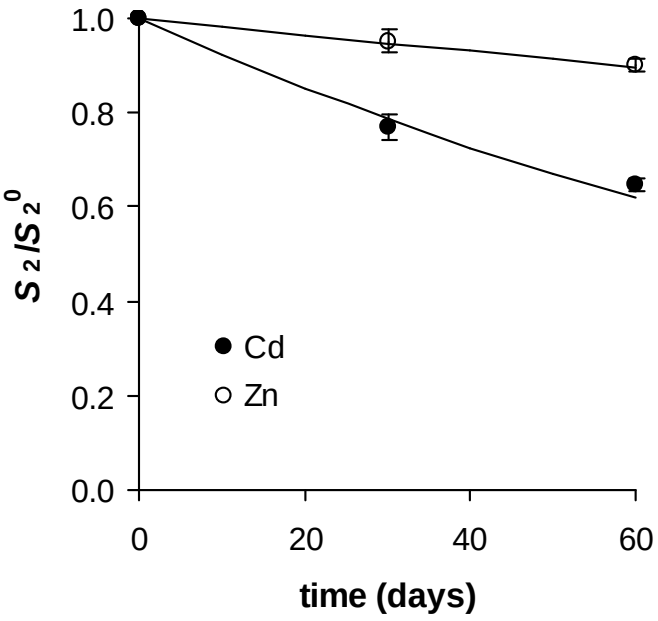

Figure 6.10 The decrease in non-labile Cd and Zn (s_2) with time. Symbols are observed values and the full lines give the modelled decrease using Eq. 6.1, with α set to 0.008 d^{-1} for Cd and 0.002 d^{-1} for Zn. Data were used from the upper part (0-1cm) of the control columns, and t=0 was taken two months after the start of the experiment, when radio-labile metal was almost completely removed.

Calculations of the Cd and Zn transport were made with the two-site model using these rate coefficients. The E value and the non-labile metal concentration were taken as the amount of type-1 sites and type-2 sites respectively, and therefore, f was equal to the fraction of labile metal (E value relative to total metal concentration). The sorption parameters k and n were identical to those of the equilibrium model where sorption was assumed to occur on labile sites only (Table 6.2), i.e., sorption was described with following equations:

$$s_1 = k \cdot c^n = f \cdot k_{\text{tot}} \cdot c^n \tag{6.3}$$

$$\frac{\delta s_2}{\delta t} = \alpha \cdot \left[(1 - f) \cdot k_{\text{tot}} \cdot c^n - s_2\right] = \alpha \cdot \left[\frac{(1 - f)}{f} \cdot k \cdot c^n - s_2\right] \tag{6.4}$$

For illustrative purpose, the calculated solid–liquid distribution of Cd, i.e., the ratio of total Cd on the solid phase to the concentration in solution, in the upper layer of the limed column after 4 months of leaching is given in Figure 6.4. This line is intermediate between

the sorption isotherm where non-labile Cd is assumed to be inert and that where all Cd is assumed to be in equilibrium with the solution phase.

The Cd and Zn profiles (Figure 6.5 and 6.6) and the breakthrough curves (Figure 6.7 and 6.8) were well predicted with the two-site model. These results indicate that non-labile metals (as determined by isotopic dilution) may become mobilized in the long term. No conclusion can be made as to the exact mechanism that caused the release of non-labile metals in this experiment. Solid-state diffusion of the metals out of a mineral phase is a possible mechanism. However, the slow dissolution of a metal-bearing phase may also explain the release of non-labile metals.

This column experiment showed that concentrations in the leachate are strongly reduced when liming the topsoil. The concentration profiles and breakthrough curves were well predicted with the CDE model, using sorption parameters obtained from batch experiments, assuming that only radio-labile metal can be desorbed. However, Cd and Zn that was initially not radio-labile was slowly released from the columns when the labile metal pool was nearly depleted. These finding indicate that non-labile Cd and Zn are not permanently fixed, but that remobilization is possible in the long term.

CHAPTER 7
Transport of Cd under acidifying conditions: a column study

Abstract

The effect of soil acidification on the transport of Cd in a contaminated sandy soil (pH = 6.1, Cd_{tot}=10 mg kg^{-1}) was studied in a column experiment. Columns were leached with 1 mM $Ca(NO_3)_2$ adjusted to pH 3 (acid treatment) or pH 5.7 (control treatment) at a pore water velocity of around 6 cm d^{-1}. The Cd concentrations in the leachate were measured weekly, and the concentration profiles of total, radio-labile and solution Cd were determined after 2, 4, and 6 months of leaching.

The concentrations in the leachate of the control columns was about 20 µg Cd l^{-1}, for the whole duration of the experiment (6 months ~ 230 pore volumes). The concentration in the leachate of the acidified columns increased from 20 to 50 µg l^{-1}. The pH front and the peak in solution concentration of Cd were found at a depth of about 2.5 cm at the end of the experiment. The Cd and proton transport was predicted with coupled convection-dispersion equations, using sorption parameters derived from batch experiments. Observed and predicted values agreed reasonably well, but the decrease in pH and concomitant increase in Cd concentration was underestimated in the lower part of the column, which is indicative of non-equilibrium in the proton transport. The model calculations predicted that most Cd present in the soil would reach the bottom of the column after between 350 and 500 pore volumes, resulting in leachate concentrations in the order of 600 µg Cd l^{-1}, which is hundredfold above the drinking water standard.

7.1 Introduction

In the northern part of Belgium, arable land highly contaminated with Cd and Zn has been converted to nature conservation areas or forest, as a result of a set aside policy. Afforestation of agricultural land results in a decrease of the soil pH, because of the termination of regular lime applications. In sandy soils, with low buffering capacity, this decrease in pH may be fast. Johnston *et al.* (1986) found that the pH of an agricultural field converted into deciduous woodland, decreased from pH 7 to pH 4.2 over a period of 100 years.

Soil acidification results in an increase in heavy metal mobility. A decrease in pH with one unit results in a decrease of the solid–liquid distribution coefficient with a factor 3 to 6 (Christensen, 1984; Temminghoff *et al.*, 1995; Chapter 3). Several transport studies have shown that enhanced soil acidification leads to increased leaching of heavy metals (e.g., Tyler, 1978; Berthelsen *et al.*, 1994). However, no attempt was made to model the transport of heavy metals in these studies.

The aim of this study was to quantify changes in Cd mobility upon soil acidification using a coupled proton-cadmium transport model. Sorption parameters of this model were obtained from batch experiments.

7.2 Materials and methods

The soil was sampled from the surface horizon (0-10 cm) from a field in Neerpelt contaminated with heavy metals by smelter emissions. The field was used as arable field until 1992. The soil had a pH (measured in 0.001 M $CaCl_2$) of 6.3, an organic C content of 2.7 % and a total metal concentration of 10.1 mg Cd kg^{-1} and 682 mg Zn kg^{-1}.

7.2.1 Proton reaction

Air-dry soil was weighed in centrifuge tubes, and a solution of 0.001 M $CaCl_2$ with various concentration of HNO_3 (0, 0.02, 0.04, 0.06, 0.08, 0.1 and 0.12 mmol HNO_3 g^{-1} soil) was added in a soil:solution ratio of 1:5 kg l^{-1}. The pH of the supernatant was measured after 1, 2, 4, and 8 days of equilibration.

Additional reaction kinetics were measured at one H^+ dose. Air-dry soil was equilibrated with a solution of 0.001 M $CaCl_2$ and 0.0013 M HNO_3 in a soil:solution ratio of 1:10 kg l^{-1}.

The tubes were shaken, and the pH of the supernatant was measured at varying time intervals (0.5, 1, 2, 7, 24, 96 and 287 hours).

7.2.2 Column experiment

Sixteen polypropylene columns (3 cm i.d.) equipped with a porous glass plate, were filled from top to bottom with 1 cm acid washed and calcinated sea sand, 5 cm air-dried soil and 1 cm acid washed and calcinated sand (Figure 6.1). A glass fibre filter was placed on top of the column to ensure homogeneous distribution of the feeding solution over the column. Sorting of the particles during packing was avoided by placing a piston of slightly smaller diameter than the column on the surface of the soil after each increment and by tapping the column. The soil was packed at a bulk density of 1.34 kg l^{-1}. The packed columns were slowly saturated from top to bottom with 0.001 M $CaCl_2$, to remove entrapped air. After one week, a 0.001 M $CaCl_2$ solution was applied by a peristaltic pump at a flow rate of 14 ml d^{-1}. A suction of 25 kPa was applied at the bottom of the columns. The different treatments were started after one week equilibration. A 0.001 M $CaCl_2$ solution acidified to pH=3 with H_2SO_4 was applied to eight colums; the other (control) columns received 0.001 M $CaCl_2$ (pH=5.7). The columns were kept at a constant temperature of 14 °C. The effluents were collected through a Teflon funnel into polypropylene bottles. Effluent samples were collected weekly and the volume was recorded by weight. The samples were acidified to pH=1 with HNO_3 and analyzed for Cd with GFAAS.

Prior to dismantlement, transport parameters (*D*, *v*) were estimated from ^{36}Cl breakthrough curves. A 2 hour $^{36}Cl^-$ pulse was applied to each column. Every 3 to 4 hours samples were collected, until complete breakthrough. Activity of ^{36}Cl in the samples was determined with a liquid scintillation counter (Packard Tricarb 1600 CA).

For each treatment, two columns were dismantled after 2 and 4 months and the remaining columns were dismantled after six months. The soil core was removed and sliced into 1 cm layers. Every layer was weighed before and after being air dried, from which the water content of every layer could be calculated. All samples were analyzed for 'total' Cd concentration by extraction with 0.43 M HNO_3 (S:L=1:10 kg l^{-1}, 2 hours of equilibration). The *E* value (cf. section 2.2.2) and solution concentration of Cd, and the pH were measured in 0.001 M $CaCl_2$ (S:L=1:10 kg l^{-1}, 1 week of equilibration).

7.2.3 Modelling

The solute transport was described with the convection-dispersion equation (CDE, eq. 1.10). The dispersion coefficient D ($cm^2\ d^{-1}$) combines the effects of molecular diffusion and of hydrodynamic dispersion caused by velocity variations in the advective transport:

$$D = \lambda \cdot v + \tau \cdot D_0 \tag{7.1}$$

where λ is the dispersitivity (cm), τ is the tortuosity factor (-), and D_0 is the diffusion coefficient in water ($cm^2\ d^{-1}$). The tortuosity factor was calculated using the relationship of Millington and Quirk (1961):

$$\tau = \frac{\theta^{7/3}}{\varphi^2} \tag{7.2}$$

where φ is the porosity ($cm^3\ cm^{-3}$).

Sorption of Cd is highly pH dependent, and therefore, the changes in solid–liquid distribution of Cd with decreasing pH must be taken into account when modelling the Cd transport in the acidified columns. The pH dependency of the sorption isotherm was quantified using following equation:

$$s_{Cd} = k' \cdot {c_H}^{m} \cdot c_{Cd} \tag{7.3}$$

where c_H is the proton concentration in solution (mol l^{-1}), and k' and m are empirically derived parameters. Combining (1.10) and (7.3) yields:

$$\frac{\delta c_{Cd}}{\delta t} + \frac{\rho}{\theta} \cdot k' \cdot {c_H}^{m} \frac{\delta c_{Cd}}{\delta t} + \frac{\rho}{\theta} \cdot c_{Cd} \cdot k' \cdot m \cdot {c_H}^{m-1} \frac{\delta c_H}{\delta t} = D_{Cd} \cdot \frac{\delta^2 c_{Cd}}{\delta z^2} - v \frac{\delta c_{Cd}}{\delta z} \tag{7.4}$$

This equation must be solved together with the equation describing the transport of protons. The 'sorption isotherm' of protons was described with:

$$s_H = a \cdot \ln c_H + b \tag{7.5}$$

where s_H is the proton concentration on the solid phase (mol kg^{-1}), and a and b are empirical parameters. Reactions of protons with the solid phase involve ion exchange and dissolution. Therefore, s_H effectively represents H^+ exchanged and H^+ consumed in mineral dissolution.

Substitution of equation 7.5 in the CDE (eq. 1.10) gives:

$$\frac{\delta c_H}{\delta t}\left(1 + \frac{\rho}{\theta} \cdot \frac{a}{c_H}\right) = D_H \cdot \frac{\delta^2 c_H}{\delta z^2} - v \frac{\delta c_H}{\delta z} \tag{7.6}$$

Equations 7.4 and 7.6 were numerically solved together, using finite differences with an explicit scheme, with the mathematical program Matlab (Release 12).

7.3 Results and discussion

7.3.1 pH buffering of soil

The pH buffer curves were measured at various equilibration times, and could be described with equation 7.5 (with the underlying assumption that activity equals concentration in these solutions with low ionic strength). The parameter *a* multiplied by a factor 2.3 (=ln10) gives the pH buffer capacity of the soil (pH BC, $cmol_c\ kg^{-1}\ pH^{-1}$), which is the amount acid (s_H) or base that must be added to change the pH with one unit:

$$\text{pH BC} = -\frac{ds_H}{dpH} \tag{7.7}$$

The pH BC (± standard error) was 3.33 (± 0.07) cmol kg^{-1} pH^{-1} after one day of equilibration, and 3.50 (± 0.06) cmol kg^{-1} pH^{-1} after 8 days of equilibration. The increase in pH BC with time is indicative that slow reactions are involved. In the pH range tested (pH 6 to 3), cation exchange and Al buffering (dissolution of $Al(OH)_3$) are the most important pH buffering mechanisms (Ulrich, 1991). For the transport calculations, the pH BC determined after one day of equilibration was used (pH BC = 3.33 cmol kg^{-1} pH^{-1} or a = 0.0145 mol kg^{-1} $\ln(H^+)^{-1}$).

Changes in pH were measured after addition of a 0.001M $CaCl_2$ solution with pH=2.9 to the soil. The pH was 4.8 after 0.5 hours of equilibration, and further increased to 5.4 within 1 day of equilibration. The pH still increased with 0.3 pH-units between 1 and 12 days of equilibration (Figure 7.1). The change in pH was modelled with a two-site model (Figure 1.4). The H^+ transfer from the equilibrium pool (s_1) to the non-equilibrium pool (s_2) was described by first-order kinetics:

$$\frac{ds_2}{dt} = k_1 s_1 - k_{-1} s_2$$

According to this model, the decrease in the fraction of H^+ in equilibrium with the solution is :

$$\frac{s_{eq}}{s_{tot}} = \frac{f \cdot (a \cdot \ln(H) + b)}{s_{tot}} = 1 - (1 - f) \cdot \left[1 - \exp(-\frac{t}{T_c}) \right] \tag{7.8}$$

where s_{eq} is the H^+ concentration on the solid phase in equilibrium with the solution, s_{tot} is the total H^+ concentration, f is the fraction of equilibrium sites, and T_c is the response time of the kinetic reaction (eq. 1.8). The sorption isotherm ($a\ln(H)+b$) derived for an equilibration time of 8 days was used, assuming that equilibrium was reached by that time.

This model, that contains two independent variables (f and T_c), was fitted to the experimental adsorption data. The data of the 3 first sampling occasions (after 0.5, 1, and 2 hours) were omitted in the regression analysis, since the two-site model did not give a good fit for all data together and therefore, only the slower kinetics were considered. A three-site model (with an equilibrium pool, and a slow and a fast reacting pool) fitted all data well. However, a two-site model was used to describe the proton transport (section 7.3.3), and therefore, the parameters for the two-site model are given. The error introduced by neglecting the fast kinetics in the transport calculations will be small (cf. section 1.4.1). Results of the non-linear regression are shown in Figure 7.1 (parameters in Table 7.1).

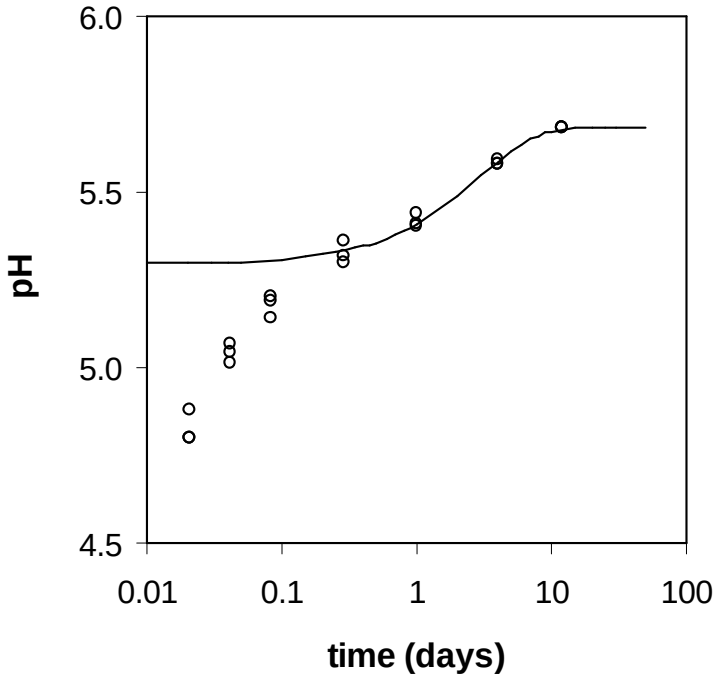

Figure 7.1 Change of pH after addition of a 0.001 M $CaCl_2$ solution with pH=2.9 to a sandy soil (pH=6.3), in a solid/liquid ratio of 1/10 kg l^{-1}. The line shows the fit of the two-site model.

Table 7.1 Parameter estimates for H^+ adsorption obtained by fitting a two-site model to the experimental data.

pool	equilibrium	non-equilibrium
fraction, f	0.47	0.53 ± 0.01
T_c (d)	-	2.92 ± 0.17

7.3.2 Effect of pH and total Cd on the solid–liquid distribution of Cd

Solution concentrations and *E* values of Cd were determined at 1 cm depth intervals after 2, 4, and 6 months of leaching in 0.001 M $CaCl_2$ (S:L=1:10 kg l^{-1}). 'Total' concentrations were determined by cold extraction with 0.43 M HNO_3. The *E* values were between 79 and 110% of the Cd concentration extracted with 0.43 M HNO_3, indicating that Cd is mainly labile.

In the control columns, the K_d^{lab} increased with decreasing total Cd concentration. The solid–liquid distribution could be described with a Freundlich isotherm:

$$s_{Cd} = 47 \cdot c_{Cd}^{0.41} \qquad (R^2 = 0.81)$$

where s_{Cd} is the labile concentration on the solid phase (mg kg^{-1}), calculated as the product of the solution concentration (c_{Cd}, mg l^{-1}) and the isotopic distribution coefficient. The parameter *n* of the Freundlich equation is unusually low in this case, which may be caused by leaching of cations (e.g., Zn) competing with Cd for sorption sites.

The pH dependence of the distribution coefficient of Cd, measured in the columns after 2, 4, and 6 months of acid leaching, is shown in Figure 7.2. The solid–liquid distribution of Cd could be described with following equation:

$$K_d^{lab} = \frac{s_{Cd}}{c_{Cd}} = 0.59 \cdot c_H^{-0.46} \qquad (R^2 = 0.98)$$

No effect of total Cd concentration was found for the acid columns. The effect of total Cd concentration was probably masked by the pH effect, since pH and Cd concentration were correlated.

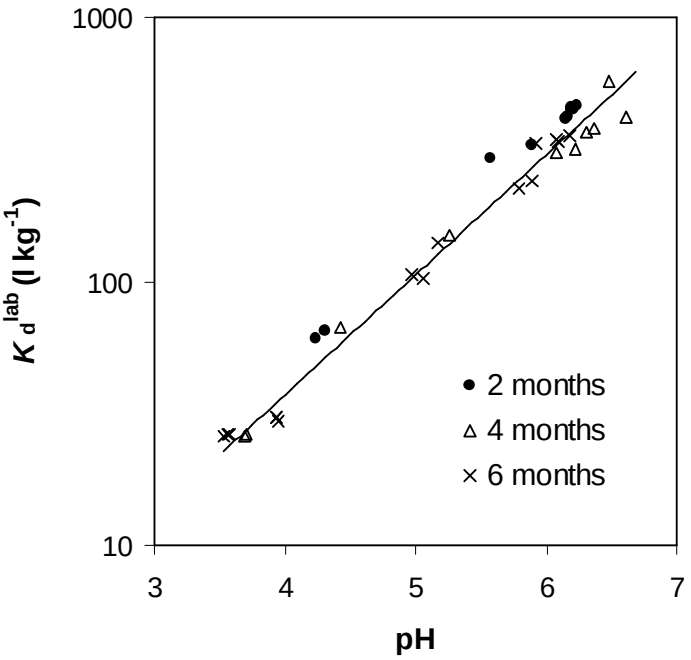

Figure 7.2 Relation between pH and K_d for the columns of the acid treatment

7.3.3 Column experiment

The parameters *v* and *D* of the convection-dispersion equation were obtained from the breakthrough of ^{36}Cl, by fitting an analytical solution of the one-dimensional convection-dispersion equation (Toride *et al.*, 1995). The breakthrough curves were well described with the CDE model, indicating that there was local equilibrium. The pore water velocity *v* was between 5.2 and 6.8 cm d^{-1}. The tortuosity factor τ was calculated with the Millington-Quirk relation (eq. 7.2), and ranged from 0.23 to 0.32. The dispersitivity λ was derived from the dispersion coefficient *D* of $^{36}Cl^-$, the diffusion coefficient D_0 (1.3 cm^2 d^{-1} for $^{36}Cl^-$) and the pore water velocity (Eq. 7.1), and ranged from 0.12 to 0.30 cm. The dispersion coefficients of Cd^{2+} and H^+ were calculated from *v*, λ, τ and D_0 (0.8 cm^2 d^{-1} for Cd and 8.1 cm^2 d^{-1} for H^+) (Eq. 7.1). The estimated dispersion coefficient ranged from 0.9 to 2.0 cm^2 d^{-1} for Cd^{2+}, and from 2.8 to 4.0 cm^2 d^{-1} for H^+. The larger dispersion coefficient of protons results from the larger diffusion coefficient. The dispersion coefficient is usually dominated by the hydrodynamic dispersion term, but the diffusion term may become important in repacked columns with slow water flow (Jury *et al.*, 1991).

The sorption parameters used in the transport model were obtained from the batch experiments (section 7.3.1 and 7.3.2). The parameters used in the transport model are shown in Table 7.2.

Table 7.2 Input parameters used in the transport model

	Parameter	Symbol	Value	Unit
Hydraulical	Pore water velocity	v	5.2 -6.8	cm d^{-1}
	Dispersion coefficients	D_{Cd}	0.9 -2.0	cm^2 d^{-1}
		D_H	2.8 – 4.0	cm^2 d^{-1}
Chemical	Sorption of Cd in control	k	47	mg^{1-n} l^n kg^{-1}
	columns (Eq. 5.3)	n	0.41	
	Sorption of Cd in acidified	k'	0.59	l kg^{-1} M^{-m}
	columns (Eq. 7.3)	m	-0.46	
	pH buffering (Eq. 7.5)	a	0.0145	mol kg^{-1} $ln(H^+)^{-1}$
Column	Length	L	5	cm
	Water content	θ	0.29 – 0.34	
	Bulk density	ρ	1.34	kg l^{-1}
Initial	Concentration in solution	c_{Cd}	0.020	mg l^{-1}
conditions		c_H	$10^{-6.3}$	mol l^{-1}
Numerical	Spatial discretization	Δz	0.1	cm
	Time discretization	Δt	0.036	day

Depth profiles of pH (in 0.001 M $CaCl_2$) were measured 2, 4 and 6 months after the start of the experiment. The control columns showed no change in pH, although the pH of the feeding solution (5.8) was slightly more acid than the pH of the soil (6.3). The pH decreased clearly in the columns that were fed with the acid solution (pH = 3) (Figure 7.3).

Figure 7.3a shows the predictions of the CDE model. The predicted pH for one layer was calculated as the arithmetic mean of the modelled pH values (not by averaging the H^+ activities), because of the linear relation between the total H^+ concentration and the pH (cf. eq. 7.7). The depth of the pH front was reasonably well predicted. However, the decrease in pH was overestimated in the upper part of the column and underestimated in the lower part. Non-equilibrium in the H^+ transport might explain these results. The prediction improved when the dispersion coefficient for proton transport, D_H, was set to 30 cm^2 d^{-1} (Figure 7.3a), i.e., about 10 times higher than the dispersion coefficient that was derived from the ^{36}Cl breakthrough and the Millington-Quirk relation (Eq. 7.2). The tortuosity factor τ of these repacked columns may possibly have been higher than was estimated with this equation, resulting in an underestimation of the proton dispersion coefficient. However, even if τ would have been as high as 0.5, the proton dispersion coefficient would have been 5.6 cm^2 d^{-1} at most. Therefore, the larger D value, that is adjusted to fit the observations, does not reflect true diffusion-dispersion, but may be seen as an effective

dispersion coefficient that combines two processes: actual dispersion and additional dispersion caused by slow reactions of protons with the solid phase.

An attempt was made to model the H^+ transport with a kinetic two-site model, that distinguishes type-I sites (s_1) on which the sorption is instantaneous, and type-II sites (s_2) on which sorption is time-dependent (cf. Figure 1.7):

$$\frac{\delta c_H}{\delta t}(1 + f \cdot \frac{\rho}{\theta} \cdot \frac{a}{c_H}) = D_H \cdot \frac{\delta^2 c_H}{\delta z^2} - v \cdot \frac{\delta c_H}{\delta t} - \frac{\rho}{\theta} \cdot \frac{\delta s_2}{\delta t} \tag{7.9a}$$

$$\frac{\delta s_2}{\delta t} = \alpha \cdot [(1 - f) \cdot (a \ln c_H + b) - s_2] \tag{7.9b}$$

where f is the fraction of equilibrium sites, and α is the first-order rate coefficient (d^{-1}). The backward rate constant, k_{-1}, as determined in the batch experiments was 0.16 d^{-1}, since

$$k_{-1} = \frac{f}{T_c} \tag{7.10}$$

When a value for α equal to k_{-1} was chosen, the predictions were nearly equal to these of the CDE model, even when assuming that f was smaller in the column experiment than in the batch experiment. A first-order coefficient considerably smaller than determined in the batch experiment had to be chosen in order to obtain a predicted pH profile that was in better agreement with the observed profile than when using the CDE model. Figure 7.3b illustrates the predictions of the two-site model when α was set to 0.025 d^{-1} and f to 0.1. The 'flux' profile (full line) represents the predicted pH values in the column. These pH values are not in equilibrium with the solid phase. The 'equilibrium' pH (after equilibration of the soil with the solution) can be calculated as:

$$pH_{eq} = -\frac{s_H - b}{2.3 \cdot a} \tag{7.11}$$

It is assumed that the pH_{eq} (dotted line in Figure 7.3b) is representative for the measured pH values since the pH was measured in soil suspensions (S:L= 1:10 kg l^{-1}) that were shaken end-over-end for one week, and therefore, nearly full equilibrium was reached (Figure 7.1).

Summarising, the proton transport exhibits considerable non-equilibrium behaviour in these columns, and the reaction kinetics determined in batch experiments, do not match these in the columns. Slow reactions due to e.g. mineral dissolution may be more pronounced in the unsaturated columns than in agitated soil suspensions. The best fit of the proton transport was still obtained by adjusting the proton dispersion coefficient.

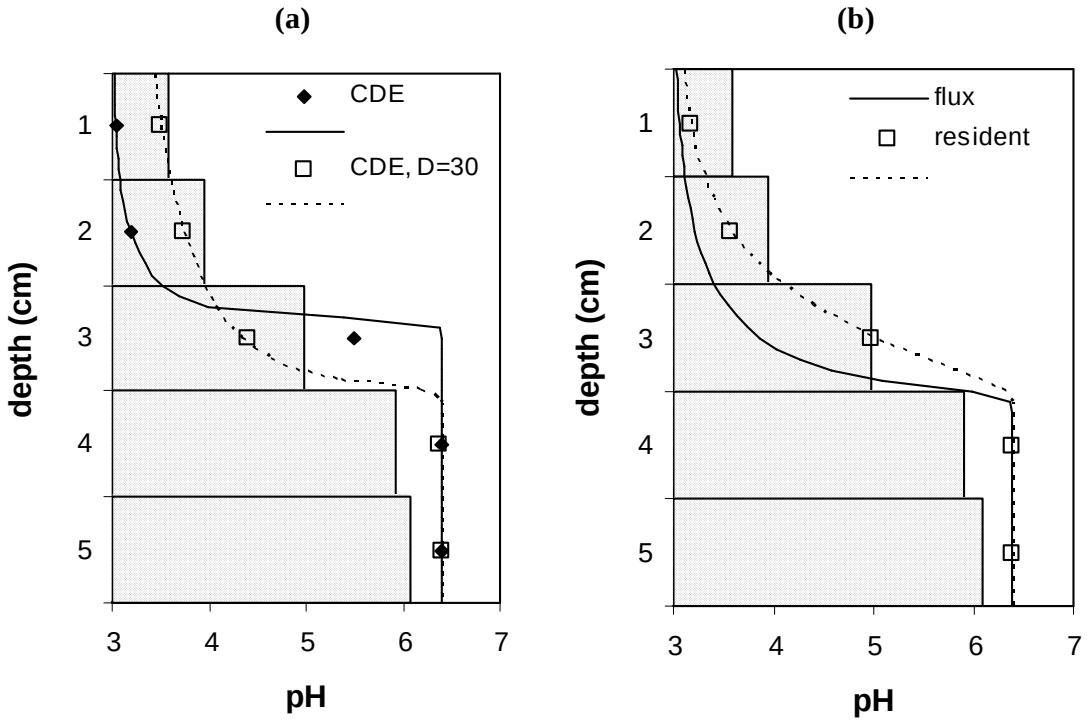

Figure 7.3 Measured (bars) and predicted (lines and symbols) depth profiles of pH after 6 months of acid leaching. (a) Predictions were made assuming local equilibrium with D_H derived from the ^{36}Cl breakthrough (D_H= 3.4 cm^2 d^{-1}, full line, ♦) or with D_H set to 30 cm^2 d^{-1} (dotted line,). (b) Predictions were made with a two-site model (and D_H= 3.4 cm^2 d^{-1}). Full explanation in text.

The measured and predicted concentration profiles of the total Cd concentration and the concentration in solution in the control columns after 6 months of leaching are shown in Figure 7.4. Only a small decrease in total Cd concentration was observed in the upper layer of the control columns, since Cd retention was high (K_d ~ 500 l kg^{-1}). The concentration profiles in the control columns were well predicted with the convection-dispersion equation, based on the local equilibrium assumption (for the labile Cd pool).

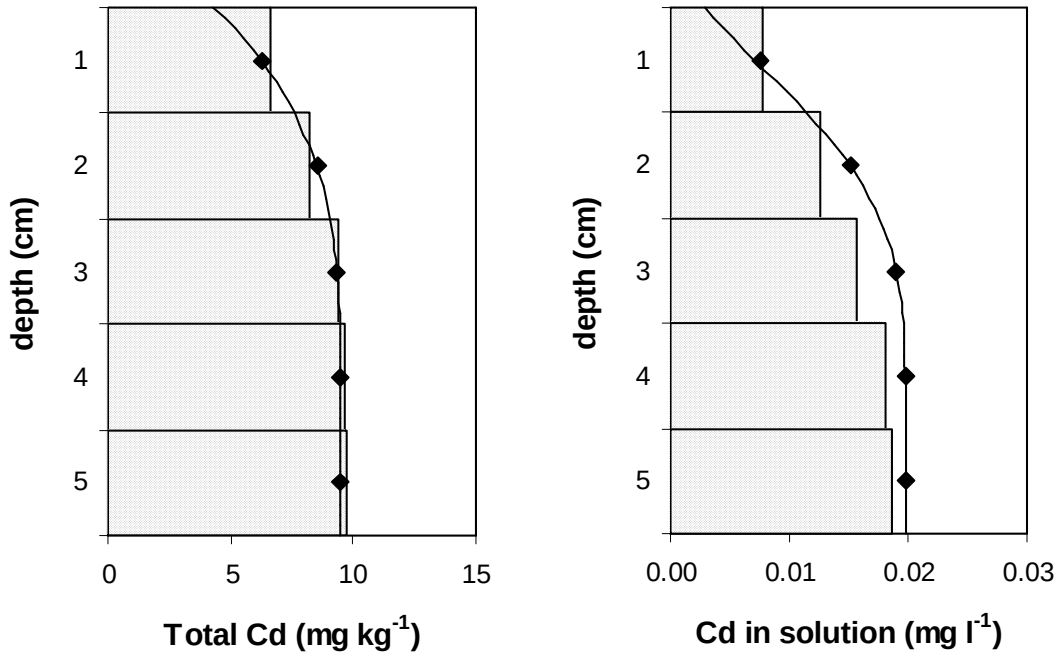

Figure 7.4 Measured (bars) and modelled (lines and symbols) depth profile of (a) total Cd concentration, and (b) Cd concentration in solution after 6 months of leaching for the control columns.

Most Cd was removed from the upper 2 cm of the acid columns after 6 months of leaching, since the strong decrease in pH resulted in weak retention of Cd in these layers (K_d~ 30 l kg^{-1}) (Figure 7.5a). Accumulation of Cd was observed in the deeper layers, where the pH was not, or only slightly affected. The solution concentrations showed a peak in the solution concentration of Cd at the depth of the pH front (Figure 7.5b). Predicted Cd profiles were in reasonable agreement with observed profiles. However, total concentration and concentration in solution were underestimated in the deeper layer of the acidified columns. This deviation between predicted and observed Cd profiles is presumably caused by non-equilibrium in the H^+ transport, since no indications of non-equilibrium for the Cd transport were found for the control columns. The Cd profiles were better predicted when model calculations were made with the parameter D_H adjusted to 30 cm^2 d^{-1} (i.e., the value that was used in order to match the predicted proton transport with the observations), or when the two-site model for proton transport was used (Figure 7.5). These findings support the hypothesis that the deviation between the observed Cd concentrations and the predictions of the CDE model are due to non-equilibrium in the H^+ transport.

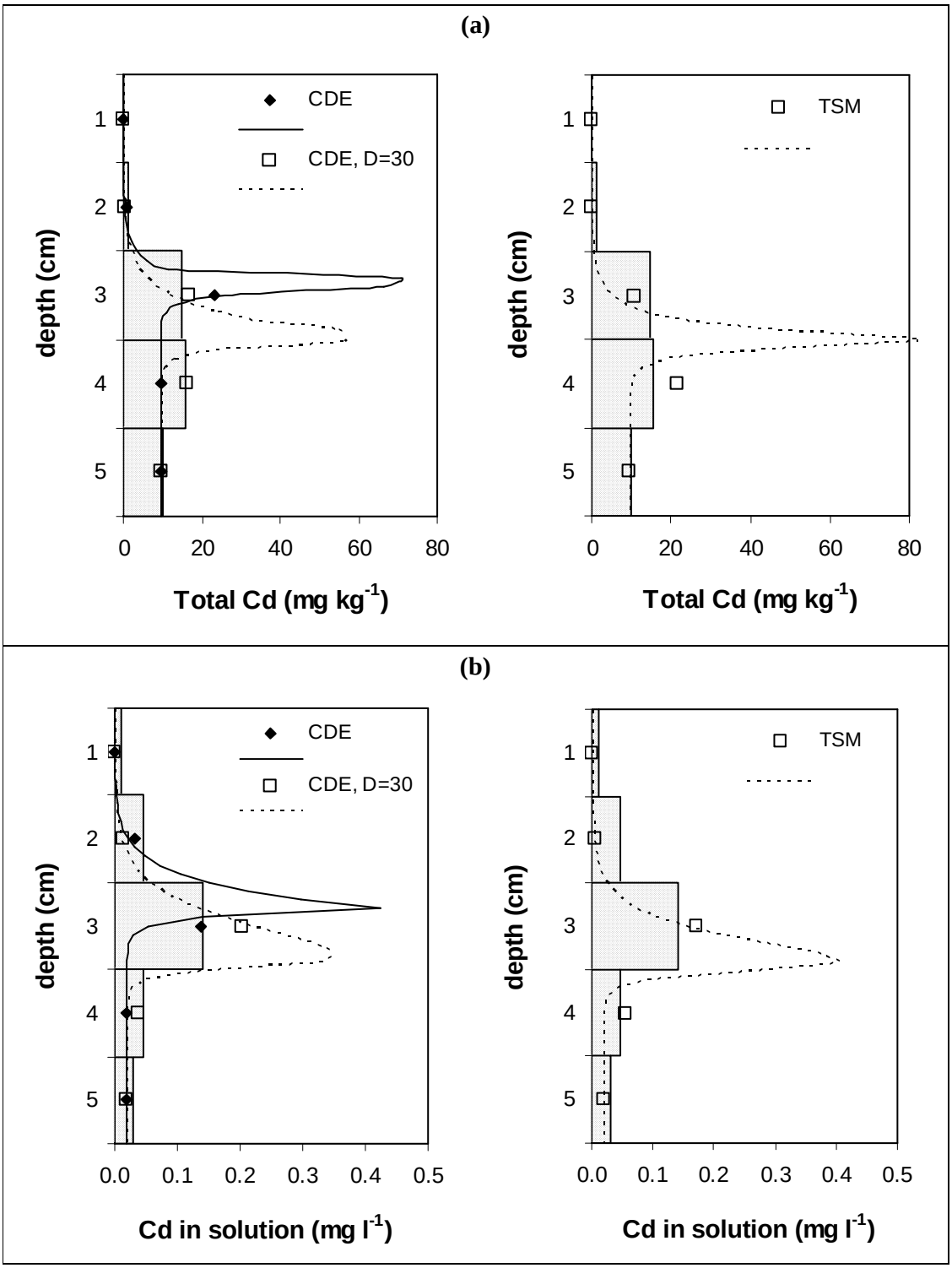

Figure 7.5 Measured (bars) and modelled (lines and symbols) depth profile of (a) total Cd concentration, and (b) Cd concentration in solution, after 6 months of acid leaching. The proton transport was modelled with the CDE model and D_H = 3.4 cm^2 d^{-1} (full lines, ♦) or D_H =30 cm^2 d^{-1} (dotted lines,), or with a two-site model (cf. Figure 7.3)

Table 7.3 gives the amounts of Cd lost by leaching, calculated from the product of leachate volume and metal concentration in the leachate, or from the decrease in the total Cd concentration. Both methods gave similar results (Table 7.3). The metal losses were larger in the acidified columns than in the control columns. The amount leached from the control columns agreed with the amount predicted to be leached from the columns according to the CDE model. The Cd concentration in the effluent of the control columns did not change within the period of observation (6 months), which was equivalent to about 230 pore volumes. Model calculations showed that a decrease in the Cd concentration in the effluent of the control columns is not to be expected before 600 pore volumes. The concentrations of Cd in the effluent of the acidified columns increased continuously, up to 0.05 mg Cd l^{-1} after 230 pore volumes. This increase is not predicted with none of the models (Figure 7.6). As a result, the amount of Cd leached from the acidified columns is larger than is predicted (Table 7.3). A sharp increase in the effluent concentration is predicted with the CDE model after about 400 pore volumes, when the Cd front reaches the bottom of the column. When the proton transport was modelled with D_H= 30 cm^2 d^{-1} or with the two-site model, an earlier breakthrough and a greater pulse spreading is predicted (Figure 7.6).

Table 7.3 The amount of Cd lost by leaching in acidified and in control columns, calculated from the metal amount recovered in the leachate or from the decrease in total Cd concentration in the soil.

time (months)	Cd lost (µg) (initial Cd content: 464 µg)				
	acidified		control		predicted
	leached	ΔCd_{tot}	leached	ΔCd_{tot}	(acidified and control)
2	20	26	13	11	14
4	26	33	26	21	28
6	86	89	42	39	43

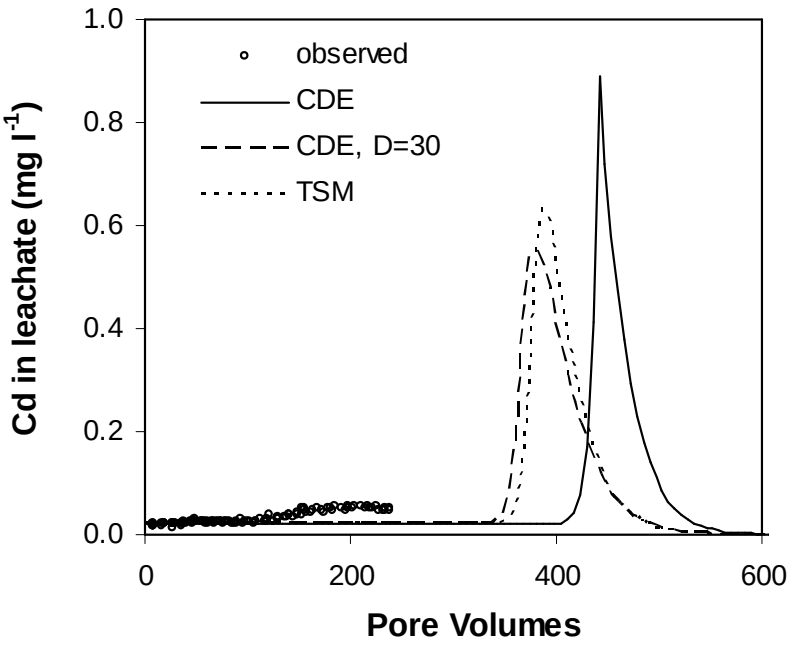

Figure 7.6 Observed (circles) and predicted (lines) Cd concentration in the effluent of the acidified columns. The proton transport was modelled with the CDE model and D_H= 3.4 $cm^2\ d^{-1}$ or D_H =30 $cm^2\ d^{-1}$, or with the two-site model.

The deviations between predicted and observed Cd concentration in the effluent and in the columns of the acid treatment indicate that H^+ in solution was not in equilibrium with the solid phase. Even when accounting for non-equilibrium with a two-site model (or by using a larger D_H), the observed increase in the Cd concentration of the effluent was still not predicted. A pH decrease in the effluent was not observed. An early decrease (i.e., before the predicted breakthrough after 400 pore volumes) in the pH of the effluent would have been another indication that non-equilibrium existed in the H^+ transport. The pH of the column effluent was regularly measured. However, these values exceeded always the original soil pH (measured in 0.001 M $CaCl_2$), e.g., the effluent pH was 6.75 ± 0.12 after 4.5 months of leaching. The pH of leachates may be higher than the pH of the soil solution due to CO_2 volatilization, caused by the lower CO_2 pressure outside the column:

$$HCO_3^- + H^+ \rightarrow H_2O + CO_2 \qquad (7.12)$$

As a result, the leachate pH cannot be used as an indicator of the pH inside the column (Reuss *et al.*, 1990).

In conclusion, the decrease in pH and mobilization of Cd in the acidified columns was reasonably predicted with coupled convection-dispersion equations (CDE) for the proton and Cd transport, using sorption parameters derived from batch experiments. However, the observed pH profile was more disperse and the Cd peak was found at greater depth than predicted with the CDE model. Better agreement between the predicted and observed profiles of H^+ and Cd was obtained when using a non-equilibrium transport model involving reaction kinetics for H^+, but with a rate constant adjusted to the column data that was much smaller than observed in batch experiments. These results indicate that proton reaction kinetics in batch experiments do not reflect *in situ* conditions. Adjusting the proton dispersion coefficient had a comparable effect on predicting the pH front as the use of a kinetic sorption model.

part III

Transport of Cd and Zn at field scale

CHAPTER 8

Field scale transport of Cd and Zn in a polluted Spodosol

Abstract

The transport of Cd and Zn was modelled in Spodosol profiles of a field polluted with heavy metals. Total, radio-labile, and solution concentrations of Cd and Zn were determined at various depths in ten profiles. Predictions of the metal transport were made assuming local equilibrium between the labile metal pool and the solution. Wick samplers were installed in 3 Spodosols (2 polluted and 1 unpolluted), and were monitored for 18 months. Concentrations of Cd and Zn in solutions collected by the wick samplers ('flux' concentrations) were in good agreement with those in soil solutions obtained by centrifugation. This good agreement supports the use of the local equilibrium assumption (LEA) for the transport calculations. Present-day Cd profiles were calculated based on the emission history of the nearby smelter, from which the production started in 1889. Observed and predicted depth profiles agreed well, except in the upper horizon where observed Cd concentrations exceeded the predicted concentrations. This may be attributed to the presence of non-labile Cd in the deposition, which was not accounted for in the retrospective modelling. The model predicted that a major part of Cd deposited on the soil has already been transported to the groundwater in the profiles with the lowest retention capacity. It was predicted that the Cd concentration in the seepage water will remain above 5 $\mu g\ l^{-1}$ for the next 170 years, and that the Zn concentration will remain above 0.5 $mg\ l^{-1}$ during the next 40 years. Liming the upper 25 cm was predicted to have limited effect on the concentrations in the seepage water, since most Cd has already been transported to depths greater than 25 cm.

8.1 Introduction

Large areas of land are contaminated with heavy metals from historical emissions of the non-ferrous industry. Groundwater pollution caused by leaching of these metals is a growing concern. Prediction of the metal transport, through model calculations, is required to evaluate the risk and extent of future groundwater pollution. Only in a few studies, the transport of Cd and Zn at field scale has been investigated. Černík *et al.* (1994) reconstructed Zn and Cu profiles of smelter contaminated soils, using a convection-dispersion model and a linear stochastic convection model. Both approaches gave a reasonable agreement between predicted and observed metal profiles. Their results indicated that, even in these soils with high pH (~ 7.5), Zn was slowly transported with a velocity of around 1 mm y^{-1}. Streck and Richter (1997b) modelled transport of Cd and Zn in a sandy soil (pH~5.3) after 29 years of controlled wastewater irrigation. The measured Cd and Zn profiles could be successfully modelled based on the local equilibrium assumption, if spatial variability of sorption was taken into account. Seuntjens (2002) evaluated the performance of a Monte-Carlo type convective-dispersive transport model to predict Cd profiles in acid sandy soils contaminated by Zn smelters.

Transport at field scale is mostly modelled based on the local equilibrium assumption (LEA). The sorption parameters that quantify the partitioning between the solid and the solution phase (e.g., K_d, in case of linear sorption) are usually based on the measurement of concentrations in isolated soil solutions or in dilute salt extracts. However, if non-equilibrium conditions prevail during the transport or if preferential flow occurs, the concentration in solutions equilibrated with the soil may overestimate the concentration in the percolating water. No experiments have yet been set-up to measure metal 'flux concentrations' in the field. Concentrations in the percolating water may be measured using *in situ* samplers, such as passive capillary samplers (PCAPS). A suction is generated by the hanging water columns, which allows the collection of soil solution from both saturated and unsaturated pores to a tension equal to that produced by the hanging column (Holder *et al.*, 1991). Therefore, the field situation is better approached than when using suction cups or pan samplers. Suction cups apply a vacuum to the soil, which may cause the collection of samples that are not representative of the solution moving to the groundwater. Pan samplers on the other hand can only collect solution from saturated pores, which may lead to a disturbance of the flow regime and a change in the soil chemical conditions above the sampler (e.g., reduction and pH increase).

In the present study, the transport of Cd was modelled in Spodosol profiles of a field polluted with heavy metals. Concentrations measured in soil solution obtained by centrifugation were used to derive the sorption parameters. This approach was validated with a comparison between the concentrations in soil solution and concentrations in solution obtained by wick samplers. Present-day Cd profiles were calculated and compared with the measured profiles, and the future leaching of Cd to the groundwater was predicted. The aim of this study was to validate the modelling approach and to unravel the major parameters controlling this transport. Since only 10 profiles were sampled, effects of spatial variability on heavy metal transport could not be studied in detail. This issue will be addressed in the next chapter.

8.2 Materials and methods

8.2.1 Soils and soil characterisation

Ten soil profiles were sampled in a polluted field in Balen. Soil characteristics and total, labile and pore water concentrations of Cd and Zn were measured, as described in section 2.2.1. A summary of soil properties and metal concentrations is given in Table 2.2.

8.2.2 Prediction of Cd transport

Transport calculations were made with the one-dimensional finite-element computer code HYDRUS-1D (Šimůnek *et al.*, 1998). The solute transport was modelled by a simultaneous solution of the Richard's equation and the convection-dispersion equation, assuming local equilibrium between the labile metal pool and the solution phase (eq. 1.10). The Cd transport was simulated from the start of the production (in 1889). For Zn, only the future transport was modelled.

The hydraulic parameters (K_s and van Genuchten parameters) were taken from Seuntjens *et al.* (1999), who studied similar soils from a nearby site (Table 8.1). No effort was made to determine these parameters exactly, since a sensitivity analysis has shown that these parameters do not significantly affect the model outcome (Seuntjens *et al.*, 2002). The longitudinal dispersitivity λ was obtained from Seuntjens *et al.* (2002), and was about 2 cm for all horizons. The boundary conditions for the water flow were constant water flux at the soil surface and zero-potential at the bottom boundary (water table). The stationary flux at the upper boundary was assumed to be 0.24 m y^{-1}, which is the long term average precipitation surplus for the region (Patyn, 1997).

Table 8.1 Hydraulic parameters for dry Spodosols in the region studied: the field-saturated hydraulic conductivity, K_s, and the van Genuchten parameters of the water retention curve (θ_r, θ_s, α_{VG}, n_{VG}) (from Seuntjens *et al.*, 1999)

horizon	K_s (cm d^{-1})	θ_r (-)	θ_s (-)	α_{VG} (-)	n_{VG} (-)
A	202	0.13	0.49	0.017	2.66
E	312	0.07	0.44	0.018	2.76
B	185	0.16	0.54	0.010	2.05
BC	600	0.09	0.45	0.018	2.87
C1	1608	0.04	0.41	0.024	4.46
C2	1104	0.,03	0.43	0.020	4.87

For the solute transport, a third-type flux boundary condition (Cauchy type) was used at the top and a second-type (zero concentration gradient or Neumann type) boundary condition at the bottom:

$$-\theta \cdot D\frac{\delta c}{\delta z} + qc = qc_{in} \qquad \text{at } z=0$$

$$\frac{\delta c}{\delta z} = 0 \qquad \text{at } z=L \qquad (8.1)$$

where q is the water flux density (cm d^{-1}), and c_{in} is the metal concentration (mg l^{-1}) in the infiltrating water (other symbols equal to those in eq. 1.10).

The solid–liquid distribution was expressed with a Freundlich type equation:

$$s=k.c^n \qquad (8.2)$$

where s is the (labile) adsorbed concentration (mg kg^{-1}), c is the concentration in solution (mg l^{-1}), and k and n are empirical parameters. A value for n of 0.8 for Cd and 0.7 for Zn was derived from batch experiments on two soil samples. The value of k was calculated from the experimentally determined metal concentrations (for each profile and soil depth):

$$k = \frac{E}{[M]_{pw}{}^n} \qquad (8.3)$$

where E is the radio-labile concentration (mg kg^{-1}), and $[M]_{pw}$ the measured concentration in the soil solution (mg l^{-1}). It was assumed that there was no change in the sorption parameters with time. The pore water concentration of Cd in the year 1889 was assumed to be 1 µg Cd l^{-1}, which is of the same order as the pore water concentration in an unpolluted

field (Houthalen). For Zn, for which only the future transport was calculated, the measured values were taken as the initial pore water concentrations.

An estimate of the historical Cd deposition rate was needed for the retrospective modelling. Seuntjens (2002) studied a nearby site and estimated the Cd emission of the neighbouring non-ferrous industry. The absolute scale of the deposition rate was estimated by integration of the experimentally derived depth profiles of the Cd concentration (Černík *et al.*, 1994; Seuntjens, 2002). The amount of Cd recovered per unit area, in the upper 2 m of the profile, was around 6 kg Cd ha^{-1} for profiles 4, 5, 7 and 9 (Table 2.6). Since model calculations indicated that leaching from these profiles was negligibly small, it was assumed that the overall Cd deposition was 6 kg Cd ha^{-1}. Cadmium amounts were considerably lower in profiles 1, 2, 3, and 6, which indicates that Cd has partly been leached from these profiles. Profiles 8 and 10 contained larger Cd amounts (respectively 11 and 26 kg ha^{-1}), and were therefore not included in the model calculations. These profiles were located nearby a smelter waste dump. Figure 8.1 shows the estimated former Cd deposition at the experimental field. It was assumed that Cd in the deposition was fully labile. This assumption seems justified, since, on average, 81% of the Cd amount present in the profile is in labile form (range 64 – 101%). For Zn, only between 12 and 55 % (mean 18%) of the total amount in the profile was labile. Therefore, the Zn transport was not modelled retrospectively.

For the prospective modelling, metal concentrations in the infiltrating water were assumed to be 0.001 mg Cd l^{-1} and 0.06 mg Zn l^{-1}, which corresponds to a future deposition rate of 2.3 g Cd ha^{-1} y^{-1} and 140 g Zn ha^{-1} y^{-1}. Measurements of wet deposition in the Netherlands indicate that the deposition rate during the period 1998-2000 was around 1 to 2 g Cd ha^{-1} y^{-1} and around 70 to 150 g Zn ha^{-1} y^{-1} (RIVM, 1999, 2001ab).

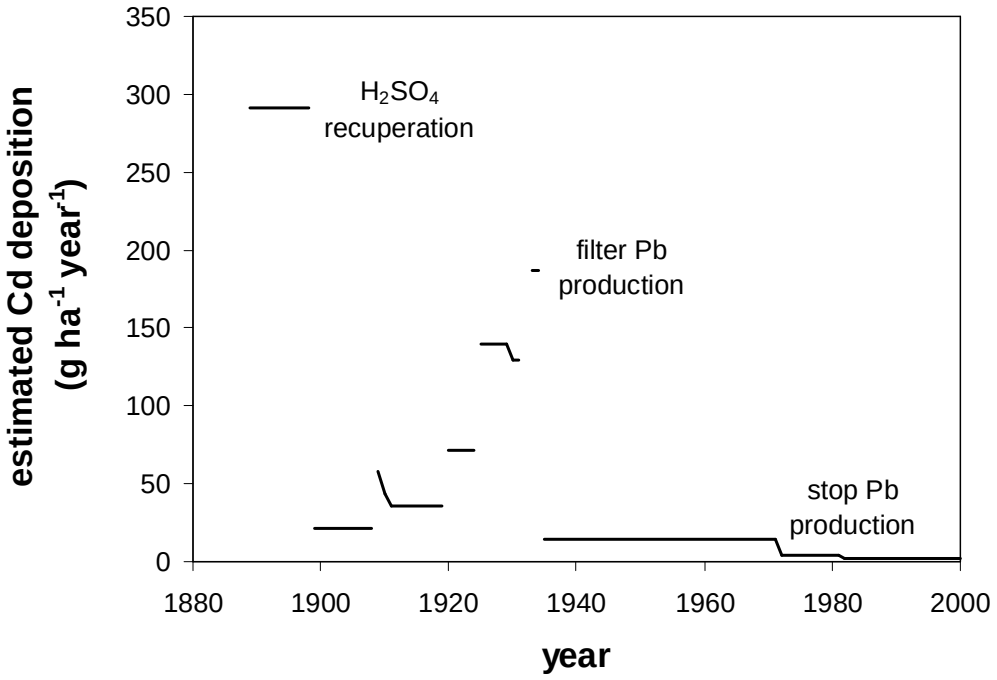

Figure 8.1 Former Cd deposition on the experimental site estimated from emission data (Seuntjens, 2002), and the Cd amount present in the soil profiles with the largest Cd mass (profiles 8 and 10 not considered).

8.2.3 Collection of soil solution with Passive Capillary Samplers (PCAPS)

The wicks used (Amatex 3/8-inch HI) were heated to 400°C, for 4 hours, to remove impurities (Knutson *et al.*, 1993). The upper end of the wicks was rolled up on a PVC-plate of 17 cm by 34 cm (2 wicks per plate), and the plate was covered with a nylon cloth. One end of the wick protruded through a hole in the plate, and was encased in a PVC pipe connected to a collection flask (Figure 8.2a). The optimal wick length was calculated according to the procedure of Rimmer *et al.* (1995).

The PCAPS were installed at 70 cm of depth, at three locations, in June 2000. A pit with a depth of about 150 cm was dug, and an excavation (60 cm depth, 10 cm height) was made in the wall. The top of the excavation was carefully levelled, and the PVC-plate with the two PCAPS units, was pushed against the top of the excavation. Wooden blocks were hammered between the bottom of the excavation and the PVC-plate, to ensure good contact between soil and PCAPS (Figure 8.2b). The excavation was refilled with soil, and the collection flasks were placed at the bottom of the pit (Figure 8.2c). The pit wall was covered with a plastic sheet and the pit was refilled.

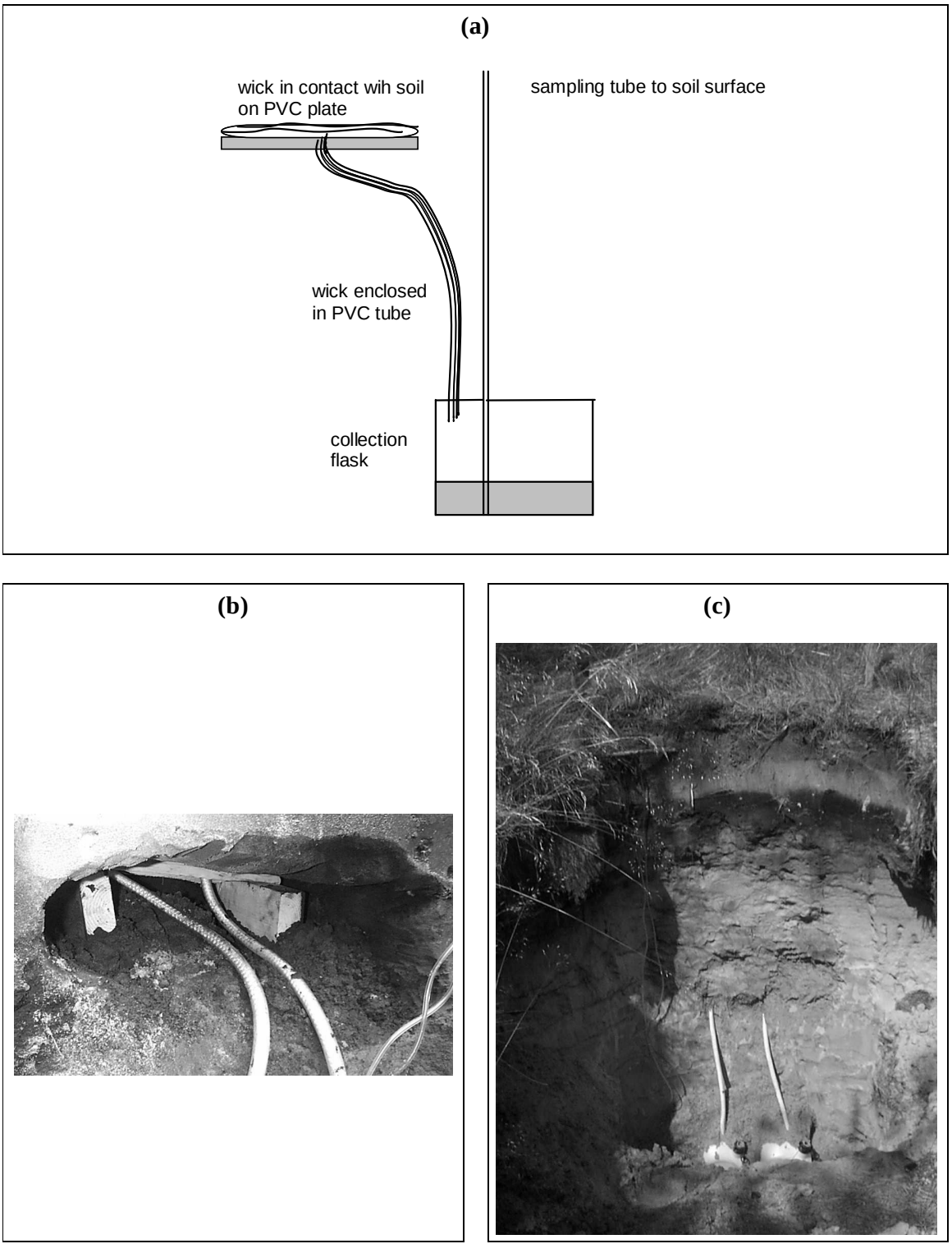

Figure 8.2 (a) Schematic picture of a passive capillary sampler, (b) excavation with wicks on PVC plate, and (c) pit after excavation is refilled with soil.

Two wick samplers were installed in two polluted Spodosols in Lommel, separated by a distance of about 150 m. One profile was a wet Spodosol (Aquod), the other profile a dry Spodosol (Placohumod). A detailed description of the profiles is given by Seuntjens *et al.* (2001a). The third wick sampler was installed in an unpolluted field in Houthalen (see section 2.2.1).

Solutions were sampled approximately bimonthly through a sampling tube running from the bottom of the collection chamber to the soil surface. The pH of the solution was measured. Concentrations of Cd, Zn, Cu, Pb, Fe, Al, Ca, Mg, Na and K in the solution were measured with ICP-OES on the solution that was acidified to pH=1 with HNO_3. Filtration (<0.45 µm) was found to have no effect on the concentrations, and therefore, no filtration step was included in the standard analysis.

At the last sampling occasion, the soil above the wick samplers was excavated. Soil solution was isolated by centrifuging the field moist soils for 1 hour at 3000*g*. The soil solution was filtered through a 0.45-µm membrane filter, acidified to pH=1 with HNO_3, and analysed with ICP-OES. The pH was determined in a water extract in a soil:solution ratio of 1:5 kg l^{-1} after 1 day of equilibration.

8.3 Results and discussion

8.3.1 Solutions sampled by wicks versus soil solution

The solutions of the first sampling occasions were discarded, because of the large pH values and the large Ca concentrations. Weathering of the fibreglass wicking material may result in solution contamination, as was also observed by Brahy *et al.* (2001) and Goyne *et al.* (2000). However, the pH and Ca concentrations declined rapidly, and did not seem to interfere with soil solution composition after some months.

Concentrations of Cd and Zn measured in the soil solution, obtained by centrifugation of the soil at the end of the experiment, agreed well with the concentrations of the solution sampled by the wick (Table 8.2, Figure 8.3). Only in the unpolluted soil, the Zn concentration in the soil solution fell outside the range of concentrations in the solutions sampled by the wick. It is possible that this is due to contamination of the soil solution since the isolation of the soil solution requires a lot of handling in the laboratory. The

concentrations in the solution sampled by the PCAPS may be interpreted as the flux concentrations (c_F), while the concentrations in the centrifugates are more representative of the resident concentration (c_R). Prediction of solute transport based on resident concentrations may lead to biased results if c_R and c_F are different. The good agreement between both methods is indicative that non-equilibrium processes, e.g., bye-pass flow and chemical non-equilibrium, do not prevail in these soils. Therefore, it seems justified to model the transport of Cd and Zn based on the local equilibrium assumption.

Table 8.2 Comparison between pore water concentrations (mean value, standard deviation of 2 replicates between parentheses) and concentrations in solutions sampled by PCAPS over a period of 18 months (mean value, range between parentheses)

	Lommel (Aquod)		Lommel (Humod)		Houthalen	
	pore water	wick	pore water	wick	pore water	wick
pH	4.18 [a]	4.6	4.65 [a]	4.6	4.77 [a]	4.8
	(0.03)	(4.1-5.5)	(0.02)	(4.0-5.5)	(0.05)	(4.3-5.6)
Cd (µg l^{-1})	17	12	17	19	1.0	0.6
	(1.3)	(6-18)	(0.6)	(14-25)	(0.1)	(0.2-2)
Zn (mg l^{-1})	0.81	0.58	0.83	0.67	0.06	0.04
	(0.05)	(0.36-0.84)	(0.02)	(0.45-0.91)	(0.01)	(0.02-0.05)
Ca (mg l^{-1})	2.1	3.8	0.9	1.6	0.38	0.9
	(0.5)	(1.1-7.8)	(0.07)	(0.7-3.8)	(0.01)	(0.2-2.9)
Mg (mg l^{-1})	0.5	0.3	0.4	0.1	0.31	0.1
	(0.1)	(0.2-0.5)	(0.07)	(0.1-0.2)	(0.01)	(0.1-0.2)
Na (mg l^{-1})	3.7	1.4	2.5	1.9	1.7	1.2
	(0.1)	(0.6-2.2)	(0.2)	(1.4-2.3)	(0.002)	(0.6-1.9)
K (mg l^{-1})	3.7	0.5	0.8	0.1	1.6	0.2
	(0.6)	(0.1-0.9)	(0.001)	(0.1-0.2)	(0.01)	(0.0-0.4)
Al (mg l^{-1})	2.0	2.3	0.8	1.6	0.29	0.9
	(0.2)	(1.0-3.8)	(0.2)	(0.3-3.0)	(0.01)	(0.3-1.3)

[a] pH measured in a soil water extract (S:L = 1/5 kg l^{-1})

The Cd and Zn concentrations are elevated in the soils of Lommel (Table 8.2). The Cd concentrations are well above the Flemish groundwater threshold of 5 µg Cd l^{-1}, although the concentration in the topsoil is only about 1 mg Cd kg^{-1}, i.e., lower than the Flemish soil clean-up value for natural and agricultural areas (2 mg Cd kg^{-1} for a standard soil with 2% organic matter and 10% clay). This discrepancy is due to the high mobility of heavy metals in these acid soils, which is also illustrated by the relatively large Cd concentration in the solution of the uncontaminated podzol.

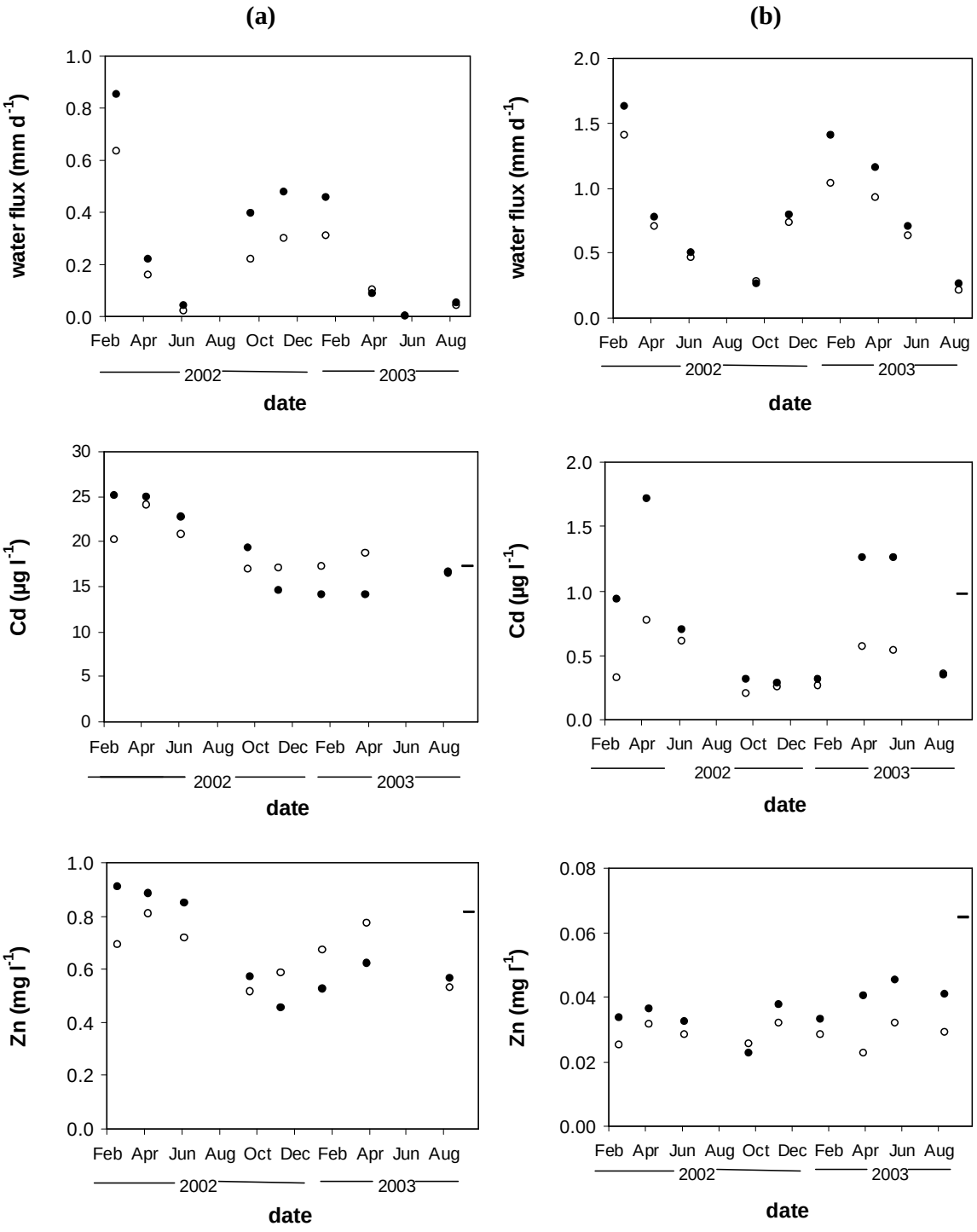

Figure 8.3 The water flux, and the concentrations of Cd and Zn measured by passive capillary samplers at 70 cm of depth in (a) a polluted podzol (Humod, Lommel), and (b) in an unpolluted podzol (Houthalen) (open and closed symbols refer to the two wicks of one sampler). The concentration in soil solution obtained by centrifugation of the soil is indicated by the dash.

The concentrations in the solutions sampled by the wick showed a temporal variation. The Ca concentrations were largest in autumn, while Al concentrations showed a peak in spring. This seasonal variation was related to the variation in pH; the pH of the solution was between 0.5 and 1 pH-unit higher in September than in April. These seasonal acidification and alkalinization phases are probably caused by nitrogen transformations. In spring, the rate of nitrification may exceed the rate of nitrate uptake, which results in a decrease of the pH in soils with low base saturation (Matzner, 1989). The lower pH in spring explains the more elevated metal concentrations between February and June (Figure 8.3).

The mean yearly drainage volume was 25 cm for the soil in Houthalen, 16 cm for the Aquod of Lommel, and 11 cm for the Humod of Lommel. The latter profile was surrounded by trees, which explains the lower flux.

8.3.2 Present-day Cd and Zn profiles

Field-averaged values of total and radio-labile concentrations of Cd and Zn are plotted in Figure 8.4. This figure also shows all measured total concentrations, illustrating the spatial variability. Total Cd and Zn concentrations decrease with depth. Labile fractions are larger for Cd than for Zn. The smallest labile fractions are observed in the topsoil (for both Cd and Zn), and in the deeper horizons for Zn (cf. section 2.3.4).

Total Cd and Zn concentrations vary considerably between profiles (Figure 8.4). Concentrations of Cd show a clear correlation with organic matter, as is illustrated in Figure 8.5 for one profile (profile 7). This profile has a clearly developed humic B-horizon, coinciding with a peak in the Cd concentration. The total Cd amount of this profile is 5.8 kg Cd ha^{-1}. No illuvial horizon was observed in profiles 2 and 6, which is reflected in the small Cd concentrations (< 0.1 mg kg^{-1}) below 10 cm of depth. These 2 profiles have the smallest Cd load (1.2 and 1.3 kg Cd ha^{-1} for profiles 2 and 6 respectively). Unless there was a large difference in Cd deposition within the field, these small Cd amounts indicate that more Cd was leached from these profiles.

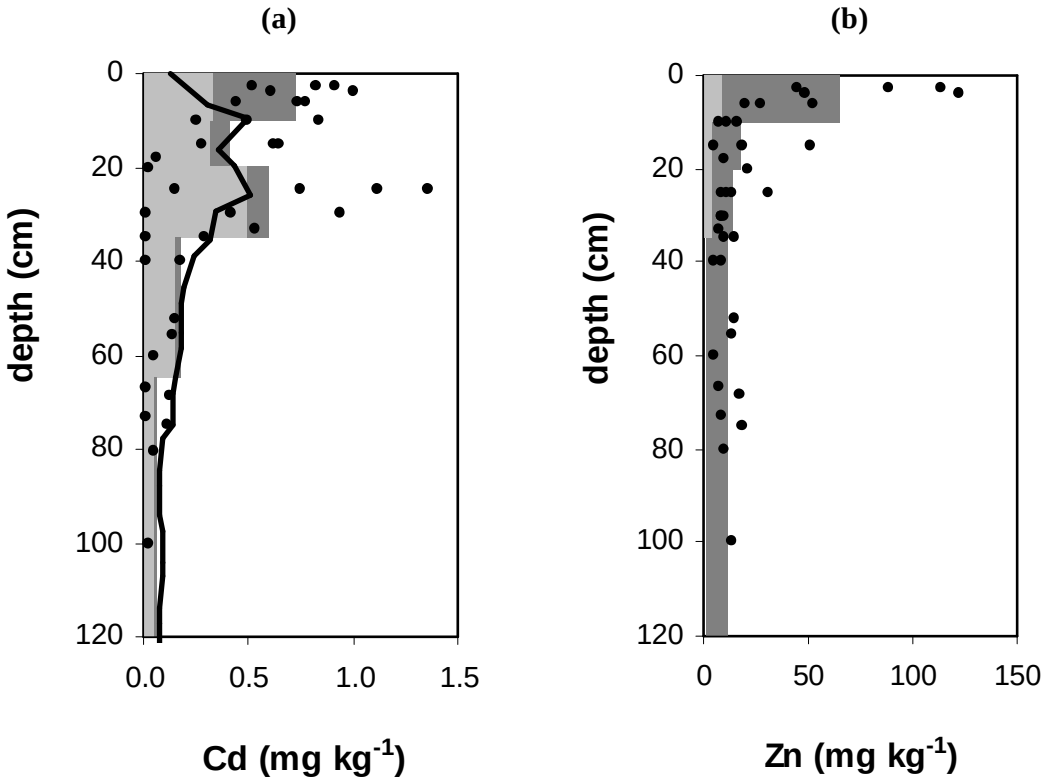

Figure 8.4 Total concentrations of (a) Cd, and (b) Zn as a function of depth. The bars denote field-averaged values of total concentrations. The light shaded area represents the field-averaged values of the radio-labile concentration (Profiles 8 and 10 not included). The line gives the total Cd concentration predicted with a convection-dispersion model.

The predicted Cd profiles correspond reasonably well with the observed profiles (Figure 8.4a and Figure 8.5). However, the total Cd concentration in the A horizon is generally underestimated. The contamination in soils surrounding smelters may be due to atmospheric deposition (primary deposition) or to secondary pollution (e.g., resuspension of contaminated soils, or roasted ores used for road construction). Cadmium and zinc are probably deposited in a partly insoluble form, which is also suggested by the low radio-labile fractions in the upper horizon. The model assumed that all Cd deposition occurred as labile Cd. Therefore, the presence of Cd in a partly insoluble form, preventing Cd to be leached, may explain the deviation between observed and predicted Cd concentration in the upper horizon. Also cycling of metals in the soil-plant environment may have contributed to the high concentrations in the A horizon.

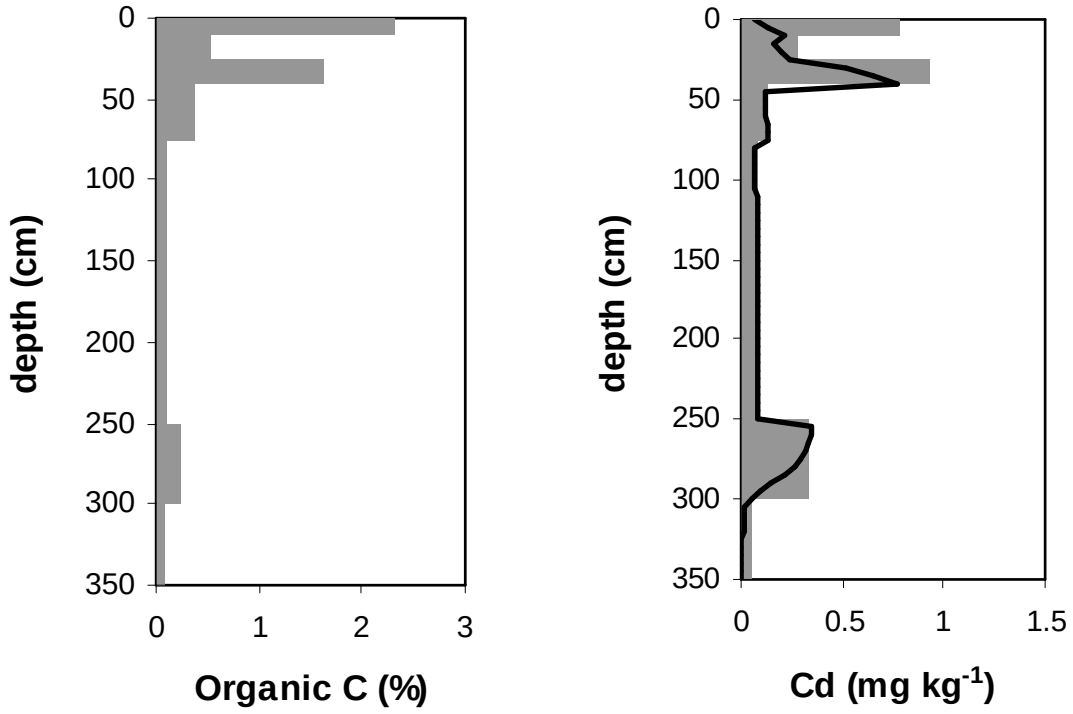

Figure 8.5 Depth profiles of organic C content and total Cd concentration for profile 7. The line gives the Cd profile predicted with the convection-dispersion equation.

No predictions of the present-day profiles were made for Zn. Most of the Zn amount deposited on the soil should be leached out according to the model predictions if it is assumed that all added Zn is labile, because of the high mobility of labile Zn at low pH. Labile Zn concentrations are indeed small, but the total Zn concentrations in the upper horizon are still elevated. We speculate that most labile Zn has been leached, while Zn that was added to the soil in a sparingly soluble form (e.g., franklinite) is only slowly released. Roberts *et al.* (2002) found that Zn in a smelter contaminated topsoil was mainly present in the Zn containing minerals franklinite ($ZnFe_2O_4$) and sphalerite (ZnS). The presence of sphalerite may be due to the emission of non-smelted ore, while franklinite is presumably formed during the roasting process.

8.3.3 Evolution of soil quality

Predicted profiles of the Cd concentration after 50 and 100 years from now are given in Figure 8.6. The concentration in the topsoil is predicted to have reached a value of around 0.1 mg Cd kg^{-1} by the year 2100. However, these predictions should be treated with care, since Cd was partly added in non-labile form. Therefore, non-labile Cd may remain present in the topsoil even after 100 years from leaching. This hypothesis is supported by the large non-labile Zn concentration in the upper horizon (on average 56 mg Zn kg^{-1}, cf. Figure 8.4b). These concentrations are much larger than non-labile Zn concentrations in the topsoil of an uncontaminated podzol with comparable soil properties (around 5 mg Zn kg^{-1}, cf. Table 2.2), despite the small retention of Zn in these profiles. This indicates that the release of non-radio-labile heavy metals (e.g., by dissolution of minerals or solid-state diffusion) is a very slow process, that may take decades or even centuries. The slow release of non-labile metals was also observed in a column experiment with a smelter contaminated soil (Chapter 6). However, the rate constant for the desorption of non-labile Zn derived from the column experiment (α=0.002 d^{-1}, Figure 6.10) cannot be used to model the metal transport at field scale. A model with this relatively large rate constant would predict that almost all non-labile Zn in the topsoil is mobilized (since most Zn has been deposited between 100 and 50 years ago, cf. Figure 8.1), which is in contradiction with the observations (Figure 8.4b). A possible explanation for the difference in desorption kinetics of non-labile metals between the column experiment and the field situation is the difference in water flux. The larger flux in the column experiment may cause accelerated weathering of the non-labile metals. It can be shown that the rate constant is proportional to the water flux if the release of non-labile metal is due to dissolution of a metal-bearing mineral.

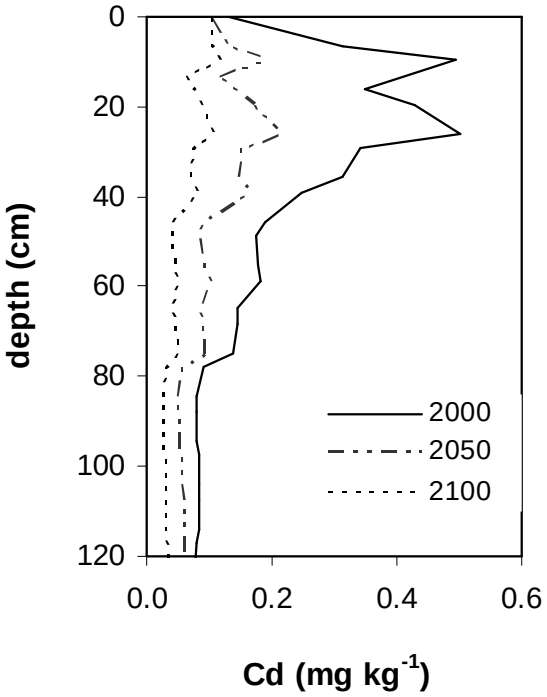

Figure 8.6 Predicted evolution of the field-averaged depth profiles of Cd, assuming constant pH, and a future Cd deposition of 2.3 g Cd ha^{-1}.

8.3.4 Concentrations in seepage water

Concentrations in the seepage water were calculated by averaging the solution concentrations at the bottom of all soil profiles. According to the model calculations, 1.7 kg Cd ha^{-1} was transported to the groundwater in the past 100 years, and 2.8 kg Cd ha^{-1} will be leached during the next 100 years at concentrations around 10 to 15 µg Cd l^{-1} (Figure 8.7). The field-averaged breakthrough curve shows a double peak. The first peak is due to transport of Cd from the profiles with lower retention capacity (profiles 1, 2, 3, and 6), while the second peak is caused by leaching from profiles with the higher retention capacity (profiles 4, 5, 7, and 9). It is possible that if profiles would have been sampled at higher density, a smooth breakthrough curve would have been obtained. However, the conclusion would presumably have been the same, i.e., the gross of Cd deposited on these soils is transported to the groundwater between 100 and 250 years after the start of the deposition. In other words, most of Cd deposited on the soil is still present in the profile and will be leached during the next 150 years.

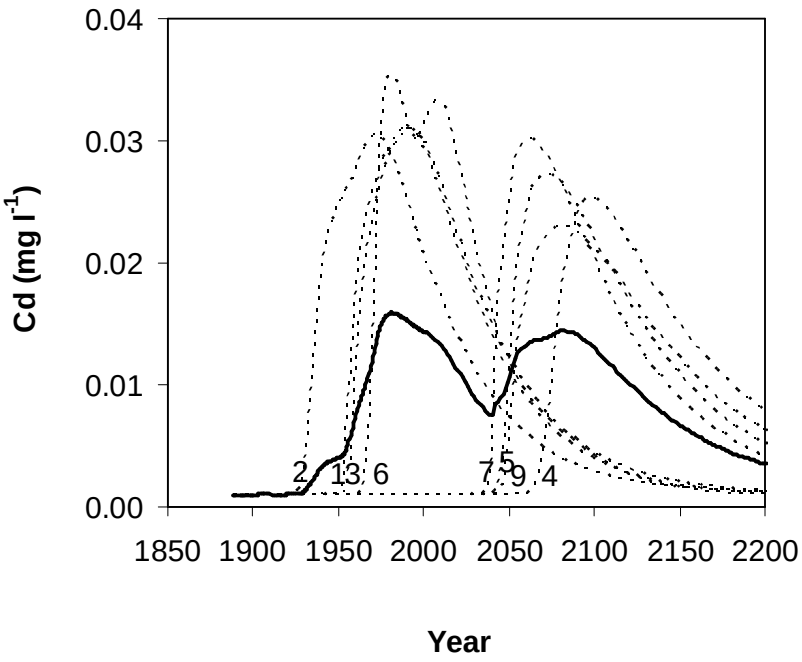

Figure 8.7 Predicted Cd concentration in seepage water for all profiles separately (dotted lines, profile indicated by label at the start of the breakthrough), and the predicted field-averaged concentration in the seepage water (full line).

No prediction of the historical Zn transport was made for reasons mentioned above. Prediction of the future transport indicates that the field-averaged concentration in the seepage water will gradually decrease and reach values below 0.5 mg Zn l^{-1} after about 50 years (Figure 8.8). Almost all radio-labile Zn will be removed after about 100 years. These predictions were made assuming that only labile Zn will be leached to the groundwater. If the total K_d is used for the calculations (i.e., if it is assumed that all metal is in equilibrium with the solution and can be leached), it is predicted that the Zn concentration in the seepage water will remain almost constant (~ 1 mg Zn l^{-1}) during the next 100 years. However, the column experiments described in Chapters 5 and 6 showed that metal leaching is strongly overestimated if non-labile Zn is assumed to be in equilibrium with the solution. It is more likely that a slow desorption of non-labile Zn will occur, resulting in long tailing of the Zn breakthrough curve at low concentrations, as was observed in a column experiment (Chapter 6, Figure 6.8).

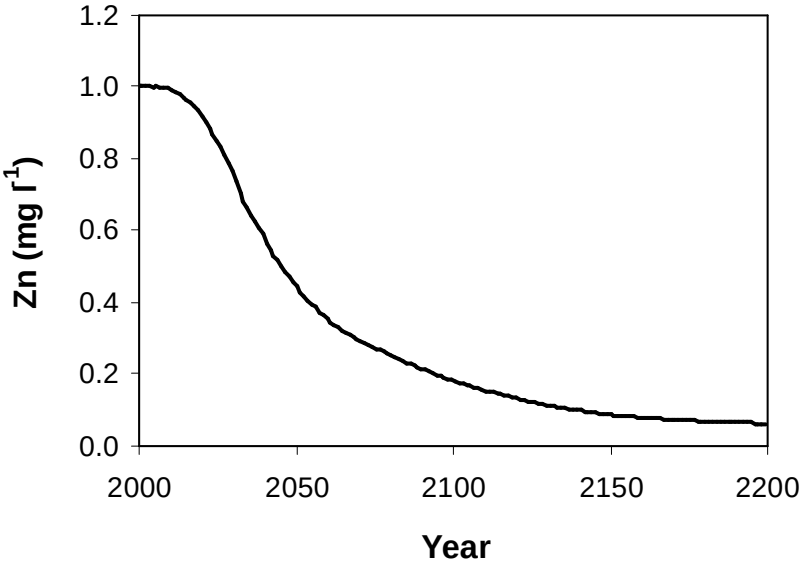

Figure 8.8 Predicted field-averaged concentration of Zn in seepage water.

The calculation of the breakthrough time (BTT) has been proposed as a simple tool to assess how fast Cd and Zn are transported to the groundwater (Ingwersen, 2001). The BTT (in years) is calculated with a piston-flow approach, which neglects local dispersion:

$$\mathrm{BTT} = \sum_i \frac{d_i}{v_i} \cdot (1 + \frac{\rho_i}{\theta_i} K_{\mathrm{d},i}) \tag{8.4}$$

where v_i is the pore water velocity (cm y^{-1}), ρ_i is the bulk density (kg l^{-1}), θ_i is the volumetric water content (cm^3 cm^{-3}), d_i is the thickness (cm) and $K_{d,i}$ is the distribution coefficient (l kg^{-1}) of the i-th horizon. Since $\rho.K_d >> \theta$, equation 8.4 can be simplified to:

$$\mathrm{BTT} = \frac{1}{q} \cdot \sum_i d_i \cdot \rho_i \cdot K_{\mathrm{d},i} \tag{8.5}$$

where q is the stationary flux at the upper boundary (23.4 cm y^{-1}). Equation 8.5 was used to calculate the breakthrough time of Cd and Zn (Table 8.3). The K_d was calculated as the slope from the Freundlich isotherm at a pore water concentration of 0.015 mg Cd l^{-1} or 0.5 mg Zn l^{-1}. The BTT of Cd calculated with the piston flow approach is in good agreement with the time (after the start from the production, i.e. 1889) where the Cd concentration in the seepage water starts to increase according to the numerical simulations. The agreement between both methods (details not shown) indicates that the BTT approach can be used to form an idea of how fast metals will be transported to the soil. The breakthrough times of Zn are smaller than those of Cd, because of the weaker retention of Zn in soils with low pH.

Table 8.3 Calculated breakthrough times (in years) of Cd and Zn

profile	1	2	3	4	5	6	7	9
cadmium	84	68	89	206	174	98	153	167
zinc	24	17	34	71	63	37	67	55

8.3.5 Liming as an option to reduce metal leaching to groundwater

Liming may be a cheap option to reduce leaching of Cd and Zn to the groundwater (cf. Chapter 6). About 3.5 ton $CaCO_3$ ha^{-1} would be needed to increase the pH of the top 25 cm with 2 pH units, since the pH buffer capacity of the topsoil is around 1 $cmol_c$ kg^{-1} pH^{-1}. Smaller lime applications – in the order of 0.3 ton $CaCO_3$ ha^{-1} y^{-1} – would be required afterwards to maintain the pH.

The effect of liming the top 25 cm was modelled assuming that the increase in pH with 2 units results in a tenfold reduction of the pore water concentrations of Cd and Zn in the top 25 cm (Chapter 4). It is predicted that 2.4 kg Cd ha^{-1} will be leached during the next 100 years when the topsoil is limed, instead of 2.8 kg Cd ha^{-1} when no action is taken (Figure 8.9a). Most Cd has already been transported to depths greater than 25 cm in most profiles, which explains the limited effect of liming. However, liming may considerably decrease the Cd concentrations in the seepage water for profiles with larger K_d values in the topsoil, where a large fraction of the Cd deposited on the soil is still present in the upper 25 cm (Figure 8.9b).

Liming was predicted to have also limited effect on the Zn concentrations in the seepage water. Other remediation procedures, such as removal of the topsoil or soil amendments, will equally have only a small impact on the Cd and Zn concentrations in the seepage water.

Deep liming (e.g. to a depth of 80 cm) on the other hand is expected to result in a stronger and earlier decrease in the concentrations of Cd and Zn in the seepage water. Deep liming will also increase the retention of Cd and Zn at depths between 25 and 80 cm below the soil surface, where in most profiles a large fraction (~ 30–50%) of the total Cd amount in the profile is present.

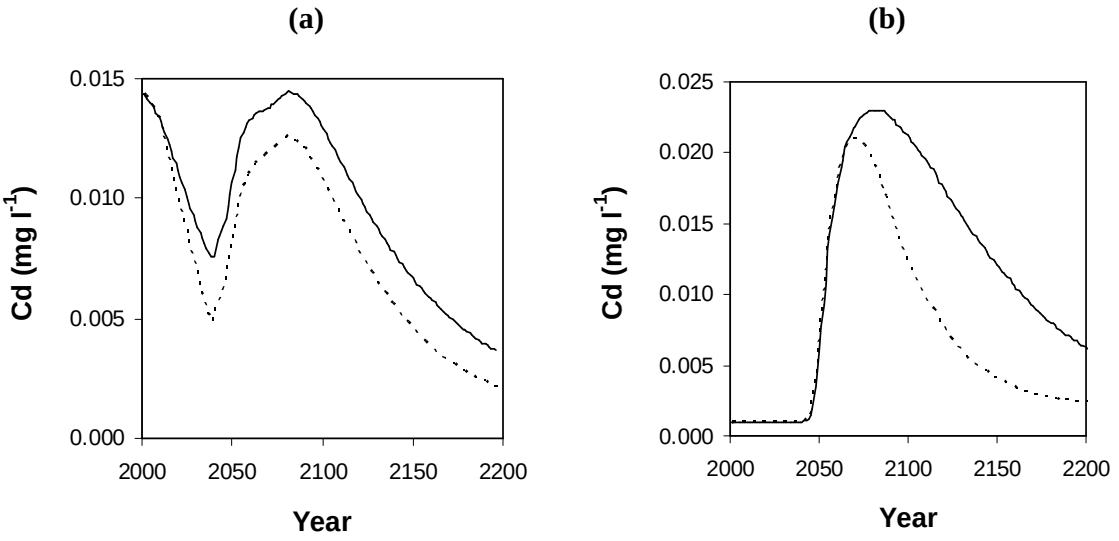

Figure 8.9 Predicted Cd concentrations in seepage water when no action is taken (full line), or when the top 25 cm is limed (dotted line). (a) Averaged value for all profiles, and (b) profile 9 only.

In conclusion, observed present-day Cd profiles agreed reasonably well with the profiles that were predicted with the local equilibrium assumption (LEA) using sorption parameters based on the concentration in soil solutions obtained by centrifugation. The use of the LEA was also supported by the good agreement between 'flux' concentrations of Cd and Zn (in solutions obtained by wick samplers) and 'resident' concentrations (in solutions obtained by soil centrifugation). Observed and predicted depth profiles agreed well, except in the upper horizon where the total Cd concentrations were underestimated. The presence of non-labile Cd in the deposition, which was not accounted for in the retrospective modelling, may explain this deviation between observed and predicted values. It is predicted that the Cd concentration in the seepage water will remain above 5 µg Cd l^{-1} for the next 170 years. Liming the top 25 cm may reduce this period to 140 years. The effect of liming the topsoil is limited since most Cd has moved down to depths greater than 25 cm.

CHAPTER 9

Mobilisation of Cd upon afforestation of agricultural land

Abstract

The set-aside of agricultural lands may result in rapid acidification of the soil. In soils contaminated with heavy metals, this acidification may lead to a strong mobilization of Cd accumulated in the plough layer. Soils were sampled in a sandy field that was set aside in 1992. The Cd concentration in the top 30 cm of this field is, on average, 10 mg kg^{-1}, most of which is labile. The coupled transport of Cd and protons was calculated for each of the 48 profiles sampled ('grid model'), using the pH buffer capacity and sorption parameters determined in batch experiments. It was predicted that the field-averaged Cd concentration in the seepage water will increase from 6 µg l^{-1} actually to 300 µg l^{-1} in 100 years, which largely exceeds the maximum permissible concentration (MPC) in groundwater of 5 µg l^{-1}. Predictions of Cd transport using field averaged soil properties yielded a later breakthrough time and a larger peak Cd concentration than predicted with the grid model, illustrating the impact of spatial variability on solute transport. Continuation of liming practices is a possible solution to prevent breakthrough of Cd at concentrations far in excess of the MPC. It is predicted that the mean Cd concentration in the seepage water will only increase from 6 to 7 µg l^{-1} in 100 years when the pH of the soil is maintained through liming.

9.1 Introduction

As a result of set-aside policy, agricultural land is converted to forest or wetland to reduce arable crop production and to restore natural ecosystems. Agricultural soils converted to forest gradually acidify. Römkens and de Vries (1995) found that pH in the topsoil of Dutch soils converted to forest, decreased from 6 to 4 within 20 to 30 years. The pH of the topsoil decreased from 7 to 4.1 over a period of 100 years in an agricultural soil that was converted to woodland (Johnston *et al.*, 1986). Acid deposition was the major cause of acidification in this soil.

It has been suggested that acidification might lead to a strong and sudden increase in plant uptake and leaching of Cd, because Cd sorption is strongly dependent on pH (Stigliani *et al.*, 1993). A decrease in pH with one unit results in a decrease of the solid–liquid distribution coefficient with about a factor of 5 (e.g., Temminghoff *et al.*, 1995; chapter 3). In chapter 7, a strong increase in pore water concentrations of Cd and accelerated leaching was observed in a column study with a contaminated sandy soil percolated with a $CaCl_2$ solution acidified to pH=3. The Cd and proton transport for this column experiment was successfully predicted by a coupled reactive transport model. In this chapter, this approach will be used to predict the Cd transport under acidifying conditions at field scale.

Solute transport at field scale is strongly influenced by soil variability. The moment of first breakthrough may be underestimated if field heterogeneity is not taken into account (van der Zee *et al.*, 1987). Transport at field scale is often modelled by representing the field as a collection of soil stream tubes that are not connected (i.e., no traversal mixing). In the Bresler-Dagan model, further developed for sorbing solutes by van der Zee *et al.* (1987), the transport within each stream tube is described by piston flow. By neglecting dispersion, analytical solutions could be derived for the solute transport. Numerical Monte Carlo simulations may be used to describe the transport in each stream tube by an equilibrium convection-dispersion equation (e.g., Seuntjens *et al.*, 2002). Both the Bresler-Dagan model and the Monte Carlo simulations use random input variables and yield probability density functions (pdf) of concentration as function of time and depth. Another approach to model field-scale transport, is the 1-D simulation of solute transport for all profiles sampled using measured parameters. In contrast to Monte Carlo simulations, this 'grid model' yields a three dimensional distribution of concentrations as output. Streck and Richter (1997b) used both the grid model and Monte Carlo simulations to model

displacement of Cd and Zn at field scale in a sandy soil after 29 years of wastewater irrigation. The differences between predictions of both models were small.

In this study, we modelled Cd transport in a sandy field that was set aside in 1992, located in the northern part of Belgium. Heavy metal concentrations in this field are elevated due to Zn smelter activities. Acid deposition is relatively large in this region, because of industrial activities and intensive cattle breeding. The transport was modelled with a grid model by solving convection-dispersion equations for coupled transport of Cd and protons for each of the 48 profiles sampled.

9.2 Materials and methods

9.2.1 Soil and soil characteristics

Soils were taken in a field that is part of a nature reserve (Hageven) in Neerpelt, situated in the 'Kempen' (northern Belgium). The field is a former arable land that was set aside in 1992. The soil is strongly contaminated with Cd and Zn due to emissions from a nearby Zn refinery that was in operation until 1995. The soil is classified as a typic haplaquod, a wet sandy soil with a plough layer. The groundwater table fluctuates between about 60 and 120 cm of depth.

Soil samples were taken in 1997, in a 20 m by 20 m grid. At each of the 48 points, samples were taken with an Edelman screw auger at 5 depths (0-15, 15-30, 30-45, 45-60, and 60-90 cm). The samples were air dried and passed through a 2 mm sieve.

The pH was measured in 0.001 M $CaCl_2$ in a 1:10 soil:solution ratio. Organic C content was measured by dry combustion (Skalar CA 100). 'Total' Cd and Zn were determined by cold extraction with 0.43 M HNO_3 in a 1:10 soil:solution ratio (Houba *et al.*, 1989). Radio-labile Cd was determined by isotopic dilution (section 1.2.2), in a 0.001 M $CaCl_2$ extract in a 1:10 soil:solution ratio. Pore water concentrations of Cd were not measured, but were approximated by the concentration in the 0.001 M $CaCl_2$ extract. The soil solution composition was determined in 2 soil profiles, and it was found that the ionic strength of the solution was between 2.0 and 4.7 mM, comparable to the ionic strength of the $CaCl_2$ extract.

Soils sampled in a nearby field, with similar soil characteristics but a larger variation in pH, were used to test whether the Cd concentration in the $CaCl_2$ extract gives reasonable estimates of the pore water concentration. Ten profiles were sampled at 6 depths. Soil

characteristics of this field are summarized in Table 3.2. The soil solution was isolated by centrifugation and analysed for Cd, Zn, and major cations by ICP-OES. Ionic strength of the solutions ranged from 0.7 to 4 mM. The Cd concentration, measured in a 0.001 M $CaCl_2$ extract, differed at most by a factor of 3 from the Cd concentration in the soil solution, except for 3 samples.

The soils of this field were also used to derive an equation relating CEC to pH (measured in 0.001 M $CaCl_2$) and organic C content. The CEC and concentrations of exchangeable bases were measured at the soil pH with silverthiourea as index cation (Chhabra *et al.*, 1975).

9.2.2 Batch experiments

Proton buffer curves were obtained by equilibrating soil samples with 0.001 M $CaCl_2$ in a 1:10 soil:solution ratio, with varying concentrations of HNO_3 (0, 0.02, 0.04, 0.06, 0.08, 0.1, and 0.12 mmol HNO_3 g^{-1}). The suspensions were shaken end over end for 24 hours, and spiked with ^{109}Cd. The samples were shaken for a further seven days, centrifuged, and the pH of the supernatant was measured. The ^{109}Cd activity of the supernatant was determined, which allowed to calculate the isotopic distribution coefficient, K_d^* (l kg^{-1}).

9.2.3 Modelling

9.2.3.1 Transport model

The sorption parameters describing the solid–liquid distribution of H^+ and Cd were derived from the batch experiments. The 'sorption isotherm' of protons was described with:

$$s_H = a \cdot \ln c_H + b \qquad (9.1)$$

where s_H is the proton concentration on the solid phase (mol kg^{-1}), c_H is the solution concentration (mol l^{-1}), and a and b are empirical parameters. As mentioned in section 7.2.3, s_H effectively represents H^+ exchanged and H^+ consumed in mineral dissolution.

The pH dependency of the solid–liquid distribution of Cd was quantified using following equation:

$$s_{Cd} = k' \cdot c_H^{\,m} \cdot c_{Cd} \qquad (9.2)$$

where s_{Cd} is the labile concentration on the solid phase (mg kg^{-1}), c_{Cd} is the solution concentration (mg l^{-1}), and k' is a parameter depending on the organic C content.

The transport was modelled by solving convection-dispersion equations for coupled transport of Cd and protons (full details in section 7.2.3):

$$\frac{\delta c_{Cd}}{\delta t}(\theta + \rho \cdot k' \cdot {c_H}^m) = \lambda_{Cd} \cdot q \cdot \frac{\delta^2 c_{Cd}}{\delta z^2} - q \cdot \frac{\delta c_{Cd}}{\delta z} - \rho \cdot c_{Cd} \cdot k' \cdot m \cdot {c_H}^{m-1} \cdot \frac{\delta c_H}{\delta t} \quad (9.3)$$

$$\frac{\delta c_H}{\delta t}(\theta + \rho \cdot \frac{a}{c_H}) = \lambda_H \cdot q \cdot \frac{\delta^2 c_H}{\delta z^2} - q \cdot \frac{\delta c_H}{\delta z} \quad (9.4)$$

Equations 9.3 and 9.4 were numerically solved together, using finite differences with an explicit scheme. It was assumed that the term θ in the left hand side of the equations could be neglected. The error (on $\delta c/\delta t$) introduced by omission of θ was mostly less than 1%, and amounted to 5% at most (for the Cd transport in the subsoil when pH was below 4). The dispersion length for the Cd transport, λ_{Cd}, was assumed to be 5 cm, which is a normal value for solute transport at comparable field scale (Černík *et al.*, 1994). However, the proton transport was calculated with a dispersion length (λ_H) of 500 cm, for reasons explained below. The stationary flux at the upper boundary, *q*, was assumed to be 23.4 cm y^{-1}, which is the long term average precipitation surplus for the region (Patyn, 1997).

The transport was simulated for each of the 48 profiles sampled. The measured buffering capacity (expressed by the parameter *a*) was used to model changes in pH upon acidification. This parameter was determined for all 240 soil samples (48 profiles at 5 depths). The dependence of the sorption parameter *k*' (eq. 9.2) on the organic C content was described with:

$$\log(k') = \log(k) + d.\ \log(\%OC) \quad (9.5)$$

where *k* and *d* are constants obtained by regression analysis (section 9.3.3). The pH and the radio-labile Cd concentrations measured in 1997 were used as the initial values. A third-type flux boundary condition (Cauchy type) was used at the top and a second-type (zero concentration gradient or Neumann type) boundary condition at the bottom (eq. 8.1). The lower boundary was taken at 90 cm of depth. The acid input was assumed to be 4.7 $kmol_c\ ha^{-1}\ y^{-1}$ (see section 9.2.3.2), which corresponds to a H^+ concentration of 0.002 M in the infiltrating water. The Cd concentration in the infiltrating water was assumed to be 0.001 mg Cd l^{-1}, corresponding to a deposition rate of 2.3 g Cd $ha^{-1}\ y^{-1}$. Estimates for Cd deposition, based on Cd concentrations in rainwater, in the Netherlands during the period 1998-2000 are in the order of 1 to 2 g Cd $ha^{-1}\ y^{-1}$ (RIVM, 1999, 2001ab). The present-day total Cd amount between 0 and 90 cm of depth is, on average, 52 kg ha^{-1}. The actual Cd

input is hence a minor part of the historical input because of the reduced emission since about 1970.

Predictions of the Cd transport were also made in case the acidification is prevented by regular liming. In this case, an acid input was assumed that is equivalent to a pH of 6.3 in the infiltrating water.

9.2.3.2 Estimation of acid input

The acidification of soil is caused by inputs of the acidifying compounds SO_2, NO_x, and NH_3. Ammonia only acidifies the soil if it is nitrified and the resultant nitrate is leached:

$$NH_4^+ + 2\ O_2 \rightarrow\ NO_3^- + 2\ H^+ +\ H_2O \qquad (9.6)$$

One mole SO_2 corresponds to 2 acid equivalents, while 1 mole NO_x or NH_3 correspond to 1 acid equivalent. Equation 9.6 seems to imply that one mole ammonia may result in the production of 2 mole H^+. However, half of the acidity in NH_4^+ originates from an acid substance (e.g., SO_2) that has transferred a proton to NH_3.

Values of acid deposition for the region studied were obtained from MIRA (VMM, 2002). These values are based on emission data, that are converted to deposition data with an atmospheric transport model. Average values in 2001 for Flanders were 1.2 $kmol_c\ ha^{-1}\ y^{-1}$ for SO_2 deposits, 1.3 $kmol_c\ ha^{-1}\ y^{-1}$ for NO_x deposits, and 2.1 $kmol_c\ ha^{-1}\ y^{-1}$ for NH_3 deposits, or a total acid deposition of 4.6 $kmol_c\ ha^{-1}\ y^{-1}$. The large contribution of NH_3 to the acid deposition is due to the intensive cattle breeding. Maps showing the regional distribution of the acid deposition indicated that the deposition in the region studied is around the mean value for Flanders. Values for H^+ deposition in rain are small in comparison and are in the order of 0.1 $kmol_c\ ha^{-1}\ y^{-1}$.

Internal proton sources may also contribute to the acidification of the soil. Ecosystems that increase in biomass acidify the soil, if net assimilation of cations exceeds that of anions. In steady-state ecosystems, however, mineralization equals assimilation and the soil does not acidify because of nutrient assimilation. Deprotonation of CO_2 or organic acids may lead to acidification. This proton source is usually of minor importance in soils with moderate or low pH. Deprotonation of CO_2 may be a significant proton source in soils where the pH exceeds the pK_a for proton dissociation of CO_2 (pK_a=6.3).

Proton balances have shown the importance of acid deposition to acidification near centers of anthropogenic activities. In central and northwestern Europe, acidic deposition

is a major fraction of the total proton loading in ecosystems with low to intermediate rates of internal proton production (van Breemen *et al.*, 1984). Therefore, the acid deposition, estimated to be 4.7 $kmol_c\ ha^{-1}\ y^{-1}$, was used as value for the total acid input.

9.3 Results and discussion

9.3.1 Soil characteristics

Selected soil characteristics are summarized in Table 9.1. The soils were sampled five years after the field was set aside, which explains the slightly lower pH in the upper layers. The plough layer (A_p) extends to a depth of 30 cm. The humic B horizon is located between 30 and 45 cm of depth. The C horizon, characterised by the yellow colour because of the small organic C content, starts at 45 cm of depth in most profiles. However, the organic C content is still larger than 1% in the 45–60 cm layer for 11 of the 48 profiles.

The HNO_3 extractable concentrations reach values up to 21 mg Cd kg^{-1} and 1080 mg Zn kg^{-1} in the plough layer (0–30 cm). Radio-labile Cd concentrations (*E* values) sometimes exceeded HNO_3 extractable Cd, indicating that not all Cd was extracted with the HNO_3 extract (Table 9.1). Total Cd concentrations were determined by *aqua regia* digestion for 5 soils from one profile. It was found that the *E* value ranged from 75 to 100% of the total Cd concentration. These large labile fractions indicate that Cd has entered the soil in soluble form or that Cd in insoluble form has been transformed to labile Cd.

The amount of Cd and Zn for each sampled profile (M_{profile}, kg ha^{-1}) was calculated by summing up the metal amount in all horizons:

$$M_{\text{profile}} = \sum_i 0.1 \cdot d_i \cdot \rho_i \cdot M_{\text{tot},i} \qquad (9.7)$$

where d_i is the horizon thickness (cm), ρ_i is the bulk density (g cm^{-3}), $M_{\text{tot},\,i}$ is the total metal content (mg kg^{-1}) of the *i*-th soil horizon, and 0.1 is a conversion factor. The total metal load ranged from 25 to 132 kg ha^{-1} for Cd and from 2220 to 8317 kg ha^{-1} for Zn. On average, 79% of Cd and 66% of Zn was present in the topsoil (0–30 cm). Figure 9.1 shows the spatial distribution of the Cd load. A similar pattern was found for Zn, indicating simultaneous deposition of Cd and Zn.

Table 9.1 Soil characteristics, HNO_3 extractable Cd and Zn concentration (Cd_{tot} and Zn_{tot}), radio-labile Cd concentration (E_{Cd}), and Cd concentration in solution (0.001 M $CaCl_2$). Values are averages for all 48 profiles (standard deviation between parentheses).

depth (cm)	pH	OC (%)	Zn_{tot} (mg kg^{-1})	Cd_{tot} (mg kg^{-1})	E_{Cd} (mg kg^{-1})	Cd_{sol} (mg l^{-1})
0–15	6.16	2.02	615	9.85	10.0	0.025
	(0.30)	(0.44)	(117)	(1.96)	(2.85)	(0.008)
15–30	6.31	1.88	596	9.46	9.96	0.023
	(0.25)	(0.42)	(140)	(2.29)	(3.66)	(0.007)
30-45	6.37	1.05	284	3.10	3.75	0.014
	(0.22)	(1.04)	(212)	(3.19)	(4.93)	(0.012)
45–60	6.37	0.98	159	1.15	1.40	0.010
	(0.21)	(1.61)	(111)	(1.85)	(2.25)	(0.012)
60–90	6.37	0.49	69	0.46	0.53	0.006
	(0.25)	(0.77)	(58)	(0.65)	(0.72)	(0.009)

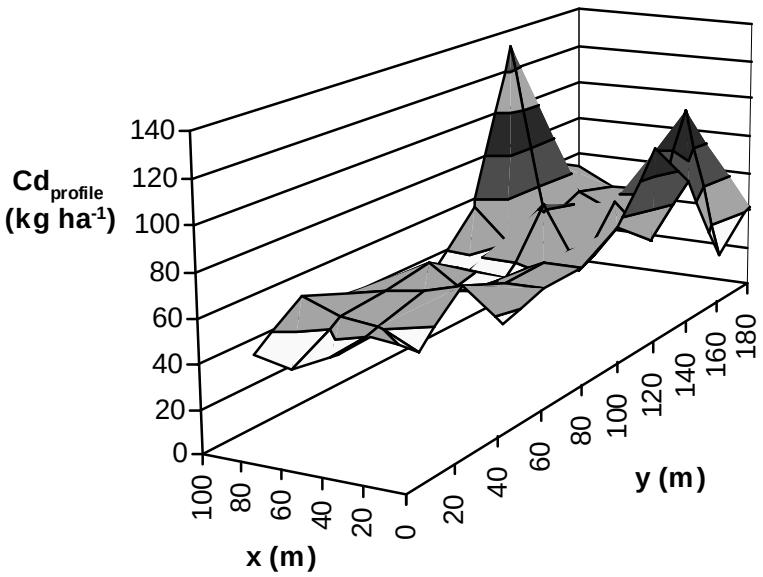

Figure 9.1 Spatial distribution of the Cd load per unit area.

9.3.2 Proton buffer capacity

The pH buffer capacity of a soil (pH BC, $cmol_c\ kg^{-1}\ pH^{-1}$) is expressed as the amount acid or base that must be added to change the pH with one unit, and is usually determined by titration of the soil. Figure 9.2 shows a titration curve, obtained by HNO_3 addition to a soil suspended in 0.001 M $CaCl_2$.

The pH buffering of a soil arises from dissolution/precipitation reactions, e.g. of $CaCO_3$ at high pH and Al compounds at low pH, and from cation exchange reactions. In the pH range 4 to 6, cation exchange is an important buffering mechanism (Reuss *et al.*, 1990). Protons added to the soil will release Al from silicate lattices. The main reaction products are non-exchangeable Al-hydroxy-cations that bind to exchange surfaces, thus leading to a reduction in the CEC, and Al^{3+} ions that exchange with base cations, thus causing a reduction in the base saturation.

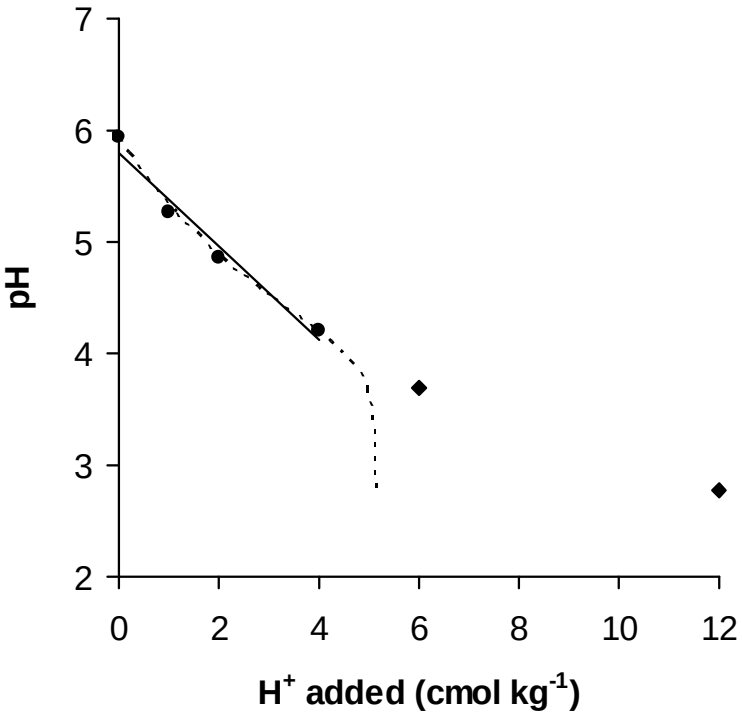

Figure 9.2 The change in pH with increasing acid load for a sandy soil (OC 2.6%). The pH BC was calculated as the reciprocal of slope of the regression line for pH values above 4 (full line). The dotted line was calculated based on the assumption that pH buffering is only related to cation exchange (model explained in text)

If soil buffer capacity is only due to cation exchange, the pH BC may be estimated from the pH dependency of the CEC, and the change in base saturation with pH:

$$\text{pH BC} = \frac{H^+_{added}}{pH_1 - pH_2} = \frac{CEC_{pH_1} \cdot BS_{pH_1} - CEC_{pH_2} \cdot BS_{pH_2}}{pH_1 - pH_2} \qquad (9.8)$$

where H^+_{added} is the amount of protons added to lower the pH from pH_1 to pH_2.

The relationship between base saturation and pH and the dependency of CEC on soil properties were estimated from data of a nearby field with larger variation in pH (Table 3.2). At constant Ca concentration, the change in base saturation with pH can be described with following equation, according to the ion exchange theory (see section 4.4.1):

$$pH = k' + 0.5 \log \frac{BS}{(1 - BS)^2} \qquad (9.9)$$

where BS is the base saturation of the ion exchange complex. The relationship between pH and BS could be well described with this equation when *k'* was set to 4.2 for a Ca concentration of 0.001 M (Figure 4.2).

The pH dependency of the CEC ($cmol_c\ kg^{-1}$) was described by a model in which the CEC of organic C increases linearly with pH and the CEC of mineral components is not pH dependent. Following regression equation was obtained:

$$CEC = 0.74 + (-1.37 + 0.53\ pH)\ \%OC \qquad (R^2=0.87,\ n=54) \qquad (9.10)$$

The change in CEC of organic C per pH unit, which is 53 ± 7 $cmol_c\ kg^{-1}\ pH^{-1}$, is in good agreement with results of other authors. Values of about 50 $cmol_c\ kg^{-1}\ pH^{-1}$ were reported by Helling *et al.* (1964), Kalisz and Stone (1980) and Aitken *et al.* (1990).

A theoretical buffer curve could be derived, by substitution of the estimated CEC (eq. 9.10) and BS (eq. 9.9) in eq. 9.8, which is illustrated in Figure 9.2 for a soil with 2.6% OC. This theoretical curve agrees well with the experimentally determined buffer curve in the pH range 4 to 6, indicating that buffering in this pH range is mainly due to cation exchange reactions. Below pH 4, the pH buffering is largely underestimated, since cation exchange buffering is negligible below this pH and pH buffering is presumably due to dissolution of Al-hydroxy compounds.

The relationship between pH and H^+ added to the soil was approximately linear for pH values above 4 (cf. Figure 9.2). Linear regressions were fitted through this part of the buffer curve, and the pH buffer capacity was calculated as the reciprocal of the slope of this

regression line (Figure 9.2). The pH BC correlated well with the organic C content, as can be seen in Figure 9.3. The result of the linear regression indicated that 79 cmol H^+ kg^{-1} of organic C is needed to lower the pH with one unit. Magdoff *et al.* (1987) found a value of 70 cmol kg^{-1} C pH^{-1} for North American forest soils. Aitken *et al.* (1990) reported values of about 90 cmol kg^{-1} C pH^{-1} for soils from Queensland (Australia). A value of 71 cmol kg^{-1} C pH^{-1} was found for weathered soils of the tropics (Oorts, 2002). The buffering of organic C is due to weakly acidic functional groups, such as carboxylic and phenolic groups.

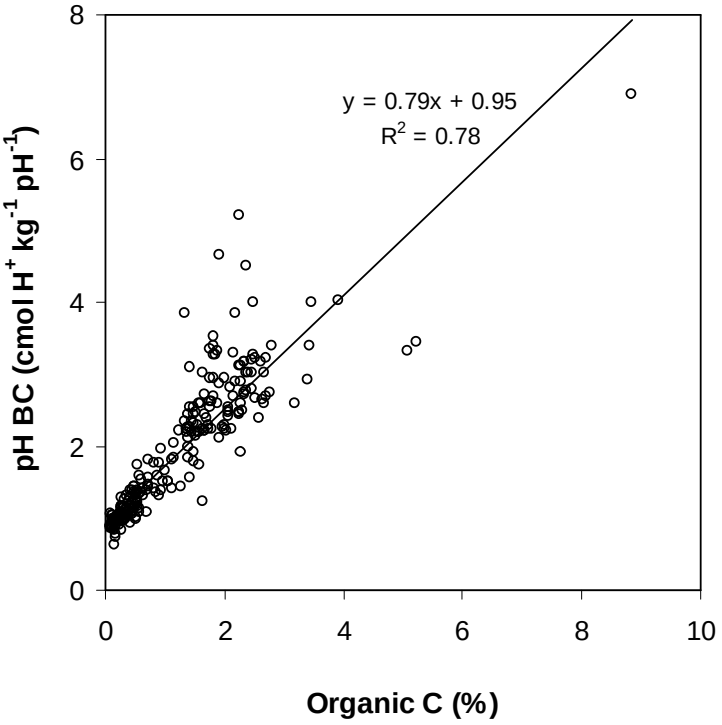

Figure 9.3 The pH buffer capacity as a function of the organic C content. Symbols are measured values (*n*=239), and the full line is the linear regression line.

According to equations 9.9 and 9.10, the CEC of organic matter is 178 $cmol_c$ kg^{-1} C at pH 6 and 73 $cmol_c$ kg^{-1} C at pH 4, and the base saturation is 0.99 at pH 6 and 0.24 at pH 4. Thus, the loss of exchangeable bases between pH 6 and pH 4 is 158 $cmol_c$ kg^{-1} C, or 79 $cmol_c$ kg^{-1} C pH^{-1}, which is the same value as that from the empirically derived regression equation (Figure 9.3). Organic C is a main contributor to the pH buffering in these soils, but the non-zero intercept in Figure 9.3 indicates that it is not the only source of pH buffering.

9.3.3 Effect of pH on solid–liquid distribution of cadmium

For all soils, the solid–liquid distribution coefficient of Cd was measured in 0.001 M $CaCl_2$ at various pH values, obtained through HNO_3 addition. Linear regression analysis of $\log K_d^*$ with respect to the pH, measured in the extract, and the organic matter content of the soil yielded the following regression equation:

$$\log K_d^* = -1.43 + 0.84 \log\%OC + 0.62\ pH \qquad (R^2 = 0.90,\ n = 1095) \qquad (9.11)$$

Since most Cd was radio-labile in these soils, the isotopic distribution coefficient was comparable with the total K_d. This regression equation agrees well with the regression equation obtained for *in situ* K_d values of 57 polluted soils (eq. 3.6, for a Ca concentration of 1 mM: $\log K_d^{lab} = -1.8 + 0.79 \log\%OC + 0.66\ pH$).

Pore water concentrations of Cd were measured for soils from a nearby field with similar soil characteristics and ionic strength, but larger variation in pH (pH between 3.9 and 6.1). Predictions of the labile K_d values, i.e., the ratio of E to the pore water concentration, were made with equation 9.11 (Figure 9.4). The predictions differed maximally by a factor of 3 from the observed K_d^{lab}, except for the soil sample with the lowest Ca concentration (Ca_{pw} = 0.1 mM). The K_d^{lab} was 7 times underpredicted for this sample, which may be explained by the stronger sorption at lower ionic strength. These results indicate that the partitioning in a 0.001 M $CaCl_2$ extract, that has a ionic strength of 3 mM, may serve as a reasonable approximation for the field situation if the ionic strength in the field is of the same order.

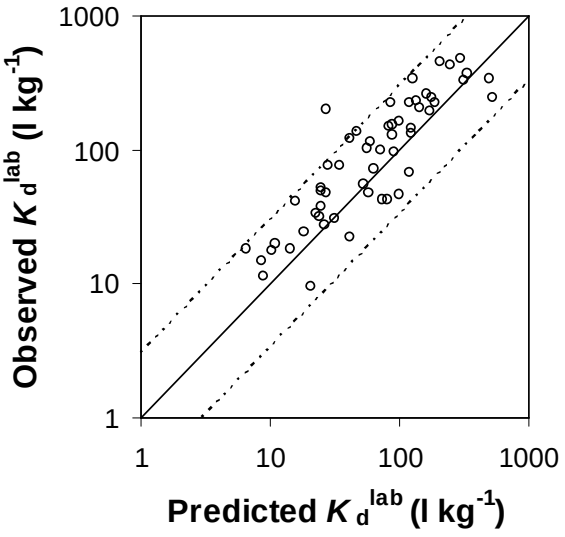

Figure 9.4 Comparison between the measured *in situ* K_d^{lab} of Cd and the values predicted with a regression equation derived from measurements in dilute salt extracts acidified with various quantities of HNO_3. The solid line is the 1:1 line and the dotted lines represent 3 times over- or underprediction.

9.3.4 Prediction of proton and Cd transport

The parameters used in the transport model are shown in Table 9.2. The sorption parameters were obtained from the batch experiments. The parameter *a* (eq. 9.1) was calculated by dividing the measured pH BC (which ranged from 0.006 to 0.069 mol H^+ kg^{-1} pH^{-1}) by a factor 2.3. The parameters *k*, *d* (eq. 9.5) and *m* (eq. 9.2) were derived from the regression equation relating the K_d of Cd to soil properties (eq. 9.11): the parameter *k* is 0.037 ($=10^{-1.43}$), *d* (describing the dependence of Cd sorption on the organic C content) is 0.84, and *m* (describing the pH dependence of Cd sorption) is -0.62.

Table 9.2 Input parameters used in the transport model

	Parameter	Symbol	Value	Unit
Hydraulical	Water flux density	q	23.4	cm y^{-1}
	Dispersion length	λ_{Cd}	5	cm
		λ_H	5 – 500	cm
Chemical	Sorption of Cd	k	0.037	
	(eq. 9.2 and 9.5)	d	0.84	
		m	-0.62	
	pH buffering (eq. 9.1)	a	0.003 – 0.03	mol kg^{-1} $ln(H^+)^{-1}$
Soil Profile	Length	L	90	cm
	Bulk density	ρ	1.35 (top) – 1.55 (bottom)	kg l^{-1}
Initial /	(Initial pH and labile Cd concentration (mg kg^{-1}) as measured)			
Boundary	Acid input (4.7 $kmol_c$ ha^{-1} y^{-1})	$c_{H,in}$	0.002	mol l^{-1}
conditions	Cd input (2.3 g $ha^{-1}y^{-1}$)	$c_{Cd,in}$	0.001	mg l^{-1}
Numerical	Spatial discretization	Δz	1	cm
	Time discretization	Δt	1	day

9.3.4.1 Proton transport

Figure 9.5 shows the calculated pH profile after 50 years (from 1997 onwards) for one profile with a pH BC of 2.8 $cmol_c$ kg^{-1} pH^{-1} in the upper 30 cm. The model predicts that the pH front will have reached a depth of 18 cm. When a dispersion length of 5 cm is used, the spreading of the pH front is within ± 10 cm, which is in contradiction with measured pH profiles (e.g., Blake *et al.*, 1999; Andersen *et al.*, 2002). These calculations were made assuming local equilibrium. However, non-equilibrium conditions are likely to prevail

during proton transport (Chapter 7). Sverdrup *et al.* (1995) modelled pH changes in an agricultural soil in Rothamsted that was converted to woodland at the end of the 18th century. They used the biogeochemical model SAFE (Simulating Acidification in Forested Ecosystems), that includes diffusion limited cation-exchange and weathering rates for mineral dissolution reactions. Measured and calculated pH profiles agreed reasonably well. We choose to describe the large spreading in the pH front by using a larger dispersion length, since it has a similar effect as the use of kinetic parameter (see chapter 7), but is mathematically easier to handle. The spreading in the calculated pH front was in good agreement with the spreading in measured pH profiles given in literature when a dispersion length of 500 cm was used.

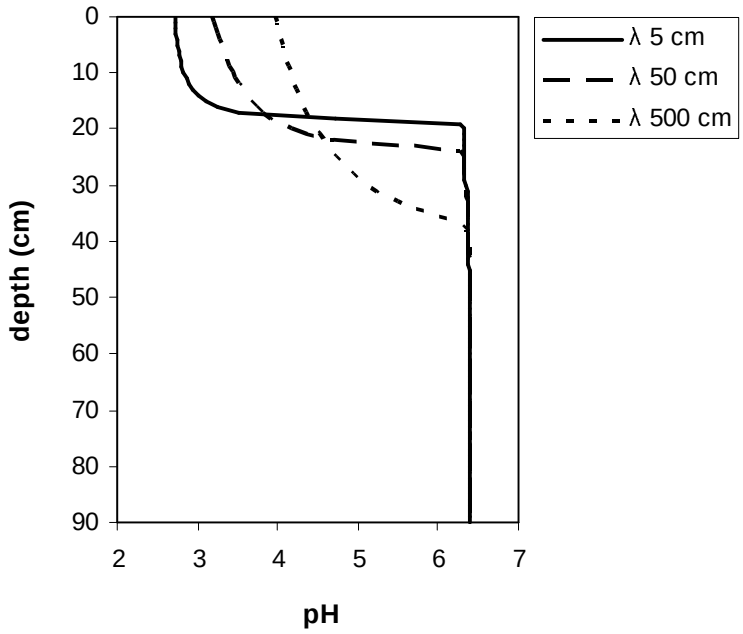

Figure 9.5 Calculated pH profile for a single profile, after 50 years (from 1997 onwards), assuming an acid input of 4.7 $kmol_c$ ha y^{-1} and no lime application. Calculations were made with a dispersion length for H^+ transport of 5, 50 or 500 cm.

All profiles were calculated with λ_H =500 cm. Figure 9.6 shows the modelled pH profiles after 50 and 100 years, averaged over all 48 profiles. The field-averaged pH profile shows larger spreading than that calculated for a single profile (cf. Figure 9.5), because of the variation in pH BC among profiles, which is related to the variation in organic C content. According to the model calculations, the pH at the bottom of the profile will already have decreased after 100 years in some of the profiles that have low organic C content (< 0.5 %) beneath 30 cm of depth.

In the field of Rothamsted, the pH of the topsoil (0-23 cm) decreased by approximately 2.5 units, and the pH of the 46–69 cm layer by 1 unit during the 110 years since the field was converted to woodland (Blake *et al.*, 1999). We predict a faster acidification, but this is not in contradiction since the sandy soil of our study has a smaller CEC, and hence a smaller buffer capacity in the subsoil than the silty clay loam soil of Rothamsted. The CEC at 50 cm of depth is about 3 $cmol_c\ kg^{-1}$ for the soil of Neerpelt, and about 20 $cmol_c\ kg^{-1}$ for the Rothamsted soil.

Afforestation may lead to a build-up of organic matter in the top layer. This increase in organic C content and the recycling of cations by vegetation may result in a slower acidification in the top layer, which was not considered in the model. However, the data of Rothamsted indicate that this effect is small and restricted to the upper centimeters of the profile (Sverdrup *et al.*, 1995), and therefore will have little effect on the Cd transport.

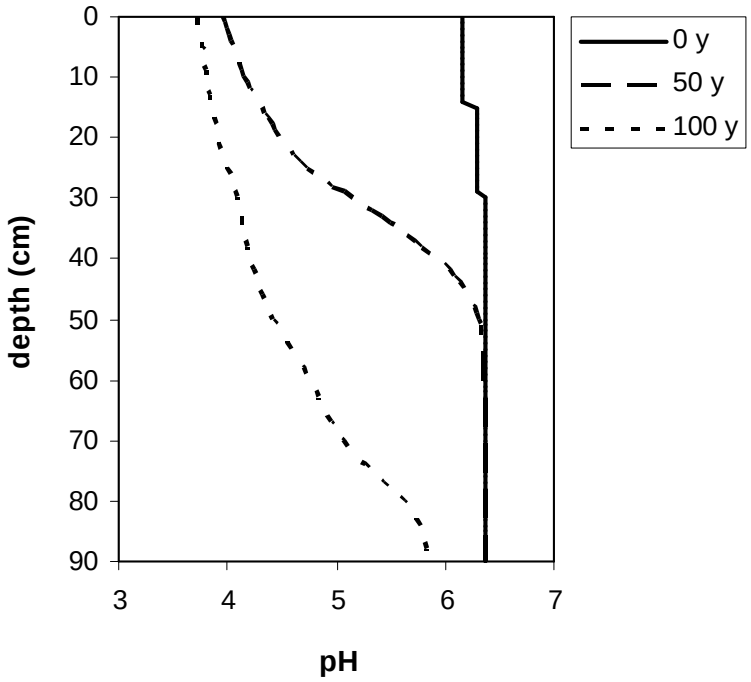

Figure 9.6 Field-averaged pH profile measured in the year 1997 (full line), and calculated pH profiles profiles after 50 and 100 years from 1997 onwards (dotted lines), assuming an acid input of 4.7 $kmol_c\ ha\ y^{-1}$ and no lime application.

9.3.4.2 Transport of Cd

Figure 9.7 shows the calculated profiles of total and solution phase Cd concentrations, averaged for all 48 profiles. When the pH is maintained, the K_d values of Cd remain in the order of 500 l kg^{-1} in the topsoil and the Cd plume travels slowly because of this relatively strong retention (Figure 9.7b). However, large increases in pore water concentrations and rapid leaching of Cd are predicted when liming is abandoned (Figure 9.7a), because of the strong decrease in pH and the resulting decrease in Cd retention.

The strong mobilization of Cd upon acidification results in very elevated concentrations in the seepage water, calculated as the average pore water concentration at the bottom of the profile (90 cm of depth). A sudden increase in the Cd concentration is predicted after about 80 years, i.e., around the year 2080 (Figure 9.8a). The concentration will reach values in the order of 0.3 mg Cd l^{-1} and will remain that high during about 30 years, according to the predictions. The maximum permissible concentration (MPC) for groundwater in Flanders is 5 µg l^{-1}. The concentration is predicted to fall below this value after 300 years, when nearly all Cd is leached to the groundwater.

These predictions indicate that the abandonment of agricultural lands that are heavily contaminated with Cd may have large environmental impacts, especially where the groundwaters are shallow. Continuation of liming practices is a possible solution to prevent breakthrough of Cd at concentrations far above the MPC of Cd in groundwater. Approximately 250 kg $CaCO_3$ ha^{-1} y^{-1} would be required to maintain soil pH, assuming that the acid deposition remains at the current level of about 5 $kmol_c$ ha^{-1} y^{-1}. It is predicted that the concentration in the seepage water will remain below 15 µg l^{-1} under that scenario (Figure 9.8b). As a result, it will take about 2000 years before all excess Cd is removed from the soil.

The Cd transport under acidifying conditions was also simulated with a model where the field was treated as one single column with average soil properties (Figure 9.8a). In this case, a later breakthrough and a larger peak concentration was predicted, i.e., the transport is predicted to be more disperse when field heterogeneity is taken into account. These results illustrate the importance of soil variability for the transport of sorbing solutes.

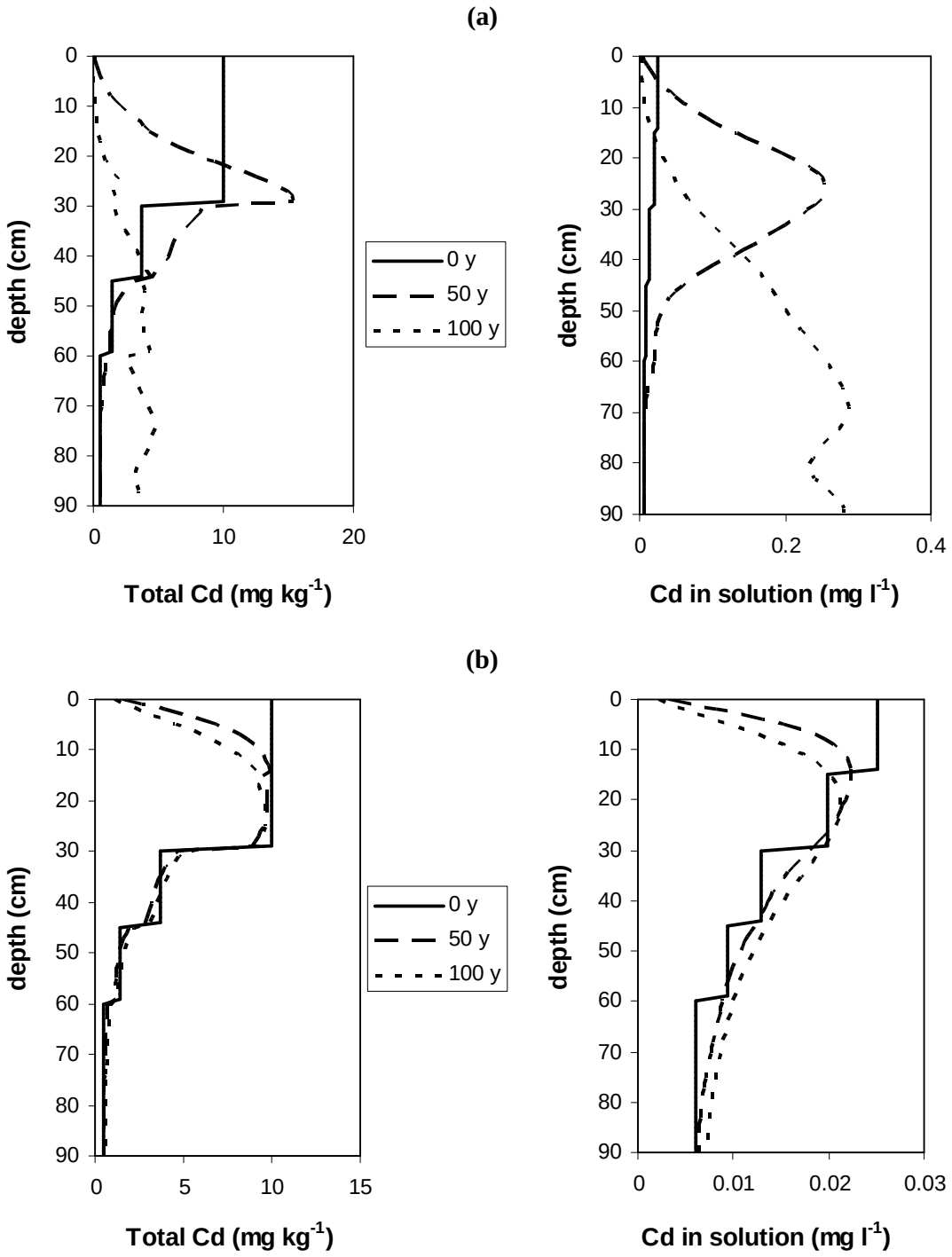

Figure 9.7 Modelled field-averaged profiles of total Cd concentrations and concentrations in solution (a) for an acid input of 4.7 $kmol_c$ ha y^{-1}, or (b) when the pH is maintained. The full line indicates the profiles measured in the year 1997, and the dotted lines represent the calculated profiles after 50 and 100 years from 1997 onwards.

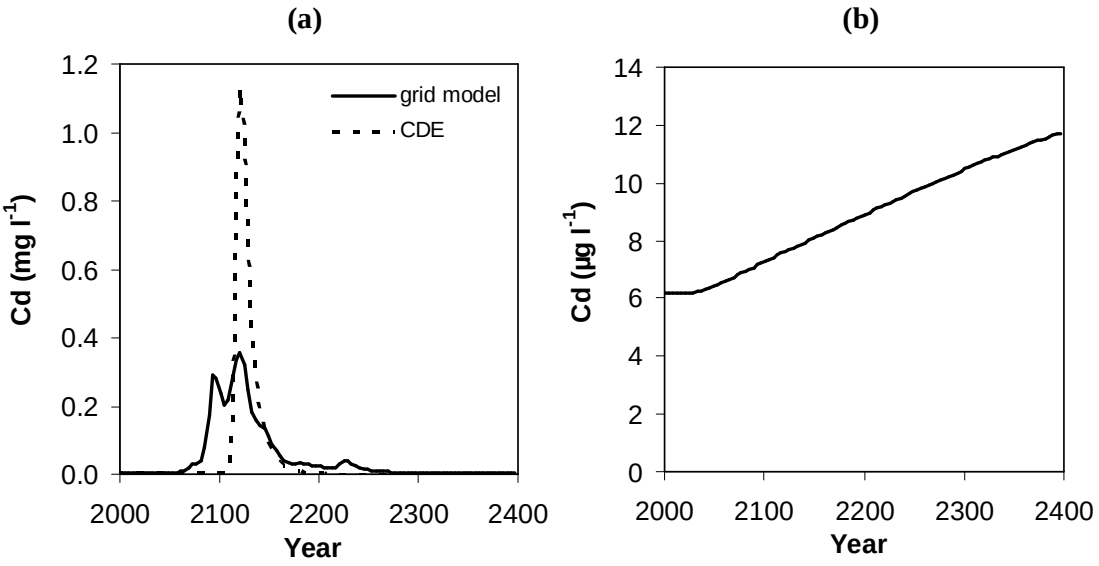

Figure 9.8 Modelled concentrations of Cd in the seepage water (a) for an acid input of 4.7 $kmol_c$ ha y^{-1}, or (b) at constant pH. (Note the difference in scale on the y-axis between panels a and b). The full line gives the simulation of the grid model, where the transport was calculated for all profiles using the measured soil properties and the convection-dispersion equation (CDE). The dotted line gives the simulation of the CDE for a single profile with field-averaged properties. The field was set-aside in 1992.

In conclusion, the set-aside of agricultural lands may result in a rapid acidification of these soils. Because a high pH (pH>6) is maintained, only a small fraction of Cd has migrated downward out of the plough layer in contaminated soils, and acidification will result in a strong mobilization of Cd accumulated in the plough layer ('chemical time bomb'). To simulate the proton transport, a very large dispersion length was used for the proton transport (λ_H = 500 cm) to predict a spreading of the soil acidification front in agreement with what is reported in the literature. It was predicted that concentrations in the seepage water will increase from 6 µg Cd l^{-1} actually to 300 µg Cd l^{-1} around the year 2100, when the pH front reaches the depth of the groundwater (90 cm of depth). Maintaining the soil pH through liming is a possible solution to prevent breakthrough of Cd at concentrations far above the maximum permissible concentration.

General conclusions

Main results and conclusions

A large area of land at the Dutch-Belgian boundary is contaminated with Cd and Zn due to atmospheric deposition of these metals from Zn smelters. Groundwater pollution caused by leaching of these metals is a growing concern. In this work, the mobility of Cd and Zn in these podzols was investigated by batch and column experiments, field observations and by model simulations at the field scale. Following conclusions were drawn:

Not all Cd and Zn in the soil is in labile form

The isotopic dilution technique was used to measure the labile metal pool (*E* value) of Cd and Zn. The %*E* values (*E* value relative to total metal concentration) of Cd were generally larger than 50%, while %*E* values of Zn were generally smaller than 50%. The %*E* values of Cd and Zn in the topsoil of a contaminated podzol were smaller than in an unpolluted podzol, indicating that the metals in the contaminated soil were added in a partly insoluble form.

Transport of labile Cd and Zn can be modelled with the local equilibrium assumption

Column experiments showed that the Cd and Zn transport in these sandy soils was well predicted with the local equilibrium assumption (LEA). Tailing of the ^{36}Cl breakthrough curves at large pore water velocities (between 12 and 30 cm d^{-1}) was indicative of physical non-equilibrium, but even in this case, breakthrough curves of Cd and Zn were reasonably described with the LEA. These model predictions assumed equilibrium between the labile pool and the solution, i.e., it is assumed that the non-labile metals cannot desorb.

Present-day vertical Cd concentration profiles in a moderately polluted field with acid sandy soils were calculated with the LEA, based on the emission history of the nearby smelter. The results of the column experiments, and the good agreement between 'resident' concentrations (measured in soil centrifugates) and 'flux' concentrations (measured in solutions sampled by wick samplers in the field) supported the use of the LEA for the transport calculations at field scale. Predicted and observed profiles agreed reasonably well, but total Cd concentrations in the topsoil were generally underestimated, probably because Cd in the deposition was partly in insoluble (non-labile) form. The predictions might improve if the speciation of Cd in the historical emission was known and if long-term weathering of the non-labile forms could be quantified.

Transport of non-labile Cd and Zn cannot be modelled with the LEA

Leaching of Cd and Zn was greatly overestimated when it was assumed that all metal (labile and non-labile) was in equilibrium with the solution phase, i.e. when the 'total' K_d was used for the transport calculations. However, a slow release of non-labile Cd and Zn was observed in columns leached with over 100 pore volumes and where the labile metal pool was nearly depleted, resulting in a longer tailing of the breakthrough curve than predicted with the equilibrium model.

The large concentrations of non-labile Zn in the upper horizons of a polluted field also indicated that the release of non-labile Zn is a very slow process, that may take decades or even centuries. The rate constant for desorption of non-labile metal derived from the column experiment could not be used to model the metal transport at field scale, which may be attributed to the large difference in water flux between the column experiment and the field situation.

Leaching of Cd and Zn depends strongly on soil chemical properties (pH, organic C)

Cadmium and zinc are (relatively) strongly sorbing solutes, and therefore, the transport of these metals is not much affected by the soil physical parameters (Černík *et al*., 1994). The sensitivity analysis of Seuntjens *et al*. (2002b) showed that the field-scale Cd flux is very sensitive to the solid–liquid distribution coefficient (K_d) and the deposition rate, while hydraulic parameters (K_s and van Genuchten parameters) have little effect.

The pH is an extremely important factor in controlling the solid–liquid distribution of Cd and Zn. Batch experiments showed that the K_d of Cd and Zn increases about five-fold per unit increase in pH. Organic matter content and ionic strength of the soil solution also affect the sorption of Cd and Zn.

As a result, land use changes that affect these soil properties (pH, OC, ionic strength) will also affect the mobility of Cd and Zn. The pH of the topsoil of sandy soils may decrease with 2 units within 20 to 30 years after conversion from agricultural land to forest (Römkens and de Vries, 1995), which will lead to an increase in solution concentrations of Cd and Zn. The effect of acidification on Cd transport was studied in a column experiment. The decrease in pH and the mobilization of Cd in these artificially acidified soil columns was reasonably predicted, but the spreading in the pH profile was more disperse than predicted, which was attributed to non-equilibrium in the proton transport.

Liming on the other hand reduces the mobility of Cd and Zn. Concentrations of Cd and Zn in the column effluent of polluted soils were strongly reduced when the topsoil was

limed. After 4 months, the amount of Cd leached from the limed columns was only half of the amount leached in control columns.

The groundwater contamination in the Kempen is likely to persist or even worsen

Large amounts of Cd and Zn are still present in the soils around the (former) Zn smelters. According to the model calculations for a polluted field with Spodosols, 1.7 kg Cd ha^{-1} was transported to the groundwater in the past 100 years and 2.8 kg Cd ha^{-1} will end up in the groundwater during the next 100 years. It was predicted that the Cd concentration in the seepage water will remain above 5 µg l^{-1} for the next 170 years. These results, and the results of Seuntjens (2002), indicate that a large part of Cd deposited on acid sandy soils around the Zn smelters in the Kempen – where the groundwater table is mostly between 0.5 and 4 m below the soil surface (Wilkens, 1999) – will reach the groundwater during the next two centuries, if no action is taken.

Abandoning agricultural land contaminated with heavy metals should be avoided, unless soil pH is controlled

Most Cd is present in the plough layer in contaminated agricultural soils, because a high pH is maintained in these soils. The set-aside of agricultural land results in a rapid acidification of sandy soils with low buffer capacity, which may lead to mobilization of Cd accumulated in the plough layer. The future Cd transport was modelled for a heavily polluted field (~ 10 mg Cd kg^{-1} in the plough layer), with sandy soils and a shallow groundwater table (~ 90 cm of depth), that was set-aside in 1992. It was predicted that most Cd will leach to the groundwater between 90 and 170 years after the field was set-aside, resulting in elevated Cd concentrations in the seepage water (~ 0.3 mg Cd l^{-1}) during this period.

Liming is recommended to avoid leaching of Cd and Zn in elevated concentrations

Liming is especially recommended in polluted arable land that is set-aside. Liming the topsoil may prevent breakthrough of Cd at concentrations far above the maximum permissible concentration.

Conventional liming was predicted to have only limited effect on the Cd and Zn transport in a field with acid sandy soils. Most Cd and Zn was already transported to depths greater than 25 cm in this field, which explains the small predicted effect of liming. Liming combined with deep ploughing will probably cause a strong decrease in the metal concentrations in the seepage water.

Outlook

During the last decades, the metal contamination in the Kempen at the Belgian-Dutch boundary has been monitored intensively, and metal transport in these soils has been studied by various researchers (e.g., Boekhold, 1992; Wilkens, 1995; Seuntjens, 2000). Since the ongoing groundwater contamination is far from over, this regional metal pollution problem deserves further attention. Current work has confirmed the validity of batch equilibrium data to predict Cd and Zn transport at the field scale, i.e. the chemical equilibrium models predicting solid-liquid partitioning can be integrated into transport models. The current work predicts that spatial variability in soil properties, affecting the solid-liquid distribution of metals, strongly affects the dispersion of the Cd and Zn breakthrough.

In this work, metal mobility was studied at laboratory scale (batch, column) and field scale. To assess the risk of metal leaching at regional scale (entire area of the Kempen), data gaps and gaps in scientific knowledge are to be filled. Integration of the available data is a first priority to assess the risk in the entire contaminated region that is >100 km^2 large. The available data of soil properties, metal concentrations and land use should be collected in a database. This would allow to determine if and where further analyses are needed, and to delineate areas where future leaching to the groundwater will be considerable. The set-aside policy for contaminated agricultural lands has to be evaluated taking into account the risk of groundwater contamination. It is predicted that large Cd concentrations in the seepage water will be reached about 100 years after the soils are set-aside, if no remedial actions are taken (Figure 9.8).

Predicting metal transport in the saturated zone (not covered in this work) may require additional knowledge. The results of unsaturated zone models need to be integrated in groundwater models to assess the implications of Cd leaching for groundwater and surface water quality. The fate of metals in wet Spodosols with alternating aerobic and reduced soil horizons is unknown, but may be a major route of metal release to surface water in large areas.

Further research efforts are also needed to account for solid phase speciation when predicting metal transport in soils. Column experiments reported here showed that leaching of Cd and Zn is largely overestimated in soils where large metal fractions are in non-labile form if it is assumed that all metal is in equilibrium in solution. The presence of small labile metal fractions in the upper horizons of contaminated soils also indicated that

the release of non-labile Cd and Zn is a very slow process. However, a column experiment of this thesis showed mobilisation of non-labile Cd and Zn when the labile metal pool was nearly depleted. The rate constant for desorption of non-labile metal derived from this column experiment could not be used to model the metal transport at field scale, which may be attributed to differences in scale and in the water flux. The release of non-labile metal is a process that should not be ignored, especially for Zn that is mainly present in non-labile forms. Additional research is needed to elucidate the mechanisms responsible for the mobilization of non-labile metals (e.g., dissolution of minerals, solid state diffusion) and to determine the rate of this process at the field scale.

References

Aitken R.L., Moody P.W., and McKinley P.G. (1990) Lime requirement of acidic Queensland soils. 1. Relationships between soil properties and pH buffer capacity. *Australian Journal of Soil Research* **28**, 695-701.

Andersen M.K., Raulund-Rasmussen K., Hansen H.C.B., and Strobel B.W. (2002) Distribution and fractionation of heavy metals in pairs of arable and afforested soils in Denmark. *European Journal of Soil Science* **53**, 491-502.

Anderson P.R. and Christensen T. H. (1988) Distribution coefficients of Cd, Co, Ni, and Zn in soils. *Journal of Soil Science* **39**, 15-22.

Bahr J.M. and Rubin J. (1987) Direct comparison of kinetic and local equilibrium formulations for solute transport affected by surface reactions. *Water Resources Research* **23**, 438-352.

Barrow N.J. (1986) Testing a mechanistic model. 2. The effects of time and temperature on the reaction of zinc with a soil. *Journal of Soil Science* **37**, 277-286.

Berthelsen B.O., Ardal L., Steinnes E., Abrahamsen G., and Stuanes A.O. (1994) Mobility of heavy metals in pine forest soils as influenced by experimental acidification. *Water Air and Soil Pollution* **73**, 29-48.

Blake L., Goulding K.W.T., Mott C.J.B., and Johnston A.E. (1999) Changes in soil chemistry accompanying acidification over more than 100 years under woodland and grass at Rothamsted experimental station, UK. *European Journal of Soil Science* **50**, 401-412.

Boekhold A.E. (1992) *Field scale behaviour of cadmium in soil.* PhD Thesis. Wageningen Agricultural University. The Netherlands.

Boekhold A.E. and van der Zee S.E.A.T.M. (1992) A scaled sorption model validated at the column scale to predict cadmium contents in a spatially-variable field soil. *Soil Science* **154**, 105-112.

Boll J., Steenhuis T.S., and Selker J.S. (1992) Fiberglass wicks for sampling of water and solutes in the vadose zone. *Soil Science Society of America Journal* **56**, 701-707.

Brahy V. and Delvaux B. (2001) Comments on "Artifacts caused by collection of soil solution with Passive Capillary Samplers". *Soil Science Society of America Journal* **65**, 1751-1752.

Bruemmer G.W., Gerth J., and Tiller K.G. (1988) Reaction-kinetics of the adsorption and desorption of nickel, zinc and cadmium by goethite. 1. Adsorption and diffusion of metals. *Journal of Soil Science* **39**, 37-52.

Černík M., Federer P., Borkovec M., and Sticher H. (1994) Modeling of heavy metal transport in a contaminated soil. *Journal of Environmental Quality* **23**, 1239-1248.

Chhabra R., Pleysier J., and Cremers A. (1975) The measurement of the cation exchange capacity

and exchangeable cations in soils: a new method. In: *Proceedings of the International Clay Conference* (ed S.W. Bailey), pp. 439-449. Applied Publishing Ltd., Wilmette, Illinois, USA.

Christensen T.H. (1984) Cadmium soil sorption at low concentrations. I. Effect of time, cadmium load, pH, and calcium. *Water Air and Soil Pollution* **21**, 105-114.

Christensen T.H. (1985) Cadmium soil sorption at low concentrations. III. Prediction and observation of mobility. *Water, Air, and Soil Pollution* **26**, 255-264.

Christensen T.H. (1987) Cadmium soil sorption at low concentrations. VI. A model for zinc competition. *Water Air and Soil Pollution* **34**, 305-314.

Christensen T.H. (1989) Cadmium soil sorption at low concentrations. VIII. Correlation with soil parameters. *Water Air and Soil Pollution* **44**, 71-82.

Curtin D., Campbell C.A., and Jalil A. (1998) Effects of acidity on mineralization: pH dependence of organic matter mineralization in weakly acidic soils. *Soil Biology and Biochemistry* **30**, 57-64.

Curtin D. and Smillie G.W. (1983) Soil solution composition as affected by liming and incubation. *Soil Science Society of America Journal* **47**, 701-707.

Curtin D. and Smillie G.W. (1995) Effects of incubation and pH on soil solution and exchangeable cation ratios. *Soil Science Society of America Journal* **59**, 1006-1011.

Dancer W.S., Peterson L.A., and Chesters G. (1973) Ammonification and nitrification of N as influenced by soil pH and previous N treatments. *Soil Science Society of America Journal* **37**, 67-69.

Dawson B.S.W., Fergusson J.E., Campbell A.S., and Cutler E.J.B. (1991) Depletion of 1st-row transition-metals in a chronosequence of soils in the reefton area of New-Zealand. *Geoderma* **48**, 271-296.

de Groot, A. C., Peijnenburg, W. J. G. M., van den Hoop, M. A. G. T., Ritsema, R., and van Veen, R. P. M. (1998) *Heavy metals in Dutch field soils: an experimental and theoretical study on equilibrium partitioning.* Report No 607220-001. National Institute of Public Health and the Environment (RIVM), Bilthoven, The Netherlands.

Degryse F., Broos K., Smolders E., and Merckx R. (2003a) Soil solution concentration of Cd and Zn can be predicted with a $CaCl_2$ soil extract. *European Journal of Soil Science* **54**, 149-157.

Degryse F., Buekers J., and Smolders E. (2003b) Radio-labile cadmium and zinc in soils as affected by pH and source of contamination. *European Journal of Soil Science.* Accepted.

Ernstberger H., Davison W., Zhang H., Tye A., and Young S. (2002) Measurement and dynamic modeling of trace metal mobilization in soils using DGT and DIFS. *Environmental Science & Technology* **36**, 349-354.

Filius A., Streck T., and Richter J. (1998) Cadmium sorption and desorption in limed topsoils as influenced by pH: Isotherms and simulated leaching. *Journal of Environmental Quality* **27**, 12-18.

Gaber H.M., Inskeep W.P., Comfort S.D., and Wraith J.M. (1995) Nonequilibrium transport of atrazine through large intact soil cores. *Soil Science Society of America Journal* **59**, 60-67.

Gerritse R.G. and Van Driel W. (1984) The relationship between adsorption of trace metals, organic matter and pH in temperate soils. *Journal of Environmental Quality* **13**, 197-204.

Goyne K.W., Day R.L., and Chorover J. (2000) Artifacts caused by collection of soil solution with passive capillary samplers. *Soil Science Society of America Journal* **64**, 1330-1336.

Hamon R.E., McLaughlin M.J., and Cozens G. (2002) Mechanisms of attenuation of metal availability in *in situ* remediation treatments. *Environmental Science & Technology* **36**, 3991-3996.

Helling, C.S., Chesters, G., and Corey, R.B. (1964) Contribution of organic matter and clay to soil cation-exchange capacity as affected by the pH of the saturating solution. *Soil Science Society of America Proceedings* **28**, 517-520.

Holder M., Brown K.W., Thomas J.C., Zabcik D., and Murray H.E. (1991) Capillary-wick unsaturated zone soil pore water sampler. *Soil Science Society of America Journal* **55**, 1195-1202.

Honeyman, B.D. and Santschi, P.H. (1988) Metals in aquatic systems. *Environmental Science & Technology* **22**, 862-871.

Houba V.J.G., Van der Lee J.J., Novozamsky I., Walinga I. (1989) *Soil and Plant Analysis, a series of syllabi, Part 5: Soil Analysis Procedures.* Department of Soil Science and Plant Nutrition, Wageningen Agricultural University, The Netherlands.

Ide G. (1992) Cadmium in de Belgische Kempen: een situatieschets. *Bodem* **3**, 119-121.

Ingwersen, J. (2001) *The environmental fate of cadmium in the soils of the waste water irrigation area of Braunschweig: Measurements, modelling and assessment*. PhD thesis. Technischen Universität Carolo-Wilhelmina. Germany.

Jersak J., Amundson R., and Brimhall G. (1997) Trace metal geochemistry in spodosols of the Northeastern United States. *Journal of Environmental Quality* **26**, 511-521.

Johnson C.E. and Petras R.J. (1998) Distribution of zinc and lead fractions within a forest spodosol. *Soil Science Society of America Journal* **62**, 782-789.

Johnston A.E., Goulding K.W.T., and Poulton P.R. (1986) Soil acidification during more than 100 years under permanent grassland and woodland at Rothamsted. *Soil Use and Management* **2**, 3-10.

Jury, W.A., Gardner, W.R., and Gardner, W.H. (1991) *Soil Physics*. Wiley New York, New York.

Kalisz P.J. and Stone E.L. (1980) Cation exchange capacity of acid forest humus layers. *Soil Science Society of America Journal* **44**, 407-413.

Kinniburgh D.G., Milne C.J., Benedetti M.F., Pinheiro J.P., Filius J., Koopal L.K., and van Riemsdijk W.H. (1996) Metal ion binding by humic acid: application of the NICA-Donnan Model. *Environmental Science & Technology* **30**, 1687-1698.

Knight B.P., Chaudri A.M., McGrath S.P., and Giller K.E. (1998) Determination of chemical availability of cadmium and zinc in soils using inert soil moisture samplers. *Environmental Pollution* **99**, 293-298.

Knutson J.H., Lee S.B., Zhang W.Q., and Selker J.S. (1993) Fiberglass wick preparation for use in passive capillary wick soil pore-water samplers. *Soil Science Society of America Journal* **57**, 1474-1476.

Knutson J.H. and Selker J.S. (1994) Unsaturated hydraulic conductivities of fiberglass wicks and designing capillary wick pore-water samplers. *Soil Science Society of America Journal* **58**, 721-729.

Kookana R.S., Naidu R., and Tiller K.G. (1994) Sorption non-equilibrium during cadmium transport through soils. *Australian Journal of Soil Research* **32**, 635-651.

Lauwerys R., Amery A., Bernard A., Bruaux P., Buchet J., Claeys F., De Plaen P., Ducoffre G., Fagard R., Lijnen P., Nick L., Roels H., Rondia D., Saint-Remy A., Sartor F., and Staessen J. (1990) Health effects of environmental exposure to cadmium: Objectives, design and organization of the Cadmibel study: A cross-sectional morbidity study carried out in Belgium from 1985 to 1989. *Environmental Health Perspectives* **87**, 283-289.

Lofts S. and Tipping E. (2000) Solid-solution metal partitioning in the Humber rivers: application of WHAM and SCAMP. *Science of the Total Environment* **251**, 381-399.

Lombi E., Zhao F.-J., Zhang G., Sun B., Fitz W., Zhang H., and McGrath S.P. (2002) In situ fixation of metals in soils using bauxite residue: chemical assessment. *Environmental Pollution* **118**, 435-443.

Magdoff F.R., Bartlett R.J., and Ross D.S. (1987) Acidification and pH buffering of forest soils. *Soil Science Society of America Journal* **51**, 1384-1386.

Matzner E. (1989) Acidic precipitation: Case study Solling. In: *Acidic precipitation. Volume I: Case studies* (eds D.C. Adriano & M. Havas), pp. 39-83. Springer-Verlag, New York.

Merckx R., Brans K., and Smolders E. (2001) Decomposition of dissolved organic carbon after soil drying and rewetting as an indicator of metal toxicity in soils. *Soil Biology & Biochemistry* **33**, 235-240.

Millington R.J. and Quirk J.M. (1961) Permeability of porous solids. *Transactions of the Faraday Society* **57**, 1200-1207.

Nakhone L.N. and Young S.D. (1993) The significance of (radio-) labile cadmium pools in soil. *Environmental Pollution* **82**, 73-77.

Nkedi-Kizza P., Biggar J.W., Selim H.M., van Genuchten M.T., Wierenga P.J., Davidson J.M., and Nielsen D.R. (1984) On the equivalence of 2 conceptual models for describing ion-exchange during transport through an aggregated oxisol. *Water Resources Research* **20**, 1123-1130.

Nowack B., Obrecht J.M., Schluep M., Schulin R., Hansmann W., and Koppel V. (2001) Elevated lead and zinc contents in remote Alpine soils of the Swiss national park. *Journal of Environmental Quality* **30**, 919-926.

Oorts, K. (2002) *Charge characteristics and organic matter dynamics in weathered soils of the tropics*. PhD Thesis. Katholieke Universiteit Leuven. Belgium.

Oste L.A., Temminghoff E.J.M., and Van Riemsdijk W.H. (2002) Solid-solution partitioning of organic matter in soils as influenced by an increase in pH or Ca concentration . *Environmental Science & Technology* **36**, 208-214.

Patyn, J. (1997) *Hydrodynamisch model SCR Sibelco*.

Reedy O.C., Jardine P.M., Wilson G.V., and Selim H.M. (1996) Quantifying the diffusive mass transfer of nonreactive solutes in columns of fractured saprolite using flow interruption. *Soil Science Society of America Journal* **60**, 1376-1384.

Reuss J. and Walthall P. (1990) Soil Reaction and Acidic Deposition. In: *Acidic Precipitation: Soils, Aquatic Processes, and Lake Acidification* (eds D. Adriano & A. Johnson), pp. 1-33. Springer-Verlag, New York.

Rimmer A., Steenhuis T.S., and Selker J.S. (1995) One-dimensional model to evaluate the performance of wick samplers in soils. *Soil Science Society of America Journal* **59**, 88-92.

RIVM (1999) *Landelijk Meetnet Regenwatersamenstelling. Meetresultaten 1998.* Report No 723101-054. National Institute of Public Health and the Environment (RIVM), Bilthoven, The Netherlands.

RIVM (2001a) *Landelijk Meetnet Regenwatersamenstelling. Meetresultaten 1999.* Report No 723101-056. RIVM, Bilthoven, The Netherlands.

RIVM (2001b) *Landelijk Meetnet Regenwatersamenstelling. Meetresultaten 2000*. Report No 723101-057. RIVM, Bilthoven, The Netherlands.

Roberts D.R., Scheinost A.C., and Sparks D.L. (2002) Zinc speciation in a smelter-contaminated soil profile using bulk and microspectroscopic techniques. *Environmental Science & Technology* **36**, 1742-1750.

Römkens P.F. and de Vries W. (1995) Acidification and metal mobilization: effects of land use changes on Cd mobility. In: Acid rain research: do we have enough answers? (eds G.J. Hey & J.W. Erisman), pp. 327-380. Elsevier Science, Amsterdam.

Römkens P.F. and Salomons W. (1998) Cd, Cu and Zn solubility in arable and forest soils: consequences of land use changes for metal mobility and risk assessment. *Soil Science* **163**, 859-871.

Ronse A., de Temmerman L., Guns M., and de Borger R. (1988) Evolution of acidity, organic matter content, and CEC in uncultivated soils of north Belgium during the past 25 years. *Soil Science* **146**, 453-460.

Sauvé S., Hendershot W., and Allen H.E. (2000) Solid-solution partitioning of metals in contaminated soils: dependence on pH, total metal burden, and organic matter. *Environmental Science & Technology* **34**, 1125-1131.

Schwertmann U. (1964) Differenzierung der eisen-oxide des bodens durch photochemische extraktion met saurer ammonium oxalat-lösung. *Zeitschrift Fur Pflanzenernahrung Und Bodenkunde* **105**, 194-202.

Seuntjens P. (2000) *Reactive solute transport in heterogeneous porous media. Cadmium leaching in acid sandy soils.* PhD Thesis. Universiteit Antwerpen. Belgium.

Seuntjens P. (2002) Field-scale cadmium transport in a heterogeneous layered soil. *Water Air and Soil Pollution* **140**, 401-423.

Seuntjens P., Cornelis C., De Brucker N., and Geuzens P. (1999) Derivation of functional layers in a podzol toposequence for simulating cadmium transport. *Physics and Chemistry of the Earth Part B-Hydrology Oceans and Atmosphere* **24**, 869-873.

Seuntjens P., Mallants D., Simunek J., Patyn J., and Jacques D. (2002) Sensitivity analysis of physical and chemical properties affecting field-scale cadmium transport in a heterogeneous soil profile. *Journal of Hydrology* **264**, 185-200.

Seuntjens P., Mallants D., Toride N., Cornelis C., and Geuzens P. (2001a) Grid lysimeter study of steady state chloride transport in two Spodosol types using TDR and wick samplers. *Journal of Contaminant Hydrology* **51**, 13-39.

Seuntjens P., Tirez K., Simunek J., Van Genuchten M.T., Cornelis C., and Geuzens P. (2001b) Aging effects on cadmium transport in undisturbed contaminated sandy soil columns. *Journal of Environmental Quality* **30**, 1040-1050.

Šimůnek, J., Huang, K., & van Genuchten, M.T. (1998) *The HYDRUS code for simulating the one-dimensional movement of water, heat and multiple solutes in variably saturated media.* Research Report No. 144. U.S. Salinity Laboratory, USDA, Riverside, California.

Sinaj S., Machler F., and Frossard E. (1999) Assessment of isotopically exchangeable zinc in polluted and non-polluted soils. *Soil Science Society of America Journal* **63**, 1618-1625.

Smolders E., Brans K., Foldi A., and Merckx R. (1999) Cadmium fixation in soils measured by isotopic dilution. *Soil Science Society of America Journal* **63**, 78-85.

Stigliani W.M., Jaffé P.R., and Anderberg S. (1993) Heavy metal pollution in the Rhine basin. *Environmental Science & Technology* **27**, 786-793.

Streck T. and Richter J. (1997a) Heavy metal displacement in a sandy soil at the field scale. 1.Measurements and parameterization of sorption. *Journal of Environmental Quality* **26**, 49-56.

Streck T. and Richter J. (1997b) Heavy metal displacement in a sandy soil at the field scale. 2.Modeling. *Journal of Environmental Quality* **26**, 56-62.

Sverdrup H., Warfvinge P., Blake L., and Goulding K. (1995) Modeling recent and historic soil data from the Rothamsted- Experimental-station, UK using SAFE. *Agriculture Ecosystems & Environment* **53**, 161-177.

Tack F.M.G., Verloo M.G., Vanmechelen L., and Van Ranst E. (1997) Baseline concentration levels of trace elements as a function of clay and organic carbon contents in soils in Flanders (Belgium). *The Science of the Total Environment* **201**, 113-123.

Temminghoff E.J.M., van der Zee S.E.A.T.M., and de Haan F.A.M. (1995) Speciation and calcium competition effects on cadmium sorption by sandy soil at various pHs. *European Journal of Soil Science* **46**, 649-655.

Tiller K.G. (1989) Heavy metals in soils and their environmental significance. *Advances in Soil Science,* **9**, 113-141.

Tiller K.G., Honeysett J.L., and De Vries M.P.C. (1972) Soil zinc and its uptake by plants. I. Isotopic exchange equilibria and the application of tracer techniques. *Australian Journal of Soil Research* **10**, 151-164.

Tipping E. (1998) Humic ion-binding model VI: an improved description of the interactions of protons and metal ions with humic substances. *Aquatic geochemistry* **4**.

Tjell, J. C. and Christensen, T. H. (1985) Evidence of increasing cadmium contents of agricultural soils. In: *Heavy Metals in the Environment*. (Ed. Lekkas, T.D.), pp. 391-393. CEP consultants, Albany, UK.

Toride, N., Leij, F.J., and van Genuchten, M.Th. (1995) *The CXTFIT code for estimating transport parameters from laboratory or field tracer experiments. Version 2.0.* Research Report No. 137. U.S. Salinity Laboratory, USDA, Riverside, California.

Trivedi P. and Axe L. (2000) Modeling Cd and Zn sorption to hydrous metal oxides. *Environmental Science & Technology* **34**, 2215-2223.

Tye A.M., Young S.D., Crout N.M.J., Zhang H., Preston S., Barbosa-Jefferson V.L., Davison W., McGrath S.P., Paton G.I., Kilham K. and Resende L. (2003) Predicting the activity of Cd^{2+} and Zn^{2+} in soil pore water from the radio-labile metal fraction. *Geochimica et Cosmochimica Acta* **67**, 375-385.

Tyler G. (1978) Leaching rates of heavy metal ions in forest soil. *Water Air and Soil Pollution* **9**, 137-148.

Ulrich B. (1991) An ecosystem approach to soil acidification. In: *Soil acidity* (eds Ulrich B. & M.E. Sumner), pp. 28-79. Springer-Verlag, Berlin Heidelberg.

Valocchi A.J. (1985) Validity of the local equilibrium assumption for modeling sorbing solute transport through homogeneous soils. *Water Resources Research* **21**, 808-820.

van Breemen N., Driscoll C.T., and Mulder J. (1984) Acidic deposition and internal proton sources in acidification of soils and waters. *Nature* **307**, 599-604.

van der Zee S.E.A.T.M. and van Riemsdijk W.H. (1987) Transport of reactive solute in spatially variable soil systems. *Water Resources Research* **23**, 2059-2069.

van Genuchten M.T. and Wierenga P.J. (1976) Mass transfer studies in sorbing porous media. I. Analytical solutions. *Soil Science Society of America Journal* **40**, 473-481.

van Genuchten M.T. and Wagenet R.J. (1989) Two-site/two-region models for pesticide transport and degredation: theoretical development and analytical solutions. *Soil Science Society of America Journal* **53**, 1303-1310.

van Genuchten M.T. and Wierenga P.J. (1977) Mass transfer studies in sorbing porous media: II. Experimental evaluation with Tritium (^3H_2O). *Soil Science Society of America Journal* **41**, 272-278.

VMM (2002) *Milieu- en Natuurrapport Vlaanderen. MIRA-T 2002. Achtergronddocument 2.13 Verzuring.* Vlaamse Milieu Maatschappij.

Weng L., Temminghoff E.J.M., and Van Riemsdijk W.H. (2001) Contribution of individual sorbents to the control of heavy metal activity in sandy soil. *Environmental Science & Technology* **35**, 4436-4443.

Wilkens B.J. (1995) *Evidence for groundwater contamination by heavy metals through soil passage under acidifying conditions*. Universiteit Utrecht. The Netherlands.

Young S.D., Tye A., Carstensen A., Resende L., and Crout N. (2000) Methods for determining labile cadmium and zinc in soil. *European Journal of Soil Science* **51**, 129-136.

Young S. D., Tye A., and Crout N. (2001) Rates of metal ion fixation in soils determined by isotopic dilution. In: *Proceedings of the Sixth International Conference on the Biogeochemistry of Trace Elements* (Eds L. Evans *et al.*,), p. 105. Guelph, Canada.

Appendix

Notations used in Appendix

pH	pH measured in 0.01 M $CaCl_2$ (Houthalen and Balen) or 0.001 M $CaCl_2$ (Neerpelt)
OC	organic C
Fe_{ox}	ammonium oxalate extractable Fe
Al_{ox}	ammonium oxalate extractable Al
Cd_{tot}	total Cd concentration
E_{Cd}	labile Cd concentration
Zn_{tot}	total Zn concentration
E_{Zn}	labile Zn concentration
Cd_{pw}	pore water concentration of Cd
Zn_{pw}	pore water concentration of Zn
Ca_{pw}	pore water concentration of Ca
DOC	pore water concentration of dissolved organic carbon

Table A.I Soil characteristics, metal concentrations, and pore water composition for the unpolluted field in Houthalen (6 profiles)

sample	depth [a]	pH	OC	Fe_{ox}	Al_{ox}	Cd_{tot}	E_{Cd}	Zn_{tot}	E_{Zn}	Cd_{pw}	Zn_{pw}	Ca_{pw}
	(cm)		(%)	(mmol kg^{-1})		(mg kg^{-1})				($\mu g\ l^{-1}$)	(mg l^{-1})	(mM)
1A	15	3.3	2.68	18	22	0.14	0.09	8.1	2.4	2.6	0.26	0.04
1B	30	3.3	2.44	19	22	0.19	0.13	6.4	1.7	4.2	0.25	0.02
1C	50	3.8	0.69	21	41	0.06	0.05	7.6	1.3	3.6	0.44	0.03
1D	90	4.0	0.29	9	33	0.02	0.02	13.7	1.0	2.3	0.23	0.02
2A	12	3.4	3.14	28	28	0.18	0.12	8.0	3.3	1.7	0.27	0.04
2B	30	3.4	2.33	20	23	0.17	0.15	3.1	1.7	2.7	0.16	0.02
2C	45	3.9	0.88	22	37	0.10	0.11	7.0	1.3	4.2	0.27	0.02
2D	90	4.1	0.21	7	29	0.02	0.02	9.2	1.0	3.8	0.53	0.04
2E	200	4.0	0.10	6	17	0.01	0.01	11.2	1.6	2.2	0.60	0.03
2F	320	4.1	0.06	5	14	0.01	0.01	10.0	2.0	3.6	nd	nd
3A	10	3.2	2.58	13	11	0.12	0.07	7.2	3.0	2.0	0.24	0.04
3B	25	3.3	1.44	10	12	0.08	0.06	2.3	1.1	2.0	0.24	0.04
3C	40	3.4	1.77	23	30	0.19	0.17	4.0	1.7	2.1	0.42	0.02
3D	65	3.9	0.49	13	27	0.02	0.03	7.4	0.7	1.5	0.36	0.04
3E	120	4.0	0.12	4	14	0.01	0.01	9.8	0.6	0.9	nd	nd
3F	280	3.9	0.09	6	12	0.02	0.01	11.2	2.1	2.5	0.67	0.04
4A	10	3.3	4.14	22	19	0.24	0.13	11.1	4.6	2.4	0.27	0.09
4B	25	3.3	1.97	15	20	0.20	0.13	4.0	2.7	2.6	0.27	0.05
4C	35	3.6	2.71	47	47	0.26	0.23	11.1	3.8	2.8	0.26	0.09
4D	55	4.0	0.69	21	34	0.09	0.05	6.7	1.2	5.3	nd	nd
4E	100	4.0	0.24	9	23	0.03	0.03	5.4	0.7	3.2	0.26	0.06
4F	200	3.9	0.14	7	23	0.02	0.02	18.7	1.4	2.2	nd	nd
5A	8	3.1	1.96	6	7	0.11	0.05	4.3	2.7	1.8	0.25	0.04
5B	20	3.2	1.79	9	10	0.10	0.06	3.6	1.7	1.6	0.18	0.03
5C	35	3.7	0.66	33	31	0.10	0.06	3.6	0.9	3.6	0.44	0.04
5D	120	4.1	0.16	8	44	0.01	0.01	9.7	0.7	1.6	nd	nd
5E	200	4.0	0.14	18	32	0.02	0.02	16.1	1.9	2.8	nd	

(**Table A.I** *continued*)

sample	depth [a]	pH	OC	Fe_{ox}	Al_{ox}	Cd_{tot}	E_{Cd}	Zn_{tot}	E_{Zn}	Cd_{pw}	Zn_{pw}	Ca_{pw}
	(cm)		(%)	(mmol kg^{-1})		(mg kg^{-1})				(µg l^{-1})	(mg l^{-1})	(mM)
6A	10	3.3	5.58	22	26	0.27	0.21	17.9	10.7	2.6	0.23	0.12
6B	25	3.4	3.46	22	25	0.26	0.21	7.6	3.9	3.4	0.25	0.06
6C	45	3.8	1.54	38	69	0.19	0.17	4.4	2.4	2.9	0.16	0.04
6D	90	3.9	0.45	11	40	0.02	0.03	10.1	1.9	2.6	nd	nd

[a] lower boundary

Table A.II Soil characteristics, metal concentrations, and pore water composition for the field in Balen (10 profiles)

sample	depth [a]	pH	OC	Fe_{ox}	Al_{ox}	Cd_{tot}	E_{Cd}	Zn_{tot}	E_{Zn}	Cd_{pw}	Zn_{pw}	Ca_{pw}	DOC
	(cm)		(%)	(mmol kg^{-1})		(mg kg^{-1})				(µg l^{-1})	(mg l^{-1})	(mM)	(mg l^{-1})
1A	5	3.8	2.16	10	17	0.52	0.26	45.0	4.1	3.8	0.30	0.08	nd
1B	15	3.8	0.97	4	9	0.25	0.26	7.1	2.0	15	0.65	0.07	9
1C	25	3.8	2.84	53	60	1.35	1.27	9.0	5.5	21	0.48	0.03	8
1D	45	4.2	0.32	10	23	0.18	0.14	4.5	0.8	13	0.29	0.03	6
1E	75	4.4	0.15	2	19	0.05	0.03	5.0	0.5	11	0.27	0.04	12
1F	325	4.5	0.05	2	9	0.02	0.02	6.5	0.6	13	0.43	0.02	38
2A	12	3.9	2.19	36	56	0.45	0.28	27.4	6.7	1.0	0.35	0.08	17
2B	24	4.2	0.65	35	64	0.07	0.05	10.1	1.5	3.9	0.35	0.03	6
2C	36	4.4	0.22	13	43	0.01	0.01	9.8	0.6	2.7	0.23	0.04	7
2D	50	4.4	0.13	9	32	0.01	0.01	9.3	0.5	3.4	0.24	0.03	6
2E	100	4.4	0.07	2	19	0.01	0.01	8.9	0.7	5.9	0.41	0.03	11
2F	150	4.4	0.08	1	13	0.01	0.01	8.1	0.8	4.7	0.30	0.04	11

(**Table A.II** *continued*)

sample	depth [a] (cm)	pH	OC (%)	Fe_{ox} (mmol kg^{-1})	Al_{ox} (mmol kg^{-1})	Cd_{tot} (mg kg^{-1})	E_{Cd} (mg kg^{-1})	Zn_{tot} (mg kg^{-1})	E_{Zn} (mg kg^{-1})	Cd_{pw} (µg l^{-1})	Zn_{pw} (mg l^{-1})	Ca_{pw} (mM)	DOC (mg l^{-1})
3A	12	3.6	3.62	44	44	0.74	0.40	51.9	11.5	4.5	0.37	0.07	45
3B	17	3.7	2.73	30	33	0.65	0.27	50.7	4.0	7.2	0.37	0.36	38
3C	25	3.8	1.69	48	62	0.75	0.47	31.1	5.1	16	0.54	0.04	20
3D	35	4.1	1.83	21	61	0.29	0.25	10.5	2.2	11	0.39	0.03	13
3E	130	4.3	0.24	9	35	0.05	0.04	9.6	0.9	17	0.75	0.06	17
3F	280	4.5	0.09	4	7	0.03	0.02	5.1	1.8	12	0.98	0.13	25
4A	6	3.6	3.23	17	18	0.83	0.18	88.5	8.3	5.0	0.39	0.13	nd
4B	12	3.7	2.51	76	63	0.84	0.80	16.0	7.6	7.3	0.41	0.03	18
4C	27	4.3	0.56	8	65	0.15	0.18	11.4	3.3	6.9	0.34	0.03	16
4D	75	4.4	0.34	2	47	0.16	0.15	15.2	3.9	9.1	0.36	0.04	7
4E	270	4.4	0.23	2	25	0.12	0.14	12.8	2.6	13	0.53	0.04	20
4F	300	4.4	0.27	3	21	0.09	0.09	16.4	3.2	14	0.69	0.05	21
5A	7	3.5	3.23	49	36	0.60	0.38	48.2	14.2	5.0	0.32	0.02	nd
5B	16	3.8	1.44	34	45	0.50	0.43	11.3	4.6	9.1	0.42	0.03	10
5C	60	4.0	0.82	17	39	0.42	0.33	8.5	2.7	10	0.49	0.04	10
5D	75	4.2	0.35	13	28	0.13	0.14	17.7	2.1	5.8	0.57	0.05	9
5E	120	4.2	0.09	3	15	0.03	0.03	13.3	1.5	6.1	0.59	0.05	18
5F	300	4.3	0.15	5	11	0.06	0.05	13.7	3.5	25	2.17	0.05	32
6A	6	3.7	2.50	25	17	0.91	0.16	113.2	6.3	2.5	0.47	0.06	nd
6B	30	4.3	0.37	12	35	0.02	0.03	21.1	2.2	10	0.62	0.06	9
6C	55	4.3	0.10	7	24	0.01	0.01	14.5	1.7	4.3	0.45	0.03	2
6D	80	4.3	0.08	6	16	0.01	0.01	7.4	0.9	2.2	0.48	0.02	2
6E	200	4.4	0.07	4	17	0.02	0.02	6.5	1.0	2.3	0.34	0.08	5
6F	350	4.4	0.09	5	24	0.03	0.02	5.5	1.3	4.4	0.49	0.05	nd

(**Table A.II** *continued*)

sample	depth [a] (cm)	pH	OC (%)	Fe_{ox} (mmol kg^{-1})	Al_{ox} (mmol kg^{-1})	Cd_{tot} (mg kg^{-1})	E_{Cd} (mg kg^{-1})	Zn_{tot} (mg kg^{-1})	E_{Zn} (mg kg^{-1})	Cd_{pw} (µg l^{-1})	Zn_{pw} (mg l^{-1})	Ca_{pw} (mM)	DOC (mg l^{-1})
7A	12	3.5	2.32	6	13	0.78	0.63	19.7	8.0	16	0.73	0.06	37
7B	22	3.6	0.54	2	8	0.28	0.24	5.1	2.7	9.1	0.42	0.04	8
7C	37	3.9	1.61	41	54	0.94	0.78	9.2	3.6	21	0.50	0.03	2
7D	70	4.3	0.38	21	64	0.14	0.11	13.5	1.1	20	0.51	0.04	4
7E	200	4.1	0.11	5	25	0.08	0.06	20.1	2.0	23	0.72	0.05	10
7F	250	4.1	0.09	3	39	0.05	0.05	23.0	4.2	19	1.30	0.05	11
7G	300	4.3	0.24	2	45	0.34	0.30	17.8	5.3	27	1.10	0.03	8
8A	16	3.8	2.43	16	28	0.52	0.28	47.2	8.9	9.4	1.12	0.11	18
8B	34	3.7	2.65	14	24	1.21	0.56	80.9	7.5	7.7	0.39	0.04	54
8C	46	3.7	2.66	53	63	2.22	1.77	25.4	14.7	28	0.94	0.05	26
8D	70	4.2	0.47	7	30	0.18	0.23	9.0	2.4	29	0.88	0.06	7
8E	100	4.3	0.21	2	23	0.11	0.13	10.1	2.4	19	0.70	0.04	12
8F	400	4.4	0.35	3	57	0.32	0.30	13.3	2.9	25	0.61	0.13	11
9A	8	3.7	2.27	24	28	1.01	0.33	123.0	12.3	2.6	0.59	0.04	48
9B	16	4.0	1.93	24	40	0.63	0.44	18.9	6.8	6.9	0.45	0.05	13
9C	26	4.0	2.82	40	87	1.11	0.90	13.7	6.1	13	0.51	0.04	8
9D	40	4.0	4.04	17	20	0.53	0.42	7.6	3.4	12	0.64	0.05	10
9E	110	4.2	0.23	14	46	0.12	0.10	18.2	2.1	18	0.62	0.12	18
9F	400	4.3	0.05	4	14	0.05	0.05	7.4	2.3	28	1.67	0.04	12
10A	12	4.0	1.78	40	30	1.83	1.27	143.3	28.3	64	4.86	0.29	11
10B	22	3.6	1.87	9	21	2.88	2.08	50.2	33.7	20	1.54	0.11	28
10C	40	3.4	2.51	18	23	2.42	2.35	65.9	57.9	22	2.25	0.10	21
10D	60	3.7	0.55	2	11	0.77	0.69	19.1	15.1	24	3.01	0.13	10
10E	100	3.9	1.44	20	62	1.59	1.45	39.2	30.8	36	3.70	0.20	12
10F	400	4.2	0.08	7	23	0.06	0.05	9.3	4.1	27	3.27	0.02	17

Table A.III Soil characteristics, metal concentrations, and pore water composition for the field in Neerpelt (10 profiles)

sample	depth [a]	pH	OC	Fe_{ox}	Al_{ox}	Cd_{tot}	E_{Cd}	Zn_{tot}	E_{Zn}	Cd_{pw}	Zn_{pw}	Ca_{pw}
	(cm)		(%)	(mmol kg^{-1})		(mg kg^{-1})				(µg l^{-1})	(mg l^{-1})	(mM)
1A	12	4.1	2.0	5.9	29	1.7	1.2	110	64	39	4.5	0.39
1B	24	4.8	1.6	6.9	33	2.2	1.5	176	152	15	3.2	0.44
1C	35	4.9	1.6	6.4	31	2.0	1.4	131	83	12	2.3	0.49
1D	45	4.7	0.9	1.7	50	0.6	0.5	43	36	6.9	1.6	0.46
1E	75	4.7	0.3	0.7	28	0.1	0.1	13	7	6.2	1.2	0.34
1F	110	4.7	0.2	0.6	24	0.1	0.1	13	7	7.8	1.0	0.32
2A	10	4.4	1.5	11	40	1.6	1.2	100	69	5.7	1.2	0.10
2B	20	5.2	1.5	11	43	1.6	1.2	143	106	5.5	1.6	0.25
2C	30	5.3	1.5	12	47	1.3	1.0	77	44	6.1	1.4	0.31
2D	45	5.1	0.3	32	38	0.2	0.2	29	16	21	2.0	0.37
2E	80	4.8	0.2	13	25	0.1	0.1	17	6	7.8	1.0	0.24
2F	115	4.7	0.1	4.3	26	0.0	0.1	13	3	3.5	0.9	0.19
3A	13	3.9	1.7	4.4	22	1.5	1.1	97	56	28	3.4	0.23
3B	26	4.8	1.6	5.0	25	1.9	1.5	146	114	28	6.0	0.68
3C	40	5.2	1.5	5.1	27	1.9	1.6	119	89	12	2.2	0.40
3D	55	4.5	1.0	1.4	25	0.8	0.6	47	35	12	1.9	0.49
3E	85	4.5	0.7	0.7	31	0.5	0.4	19	14	16	1.8	0.58
3F	115	5.1	0.5	0.5	39	0.3	0.3	14	8	10	0.7	0.28
4A	12	4.0	2.2	5.0	23	1.4	1.0	118	57	30	3.5	0.42
4B	24	4.2	1.8	6.0	29	1.9	1.5	119	82	28	3.4	0.32
4C	36	4.5	1.5	5.2	34	1.6	1.3	110	84	17	2.8	0.48
4D	50	4.8	0.7	1.3	45	0.5	0.5	50	39	12	2.7	0.48
4E	80	4.7	0.4	0.5	32	0.1	0.1	19	13	7.6	1.5	0.41
4F	105	4.8	0.3	0.3	26	0.1	0.1	17	7	4.5	1.2	0.37

(**Table A.III** *continued*)

sample	depth [a] (cm)	pH	OC (%)	Fe_{ox} (mmol kg^{-1})	Al_{ox} (mmol kg^{-1})	Cd_{tot} (mg kg^{-1})	E_{Cd} (mg kg^{-1})	Zn_{tot} (mg kg^{-1})	E_{Zn} (mg kg^{-1})	Cd_{pw} (µg l^{-1})	Zn_{pw} (mg l^{-1})	Ca_{pw} (mM)
5A	13	5.0	2.2	20	32	5.5	4.3	479	325	28	6.2	0.51
5B	26	5.4	1.6	18	29	5.5	4.6	523	387	20	4.5	0.52
5C	40	5.9	2.0	27	34	5.7	4.8	567	349	15	2.3	0.65
5D	60	5.8	0.9	13	22	3.6	3.1	323	172	21	3.2	0.45
5E	80	5.6	0.2	1.4	13	0.5	0.5	69	44	10	1.7	0.34
6A	13	4.4	2.4	28	40	6.2	4.9	349	216	40	6.5	0.34
6B	26	5.3	2.2	28	39	7.6	6.2	729	591	27	5.4	0.37
6C	40	5.6	1.7	11	44	3.8	3.2	525	418	17	4.2	0.48
6D	60	5.6	0.8	2.3	24	0.6	0.5	121	86	5.1	2.0	0.50
6E	80	5.5	0.5	0.9	15	0.2	0.2	54	39	4.3	1.3	0.45
7A	10	5.2	2.4	12	46	4.4	3.7	434	328	11	3.0	0.60
7B	20	5.6	2.0	12	46	4.6	3.9	416	282	8.4	1.8	0.55
7C	30	5.9	2.1	10	46	4.6	3.9	442	286	8.0	1.5	0.53
7D	40	6.0	1.8	4.7	70	1.8	1.5	194	134	4.1	0.7	0.51
7E	65	6.0	0.4	1.1	31	0.3	0.3	36	20	6.9	0.9	0.93
7F	90	6.0	0.2	0.8	24	0.1	0.2	15	7	1.1	0.3	0.37
8A	10	4.7	2.3	17	38	3.1	2.3	239	130	32	4.5	0.39
8B	20	5.3	1.8	17	39	4.9	3.8	462	316	29	4.9	0.38
8C	30	5.6	1.6	9.3	30	4.5	3.1	464	284	13	3.2	0.67
8D	45	5.7	0.5	1.8	30	0.8	0.6	116	66	13	2.2	0.57
8E	80	5.8	0.2	0.6	19	0.2	0.1	27	12	4.9	0.6	0.53

(**Table A.III** *continued*)

sample	depth [a]	pH	OC	Fe_{ox}	Al_{ox}	Cd_{tot}	E_{Cd}	Zn_{tot}	E_{Zn}	Cd_{pw}	Zn_{pw}	Ca_{pw}
	(cm)		(%)	(mmol kg^{-1})		(mg kg^{-1})				($\mu g\ l^{-1}$)	(mg l^{-1})	(mM)
9A	10	4.8	2.7	16	30	5.5	4.3	441	277	28	4.7	0.59
9B	20	5.4	2.1	11	28	6.0	4.5	523	356	17	4.2	0.70
9C	30	5.7	2.4	13	31	5.7	4.7	574	385	11	2.2	0.64
9D	50	6.1	2.5	4.7	41	1.2	0.8	107	60	2.5	0.5	0.67
9E	70	6.1	2.5	3.7	50	0.5	0.4	42	27	1.8	0.3	0.64
9F	90	5.9	0.6	1.0	19	0.2	0.2	18	9	2.5	0.3	0.81
10A	12	4.9	2.0	18	34	5.6	4.5	412	303	46	8.3	0.56
10B	24	5.4	1.8	19	35	6.4	4.9	634	433	24	5.3	0.53
10C	36	5.7	1.6	8.2	23	3.9	3.4	411	313	15	3.1	0.44
10D	50	5.8	0.5	1.7	15	0.7	0.5	107	79	12	2.4	0.47
10E	80	5.8	0.2	0.7	24	0.3	0.2	18	7	10	0.5	0.63

[a] lower boundary